DEVELOPMENT OF QUALITY ASSESSMENT METHODS FOR WOOD IMAGES

HESHALINI A/P RAJAGOPAL @ RAMASAMY

FACULTY OF ENGINEERING
UNIVERSITY OF MALAYA
KUALA LUMPUR

2021

DEVELOPMENT OF QUALITY ASSESSMENT METHODS FOR WOOD IMAGES

HESHALINI A/L RAJAGOPAL @ RAMASAMY

THESIS SUBMITTED IN FULFILMENT OF THE REQUIREMENTS FOR THE DEGREE OF DOCTOR OF PHILOSOPHY

FACULTY OF ENGINEERING
UNIVERSITY OF MALAYA
KUALA LUMPUR

2021

UNIVERSITY OF MALAYA

ORIGINAL LITERARY WORK DECLARATION

Name of Candidate: **Heshalini A/P Rajagopal @ Ramasamy**

Registration/Matric No: **KHA 160066**

Name of Degree: **Doctor of Philosophy**

Title of Project Paper/Research Report/Dissertation/Thesis ("this Work"):

Development of Quality Assessment Methods for Wood Images

Field of Study: Image Processing

I do solemnly and sincerely declare that:

(1) I am the sole author/writer of this Work;
(2) This Work is original;
(3) Any use of any work in which copyright exists was done by way of fair dealing and for permitted purposes and any excerpt or extract from, or reference to or reproduction of any copyright work has been disclosed expressly and sufficiently and the title of the Work and its authorship have been acknowledged in this Work;
(4) I do not have any actual knowledge nor do I ought reasonably to know that the making of this work constitutes an infringement of any copyright work;
(5) I hereby assign all and every rights in the copyright to this Work to the University of Malaya ("UM"), who henceforth shall be owner of the copyright in this Work and that any reproduction or use in any form or by any means whatsoever is prohibited without the written consent of UM having been first had and obtained;
(6) I am fully aware that if in the course of making this Work I have infringed any copyright whether intentionally or otherwise, I may be subject to legal action or any other action as may be determined by UM.

Candidate's Signature　　　　　　Date: 30/04/2021

Subscribed and solemnly declared before,

Witness's Signature　　　　　　Date:

Name:

Designation:

DEVELOPMENT OF QUALITY ASSESSMENT METHODS FOR WOOD IMAGES

ABSTRACT

Image Quality Assessment (IQA) is a vital element in improving the efficiency of an automatic recognition system of various wood species. There is a need to develop a No-Reference Image Quality Assessment (NR-IQA) system as a perfect and distortion free wood images may be impossible to be acquired in the dusty and dark environment in timber factories. Many IQAs which focus on some image of interest such as natural images have been proposed. However, an IQA specifically for wood images have not been proposed so far. Hence, this thesis proposes two No-Reference IQA (NR-IQA) metrics, Modified BRISQUE Wood Image Quality Assessment (MBW-IQA) and GLCM and Gabor Wood Image Quality Assessment (GGW-IQA) to assess the quality of wood images. Firstly, Support Vector Machine (SVM) Regression (SVR) was trained using Generalized Gaussian Distribution (GGD) and Asymmetric Generalized Gaussian Distribution (AGGD) features calculated for wood images together with the mean opinion score (MOS) obtained from subjective evaluation to develop the MBW-IQA. Secondly, SVR was trained using Gray Level Co-Occurrence Matrix (GLCM) and Gabor features calculated for wood images together with the MOS to develop the GGW-IQA metric. The MBW-IQA and GGW-IQA metrics are compared with one of the established NR-IQA metrics, namely, Blind/Referenceless Image Spatial Quality Evaluator (BRISQUE), Deep Neural Network IQA (deepIQA), Deep Bilinear Convolution Neural Network (DB-CNN) and five Full Reference-IQA (FR-IQA) metrics known as MSSIM, SSIM, FSIM, IWSSIM and GMSD. Results shows that the GGW-IQA outperforms the MBW-IQA, BRISQUE, deepIQA, DB-CNN and all the FR-IQA metrics. Moreover, the GGW-IQA

metric is beneficial in wood industry as a distortion free reference image is not needed to evaluate the wood images.

Keywords: Wood images, NR-IQA, MBW-IQA, GGW-IQA, BRISQUE, deepIQA, DB-CNN, FR-IQA

PEMBANGUNAN KAEDAH PENILAIAN KUALITI BAGI IMEJ KAYU

ABSTRAK

Penilaian Kualiti Imej (IQA) adalah elemen penting dalam meningkatkan kecekapan sistem pengenalan automatik pelbagai spesies kayu. Terdapat keperluan untuk membangunkan Sistem Penilaian Kualiti Tanpa Rujukan (NR-IQA) sebagai imej kayu bebas yang kurang sempurna dan mungkin tidak dapat diperoleh dalam persekitaran yang berdebu dan gelap di kilang-kilang balak. Banyak kaedah IQA yang fokus kepada imej tertentu seperti image semulajadi telah dicadangkan. Akan tetapi, kaedah IQA bagi imej kayu belum dicadang setakat ini. Oleh itu, tesis ini mencadangkan dua NR-IQA, Modified BRISQUE Wood Image Quality Assessment (MBW-IQA) and GLCM and Gabor Wood Image Quality Assessment (GGW-IQA) untuk menilai kualiti imej kayu. Pertama, Regresi Mesin Sokongan Vektor (SVM) (SVR) telah dilatih menggunakan GGD dan AGGD yang dikira untuk imej kayu bersama dengan skor pendapat min (MOS) yang diperoleh daripada penilaian subjektif untuk membangunkan metric, MBW-IQA. Kedua, SVR dilatih menggunakan ciri GLCM dan Gabor yang dikira untuk imej kayu bersama dengan skor MOS untuk membangunkan metric, GGW-IQA. Metrik MBW-IQA dan GGW-IQA yang dicadangkan dibandingkan dengan Pengukur Kualiti Spatial Imej Blind / Referenceless (BRISQUE), Deep Neural Network IQA (deepIQA), Deep Bilinear Convolution Neural Network (DB-CNN) dan lima metrik Rujukan IQA (FR-IQA) yang dikenali sebagai MSSIM, SSIM, FSIM, IWSSIM dan GMSD. Keputusan menunjukkan bahawa metrik GGW-IQA mengatasi MBW-IQA, BRISQUE, deepIQA, DB-CNN dan semua metrik FR-IQA. Selain itu, GGW-IQA yang dicadangkan bermanfaat dalam industri kayu sebagai imej rujukan bebas distorsi tidak diperlukan untuk menilai imej kayu.

Kata Kunci: Imej Kayu, NR-IQA, MBW-IQA, GGW-IQA, BRISQUE, deepIQA, DB-CNN, FR-IQA

ACKNOWLEDGEMENTS

This thesis has benefited greatly from the support of many people, some of whom I would sincerely like to thank here:

The supervisors of my PhD research, Dr Norrima Binti Mokhtar and Dr Anis Salwa Binti Mohd Khairuddin for offering me such an interesting topic of investigation. Their continuous guiding, constant support and invaluable suggestions and advices have given me the confidence to complete this research work.

All the authors of the image databases and quality metrics, to share their source codes and results of the tests. Without the unselfishness in sharing the knowledge and data, the comparison studies would not be possible. I would like to also thank all the thirthy subjects, staff from Tapak Semaian Mantin, Jabatan Perhutanan Negeri Sembilan, staff and students from Department of Electrical and Electronic Engineering, Manipal International University (MIU) who were involved in the subjective evaluation for the wood images.

All the people behind the offices of the Department of Electrical Engineering and Faculty of Engineering, University of Malaya for giving me the opportunity to pursue my education.

Last but not least, I would like to thank my parents, Mr Rajagopal Nallasamy, Mrs Mageswari Gurusamy, my husband, Dr Krishna Kumar Suppaiah, my siblings, Captain Sridharn Rajagopal, Major Prabhakaran Rajagopal, my two childrens, Rishivanth Krishna Kumar, Mershivany Krishna Kumar, niece and nephews, Mognesh Sridhran, Prithyka Prabhakaran and Yeashveer Prabhakaran and friends for their thorough support and encouragement throughout the difficult times. Not to be forgotten for the gratitude to those who have helped me but not mentioned here.

TABLE OF CONTENTS

LIST OF FIGURES

LIST OF TABLES

LIST OF ABBREVIATIONS

AGGD	:	Asymmetric Generalized Gaussian Distribution
BRISQUE	:	Blind/Referenceless Image Spatial Quality Evaluator
DB-CNN	:	Deep Bilinear Convolution Neural Network
deepIQA	:	Deep Neural Network Image Quality Assessment
FR-IQA	:	Full Reference Image Quality Assessment
FSIM	:	Feature SIMilarity
GGD	:	Generalized Gaussian Distribution
GGW-IQA	:	GLCM and Gabor Wood Image Quality Assessment
GLCM	:	Gray Level Co-Occurrence Matrix
GMSD	:	Gradient Magnitude Similarity Deviation
GN	:	Gaussian White Noise
IQA	:	Image Quality Assessment
IW-SSIM	:	Information Weighted SSIM
MB	:	Motion Blur
MBW-IQA	:	Modified BRISQUE Wood Image Quality Assessment
MSCN	:	Mean Subtracted Contrast Normalized
MS-SSIM	:	Multiscale SSIM
NR-IQA	:	No Reference Image Quality Assessment
PLCC	:	Pearson Linear Correlation Coefficient
RMSE	:	Root Mean Square Error
RR-IQA	:	Reduced Reference Image Quality Assessment
SSIM	:	Structural Similarity Index Metrics
SVM	:	Support Vector Machine
SVR	:	Support Vector Machine (SVM) Regression

LIST OF APPENDICES

CHAPTER 1: INTRODUCTION

Wood is a plant tissue with a characteristic porous and fibrous structure, which is widely used for furniture, millwork, flooring, building construction, paper production, and as a source of energy (Shivashankar, 2018).The demand for wood is increasing day by day where it is used for many purposes mainly for construction of building, paper, furniture, cooking utensils and sports equipment (Shivashankar, 2018). In the South East Asia region, Malaysia is one of the timber-producing countries other than Indonesia and Laos (Noor, Kadir, & Muhamad, 2020). According to the Minister of Plantations Industries and Commodities, YB Dato' Dr Mohd Khairuddin Bin Aman Razali, for decades, the timber industry has played an important role in the socioeconomic development in Malaysia. The timber industry has become the main contributor to the Malaysia's export revenue. Malaysian wood and wood products especially furniture has been exported to over 160 countries around the world. The timber sector also provides employment to about 240,000 workers and as to date there are about 3,500 number of mills still in operation. For the year of 2019, the timber sector has contributed 1.6% to the gross domestic product (GDP) and 2.3% of the Malaysia's total merchandise export with total exports of RM22.5 billion for timber and timber-related products. From January to November 2020, timber-based products have contributed 14.9% to the export of commodity products.

Every wood species has their unique physical properties such as knot, colour, structure and density which determines its usage and price (Barmpoutis, Dimitropoulos, Barboutis, & Grammalidis, 2018; Funck, Zhong, Butler, Brunner, & Forrer, 2003; Longuetaud et al., 2012; Shivashankar, 2018; Zamri, Cordova, Khairuddin, Mokhtar, & Yusof, 2018). For example, mahogany is used mainly for fine furniture crafting as it is a medium-dense hardwood. It is also essential to choose the right wood for construction of building to ensure the safety and durability of the building. The characteristic of the wood with specific applications has made the selection of wood became crucial in timber industry.

Besides that, fraudulent labeling practiced by some timber exporters will reduce the country's incomes generated by tax. This happened when lower tax is imposed on high quality wood that is mislabeled as low quality (R. Li, Buongiorno, Turner, Zhu, & Prestemon, 2008). In addition, illegal logging of high quality wood also takes place where the timber industries were given permit by the authority to cut down different wood but some of the timber industries tend to cut down higher quality wood in the forest. A study by the American Forest & Paper Association has estimated that illegal logging depresses world timber prices by between 7% and 16%, depending on the product. This causes the world to loose of at least US$460 million each year (R. Li et al., 2008). In Malaysia, illegal logging accounted for 14–25% of the total timber production in the country (Noor et al., 2020). The illegal logging effects the economy through tax and premium evasion which causes loss of government income. It is estimated that the amount of government loss due to illegal logging stood at US$10 billion per annum (Noor et al., 2020).

To rectify these issues, timber industries and supervisory agencies have made efforts to appoint certified personnel to identify quality of wood via manual inspection to ensure that the timber industries are trading the correct timber species and correct timber is being used to manufacture the wood products. Furthermore, supervisory agencies have to verify that the timbers have not been cut down illegally from the forests (Gazo, Wells, Krs, & Benes, 2018; Yusof, Khalid, & Anis, 2013). However, manual inspection takes longer time, hectic work and subjective (Gazo et al., 2018; Shivashankar, 2018). Hence, wood image processing such as wood slice recognition and wood texture analysis are performed to judge the physical properties and economic value of different wood species correctly

(Guang-sheng & Peng, 2012; Pan & Kudo, 2011). In addition, wood slice recognition and wood texture analysis could detect wood species accurately and this could decrease the economic losses due to mislabeling of a good quality wood with a lower quality.

However, in order to perform these image processing and recognition tasks, good quality wood images are needed. A low-quality image may produce an inaccurate result from the wood slice recognition and texture analysis. However, it may not be possible to obtain a perfect image due to the dusty, high temperature and poor illumination environment in the timber factories (Ratnasinga, Ioras, Swan, Yoon, & Thanasegar, 2011). Therefore, a feedback system prior to image processing and recognition tasks must be implemented to avoid wood species misclassification. If the initial image obtained is of low quality, the feedback system will automatically inform the operator either to acquire a new image after taking the corrective action such as cleaning the camera lens, station and wood surface.

Prior studies on wood slice recognition based on image processing can be found in work of (Barmpoutis et al., 2018; Khalid, Lee, Yusof, & Nadaraj, 2008; Venkatachalapathy & Sudhakar, 2014; Zamri et al., 2018). In Khalid et al., Venkatachalapathy & Sudhakar and Zamri et al., the wood images were enhanced before performing the recognition tasks in order to obtain clearer texture properties from the images. However, the wood images quality was not assessed before the pre-processing and recognition tasks. This means that some of the images may be enhanced even though they were already of good quality. In this case, the enhancement is redundant and contributes to additional computational process. Furthermore, enhancement process ignores the dynamical information of image channels (Barmpoutis et al., 2018). If the images were assessed beforehand, images with low quality could be identified, and corrective actions could be taken to obtain higher quality images to be used for recognition tasks. Hence, the recognition rate can be increased than the one obtained without quality assessment**.**

There are two types of image quality assessment (IQA) which are objective and subjective evaluations. Subjective evaluation is the scores given by human subjects based on their judgment on the image quality while objective assessment is a method defined mathematically to assess images (L.S. Chow, Rajagopal, & Paramesran, 2016). Subjective evaluation is often assumed as the benchmark or gold standard in the image quality assessment. However, subjective evaluation is not practical as it is time consuming. Therefore, objective assessment is used as an alternative to the subjective evaluation. The aim of the objective assessment is to be consistent and in close agreement with subjective evaluation (H.R. Sheikh, Sabir, & Bovik, 2006)**.** In this study, Full Reference Image Quality Analysis (FR-IQA) is chosen as an objective assessment to evaluate the wood images. FR-IQA evaluates an image by comparing the image with its reference image where the reference image has to be a distortion free image. -(Chandler, 2013; Gulame, Joshi, & Kamthe, 2013).

In this research, firstly the importance of IQA module to improve the rate of wood species recognition system was studied. The wood images were motion-blurred due to imperfections in the imaging and capturing process. Then, IQA module was used to monitor the quality of images before proceeding to the next stage which is the feature extraction process. The IQA module will determine whether the image has to undergo the image deblurring process based on the image quality value. If the image is of low quality based on the image quality value obtained, then the image will be deblurred before the feature extraction procedure. A reliable motion deblurring technique, which is based on Lucy–Richardson algorithm, was used to enhance the motion-blurred images before proceeding to the next stage, which is the feature extraction process. Then, a statistical feature extraction technique was proposed to extract 24 features from each wood image. Finally, a Support Vector Machine (SVM) was used to classify the 20 tropical wood species. This study shows that the rate of wood species recognition or identification system can be improved with the IQA module.

Next, thirty human subjects with normal vision acuity, eleven staff from Tapak Semaian Mantin, Jabatan Perhutanan Negeri Sembilan and nineteen students and staff from Department of Electrical and Electronic Engineering, Manipal International University (MIU), Nilai, Malaysia were selected to evaluate the wood images and the scores obtained from the subjective human evaluation are represented in Mean Opinion Score (MOS) form. The five objective FR-IQA metrics: Structural Similarity Index (SSIM) (Zhou Wang, Simoncelli, & Bovik, 2003), Multiscale SSIM (MS-SSIM) (Zhou Wang et al., 2003), Feature Similarity (FSIM) (L. Zhang, Zhang, & Mou, 2011), Information Weighted SSIM (IW-SSIM) (Zhou Wang & Li, 2011) and Gradient Magnitude Similarity Deviation (GMSD) (Xue, Zhang, Mou, & Bovik, 2014) are regarded as the benchmark and compared with the subjective MOS. The correlation between the MOS and the FR-IQA metrics will be computed using Pearson Linear Correlation Coefficient (PLCC) and Root Mean Squared Error (RMSE). The subjective MOS will be used to develop the NR-IQA metrics for wood images.

The noisy and dusty environment in timber factories may not be able to produce a perfect reference image to assess the quality of an image. Therefore, the reference images used in the previous studies might be subjected to a small degree of distortions. In fact, the FR-IQA metrics can only provide a relative measure of the image quality for various distorted images compared to the so-called 'reference image'. Apparently, FR-IQA is not the best way to evaluate wood images. Hence, NR-IQA is a more suitable method to evaluate wood images as they do not require any reference image.

Two NR-IQAs were proposed. The first NR-IQA method is based on a modification of a widely-used NR-IQA, the Blind/Referenceless Image Spatial Quality Evaluator (BRISQUE) model is proposed. The first NR-IQA method is known as Modified BRISQUE Wood Image Quality Assessment, MBW-IQA. BRISQUE is an IQA model, which considers the luminance and image features of the natural images and it is not a distortion-specific model (Mittal, Moorthy, & Bovik, 2012). The BRISQUE model is trained with subjective scores to enable emulation of human judgement on the quality of the images. Modification of the BRISQUE model for wood analysis is required, as it was designed to evaluate natural images. The MBW-IQA is compared with BRISQUE, Deep Neural Network IQA (deepIQA), Deep Bilinear Convolution Neural Network (DB-CNN) and five types of established FR-IQA metrics, i.e. Structural Similarity Index (SSIM) (Zhou Wang et al., 2003), Multiscale SSIM (MS-SSIM) (Zhou Wang et al., 2003), Feature Similarity (FSIM) (L. Zhang et al., 2011), Information Weighted SSIM (IW-SSIM) (Zhou Wang & Li, 2011) and Gradient Magnitude Similarity Deviation (GMSD) (Xue et al., 2014). The relative performances in terms of efficiency of the MBW-IQA, BRISQUE, deepIQA, DB-CNN and FR-IQAs are determined based on the correlation between the expert mean opinion scores (MOS) and the metrics using Pearson Linear Correlation Coefficient (PLCC) and Root Mean Squared Error (RMSE) (L.S. Chow et al., 2016).

Second NR-IQA is designed using widely used features for wood recognition, Gray Level Co-Occurrence Matrix (GLCM) and Gabor features to evaluate wood images. This NR-IQA metric is known as GLCM and Gabor Wood Image Quality Assessment, GGW-IQA. SVR was trained using GLCM and Gabor features calculated for wood images and the mean opinion score (MOS) which was obtained from subjective evaluation. The

GGW-IQA is compared with the MBW-IQA, BRISQUE, deepIQA, DB-CNN and the same five FR-IQA metrics, SSIM, MS-SSIM, FSIM, IW-SSIM and GMSD.

1.1 Objectives of Dissertation

The objectives of this dissertation are outlined as follow:

- To perform both subjective and objective assessment of Full Reference Image Quality Assessment (FR-IQA) for wood images.
- To propose a No Reference Image Quality Assessment (NR-IQA) method for assessing the image quality of wood images by modifying well-established NR-IQA, BRISQUE.
- To propose GLCM and Gabor features based No Reference Image Quality Assessment (NR-IQA) method to evaluate wood images.

1.2 Scope of Research

The scopes of the research in this dissertation are as follows. Firstly, the need of Image Quality Assessment (IQA) module to improve the accuracy of wood species recognition system were studied and proven. Then, subjective and objective assessment are performed on wood images to analyse the quality of wood images for wood species recognition purposes. Several distorted images are generated from the reference images by applying Gaussian White Noise and Motion Blur at various levels of distortions for comparison purposes. Thirty subjects, eleven staff from Tapak Semaian Mantin, Jabatan Perhutanan Negeri Sembilan, nineteen students and staff from Department of Electrical and Electronic Engineering, Manipal International University (MIU), Nilai were selected to assess the distorted images for the subjective evaluation. The scores obtained from the subjects were transformed into Mean Opinion Score (MOS). In the objective evaluation, five Full Reference-IQA (FR-IQA) metrics, namely MSSIM, SSIM, FSIM, IWSSIM and

GMSD were used to evaluate the distorted images. The objective FR-IQAs were used as the benchmark to validate the subjective MOS obtained for wood images. The relationship between the subjective MOS and objective FR-IQAs are examined using performance metrics namely PLCC and RMSE.

Secondly, two NR-IQA metrics were proposed to assess wood images. Blind/Referenceless Image Spatial Quality Evaluator (BRISQUE) is modified by training the Support Vector Machine (SVM) Regression (SVR) with the MOS and the locally normalized luminance coefficients of the wood images to develop the first NR-IQA metric, MBW-IQA. The second NR-IQA metric, GGW-IQA were designed using widely used features for wood species recognition, Gray Level Co-Occurrence Matrix (GLCM) and Gabor features to evaluate wood images. SVR was trained using GLCM and Gabor features calculated for wood images and the mean opinion score (MOS) which was obtained from subjective evaluation.

Lastly, the proposed NR-IQA metrics, MBW-IQA and GGW-IQA are compared with one of the established NR-IQA metrics, namely, Blind/Referenceless Image Spatial Quality Evaluator (BRISQUE), Deep Neural Network IQA (deepIQA), Deep Bilinear Convolution Neural Network (DB-CNN) and five Full Reference-IQA (FR-IQA) metrics known as MSSIM, SSIM, FSIM, IWSSIM and GMSD. The efficiency of the proposed NR-IQA metrics, MBW-IQA and GGW-IQA are shown in the form of PLCC and RMSE values calculated between the metrics and MOS.

1.3 Organization of Dissertation

This dissertation is organized as follows. Chapter 1 explains the background of the study, problem statements, research objectives and scope of the research. Chapter 2 reviews the related works on image quality assessment for images. The reviews are based on FR-IQA and NR-IQA studies done for images. Chapter 3 discusses on the application of Image Quality Assessment (IQA) module to motion-blurred wood images for wood species identification system. In this chapter, the importance of IQA module in the wood species recognition system were explained and proven. Chapter 4 discusses on the correlation between subjective and objective assessment of wood images. A wood database which contains the reference images, distorted images and MOS is created. Chapter 5 and 6 discusses the two NR-IQA metrics designed to assess wood images. Chapter 5 explains the proposed first NR-IQA metric, MBW-IQA which is a modified method based on an existing state-of-the-art method, BRISQUE. Chapter 6 explains the proposed second NR-IQA method, GGW-IQA developed using GLCM and Gabor features. Finally, Chapter 7 presents the conclusion of the work in this dissertation and discusses the future works in image quality assessment of wood images.

CHAPTER 2: LITERATURE REVIEW

The demand for wood is increasing day by day where it is used for many purposes mainly for construction of building, paper, furniture, cooking utensils and sports equipment (Shivashankar, 2018). Every wood species has their unique physical properties such as knot, colour, structure and density which determines its usage and price (Barmpoutis et al., 2018; Funck et al., 2003; Longuetaud et al., 2012; Shivashankar, 2018; Zamri et al., 2016, Yusof et al., 2013b).

The need for wood recognition system is becoming critical in areas of forest management. Effectiveness in forest management is important to the timber industries with the intention to sustain and improve productivity and quality of the timber products in furniture industries and housing industries (Ibrahim, Khairuddin, Abu Talip, Arof, & Yusof, 2017). The accurate classification of wood species is needed to ensure that the timber merchandise has the required properties which are the optimized features. As example, the precise wood species must be used for the safety in construction industries. Choosing and ensuring the correct wood to be used is very important to construct a dependable roof truss. Besides that, fraudulent labeling practiced by some timber exporters will reduce the country's incomes generated by tax. This happened when lower tax is imposed on high quality wood that is mislabeled as low quality (R. Li et al., 2008). Therefore, in order to manage forest resources effectively, timber industries must certify that they are trading the correct timber species, and supervisory agencies have to verify that the timbers have not been cut down illegally from the forests.

To rectify this issue, manufacturers have made efforts to appoint certified personnel to identify quality of wood via manual inspection (Gazo et al., 2018; Yusof et al., 2013a). However, manual inspection takes longer time, hectic work and subjective (Gazo et al., 2018; Shivashankar, 2018). Hence, wood image processing such as wood slice recognition and wood texture analysis are performed to judge the physical properties and economic value of different wood species correctly (Guang-sheng and Peng, 2012; Pan and Kudo, 2011). In addition, wood slice recognition and wood texture analysis could detect wood species accurately and this could decrease the economic losses due to mislabeling of a good quality wood with a lower quality.

However, in order to perform these image processing and recognition tasks, good quality wood images are needed. A low-quality image may produce an inaccurate result from the wood slice recognition and texture analysis. However, it may not be possible to obtain a perfect image due to the dusty, high temperature and poor illumination environment in the timber factories (Ratnasinga et al., 2011). Therefore, a feedback system prior to image processing and recognition tasks must be implemented to avoid wood species misclassification. If the initial image obtained is of low quality, the feedback system will automatically inform the operator either to acquire a new image after taking the corrective action such as cleaning the camera lens, station and wood surface.

Prior studies on wood slice recognition based on image processing can be found in work of (Barmpoutis et al., 2018; Khalid et al., 2008; Venkatachalapathy & Sudhakar, 2014; Zamri et al., 2018). In Khalid et al., Venkatachalapathy & Sudhakar and Zamri et al., the wood images were enhanced before performing the recognition tasks in order to obtain clearer texture properties from the images. However, the wood images quality was not assessed before the pre-processing and recognition tasks. This means that some of the images may be enhanced even though they were already of good quality. In this case, the enhancement is redundant and contributes to additional computational process. Furthermore, enhancement process ignores the dynamical information of image channels

(Barmpoutis et al., 2018). If the images were assessed beforehand, images with low quality could be identified, and corrective actions could be taken to obtain higher quality images to be used for recognition tasks. Hence, the recognition rate can be increased than the one obtained without quality assessment**.**

Image Quality Assessment (IQA) can be divided into two categories, namely subjective and objective evaluation. Subjective evaluation is where the images will be evaluated by the human subjects and scores will be given based on their perception on the quality of the images whereas objective evaluation uses mathematical algorithm to produce quality score of the images. Although subjective evaluation is regarded as the gold standard in IQA, it is impractical as it is costly and time consuming. Therefore, objective evaluation is preferred compared to subjective evaluation. The ultimate goal of objective evaluation is to mimic the quality predictions of an average human observer (Z.; Wang, 2011).

There are three types of objective evaluation namely Full-Reference-IQA (FR-IQA), Reduced Reference-IQA (RR-IQA) and No-Reference/Blind IQA (NR-IQA) (Chandler, 2013; Gulame et al., 2013). Figure 2.1 illustrates the categories of Image Quality Assessment (IQA).

FR-IQA evaluates an image by comparing the image with its reference image while NR-IQA evaluates an image without its reference image. On the other hand, RR-IQA assesses an image using partial information from the reference images. NR-IQA is the most suitable metric to assess wood images as the noisy and dusty environment in timber factories may not be able to produce a perfect reference image to assess the quality of an image.

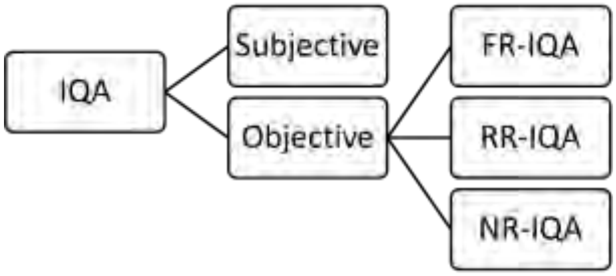

Figure 2.1: Categories of Image Quality Assessment (IQA)

2.1 Full Reference Image Quality Assessment (FR-IQA)

FR-IQA is an objective assessment which evaluates an image by comparing the image with its reference image. The reference images have to be perfect or distortion free image for an accurate image quality evaluation. There are several widely cited and established FR-IQA metrics, namely Structural Similarity Index (SSIM) (Zhou Wang et al., 2003), Multiscale SSIM (MS-SSIM) (Zhou Wang et al., 2003), Feature Similarity (FSIM) (L. Zhang et al., 2011), Visual Information Fidelity (VIF) (Hamid Rahim Sheikh & Bovik, 2006), Information Weighted SSIM (IW-SSIM) (Zhou Wang & Li, 2011) and Gradient Magnitude Similarity Deviation (GMSD) (Xue et al., 2014). Their formulas and brief description are given in Table 2.1. In Table 2.1, $r(x,y)$ denotes the reference image and $t(x,y)$ denotes the distorted image. n_x and n_y are the size of the image in pixels across x and y dimensions. Both $r(x,y)$ and $t(x,y)$ should have the same size. These FR-IQA metrics were tested on several natural images database, namely TID2008, CSIQ and LIVE and are suitable to evaluate images distorted with Gaussian White Noise and Motion Blur.

The main goal of IQA is to model an objective assessment metric that is very close to the human subjective evaluation (H.R. Sheikh et al., 2006). To achieve this goal, several researchers have produced databases to carried out experiments using the subjective based FR-IQA on natural images. To the best of our knowledge, there are ten publically available databases, namely Tampere Image Database (TID 2013) (Nikolay Ponomarenko et al., 2015), TID2008 (N Ponomarenko et al., 2008), LIVE, (H.R. Sheikh et al., 2006), CSIQ (Larson & Chandler, 2010), Image and Video Communication Database (IVC) (Patrick Le Callet, 2005), Media Information and Communication Technology Database (MICT) ("MICT Image Quality Evaluation Database," n.d.), Wireless Imaging Quality Database (WIQ) (Engelke, U., Kusuma, M., Zepernick, H. J., & Caldera, 2009), Cornell-A57 Database (A57) (Chandler & Hemami, 2007), KonIQ-10K (J. Wang & Wang, 2014) and LIVE In the Wild (Bovik, 2016).

Few researchers have produced database on MR images and underwater images. A database on MR images which incorporates subjective based FR-IQA on Magnetic Resonance Image (MRI) images was generated (Li Sze Chow, Rajagopal, & Paramesran, 2016). The MRI database consists of 25 original reference images and 750 distorted images. The reference images were distorted with two types of distortions: Gaussian White Noise, Gaussian Blur, DCT compression, JPEG compression and JPEG2000 compression. Twenty-eight subjects were chosen to evaluate the images.

Recently, a database on underwater images was generated . The database comprises of 30 ground-truth images and 900 synthetic underwater images of the same scene, called synthetic underwater image dataset (SUID). The reference images were distorted with different turbidity types and degradation levels by reconstructing four common underwater challenge scenes including greenish scene, bluish scene, low-light scene, hazy scene. The reference and distorted images were evaluated by fifty human subjects (Hou et al., 2020). These databases are always used to measure the efficiency of newly designed quality metrics model by comparing it with the subjective scores.

The details of these databases are as shown in Table 2.2. These databases are also used to model automated image quality assessment which is known as No-Reference

Image Quality Assessment (NR-IQA). NR-IQA will be explained further in the next section.

To the best of our knowledge, subjective based FR-IQA on wood images has not been done. The noisy and dusty environment in timber industry may not be able to produce a distortion-free image. If there is no perfect reference image, it means that the FR-IQA metrics can only provide a relative measure of image quality in comparison to the so-called ‘reference image’. In other words, it is not an ideal IQA method for wood images. Therefore, NR-IQA is a more appropriate method to evaluate the quality of wood images. So far, NR-IQA on wood images has not been studied yet as there is no study on subjective based FR-IQA on wood images.

Table 2.1: FR-IQA Algorithm

No	IQA Algorithm	Year	Description
1	Structural Similarity Index Metrics (SSIM)(Zhou Wang, Bovik, Sheikh, & Simoncelli, 2004)	2004	Captures the loss in the structure of the image. $$SSIM = \frac{(2\mu_r\mu_t + C_1)(2\sigma_{rt} + C_2)}{(\mu_r^2 + \mu_t^2 + C_1)(\sigma_r^2 + \sigma_t^2 + C_2)} \quad (2.1)$$ where μ_r and μ_t are the mean intensity for the reference and distorted images respectively; σ_r and σ_t are the standard deviation for the reference and distorted images respectively; σ_{rt} is estimated as: $$\sigma_{rt} = \frac{1}{N-1}\sum_{i=1}^{N}(r_i - \mu_r)(t_i - \mu_t) \quad (2.2)$$

No	IQA Algorithm	Year	Description
			where $C_1 = (K_1 L)^2$ and $C_2 = (K_2 L)^2$ where L is the dynamic range of the pixels values (i.e. 255 for 8-bit grayscale images, as in our case), K_1 = 0.01 and K_2 = 0.03.
2	Multiscale SSIM (MS-SSIM)(Zhou Wang et al., 2004)	2004	Mean of SSIM that evaluates overall image quality by using a single overall quality. $$MSSIM\ (r,t) = \frac{1}{M}\sum_{j=1}^{M} SSIM(r_j\,, t_j) \quad (2.3)$$
3	Feature SIMilarity (FSIM)(L. Zhang et al., 2011)	2011	A low-level feature based image quality assessment which used two types of features: Phase Congruency (PC) and Gradient Magnitude (GM). **Ω** represents the whole image spatial domain. $$FSIM\ (r,t) = \frac{\sum_{x\in\Omega} S_L(x).PC_m(x)}{\sum_{x\in\Omega} PC_m(x)} \quad (2.4)$$

No	IQA Algorithm	Year	Description
			where $PC_m(x) = max\big(PC_r(x).PC_t(x)\big)$ (2.5) $S_L = [S_{PC}(x)]^{\alpha}[S_G(x)]^{\beta}$ (2.6) where $S_{PC}(x) = \frac{2PC_r(x).PC_t(x)+T_1}{PC_r^2(x)+PC_t^2(x)+T_1}$ (2.7) $S_G(x) = \frac{2G_r(x).G_t(x)+T_2}{G_r^2(x)+G_t^2(x)+T_2}$ (2.8)
4	Information Weighted SSIM (IW-SSIM)(Zhou Wang & Li, 2011)	2011	Obtained by combining content weighting with MS-SSIM. $IW - SSIM = \frac{\sum_i \omega_{j,i}\, c(r_{j,i},t_{j,i})s(r_{j,i},t_{j,i})}{\sum_i \omega_{j,i}}$ (2.9)

No	IQA Algorithm	Year	Description
			where $c(r_{j,i}, t_{j,i}) = \frac{2\sigma_r\sigma_t + C_2}{\sigma_r^2 + \sigma_t^2 + C_2}$ (2.10) and $s(r_{j,i}, t_{j,i}) = \frac{\sigma_{rt} + C_3}{\sigma_r\sigma_t + C_3}$ (2.11) where σ_r and σ_t are the standard deviation for the reference and distorted images respectively; σ_{rt} is estimated as: $\sigma_{rt} = \frac{1}{N-1}\sum_{i=1}^{N}(r_i - \mu_r)(t_i - \mu_t)$ (2.12)

No	IQA Algorithm	Year	Description
			where $C_1 = (K_1L)^2$, $C_3 = (K_2L)^2/2$ where L is the dynamic range of the pixels values (i.e. 255 for 8-bit grayscale images, as in our case), $K_1 = 0.01$ and $K_2 = 0.03$.
5	Gradient Magnitude Similarity Deviation (GMSD) (Xue et al., 2014)	2014	Computes the pixel-wise similarity between the gradient magnitude maps of the reference and distorted images to create a Local Quality Map (LQM) of the distorted image. $$GMSD = \sqrt{\frac{1}{N}\sum_{i=1}^{N}(GMS(i) - GMSM)^2} \quad (2.13)$$ where N represents the total number of pixels in the image and $$GMS\ (i) = \frac{2m_r(i)m_t(i)+c}{m_r^2(i)+m_t^2(i)+c} \quad (2.14)$$

No	IQA Algorithm	Year	Description
			where $m_r(i)$ and $m_t(i)$ denotes the gradient magnitude of the reference and distorted images. And $GMSM = \frac{1}{N}\sum_{i=1}^{N} GMS(i)$ (2.15)

Table 2.2: Image Databases

Database	Year	Website Link	No. of Reference Images	No. of Distorted Images	No. of Distortion Types	Type of Image	No. of Subjects
TID2013	2013	http://www.ponomarenko.info/tid2013.htm	25	3000	24	Colour	971
TID2008	2008	http://www.ponomarenko.info/tid2008.htm	25	1700	17	Colour	838
CSIQ	2010	https://computervisiononline.com/dataset/1105138666	30	866	6	Colour	35
LIVE	2006	http://live.ece.utexas.edu/research/quality/subjective.htm	29	779	5	Colour	161
IVC	2005	http://ivc.univ-nantes.fr/en/databases/IRCCyN_IVC_Toyama_LCD/	10	185	4	Colour	15
MICT	2008	http://mict.eng.u-toyama.ac.jp/mictdb.html	14	168	2	Colour	16
WIQ	2009	https://computervisiononline.com/dataset/1105138665	7	80	5	Gray	60
A57	2007	http://vision.eng.shizuoka.ac.jp/A57/a57_db.zip	3	54	6	Gray	7
LIVE In the Wild	2016	http://live.ece.utexas.edu/research/ChallengeDB/index.html	1169	1169	-	Colour	175

Database	Year	Website Link	No. of Reference Images	No. of Distorted Images	No. of Distortion Types	Type of Image	No. of Subjects
KonIQ-10K	2014	http://database.mmsp-kn.de/koniq-10k-database.html	10073	10073	-	Colour	120
MRI	2016	https://www.sciencedirect.com/science/article/abs/pii/S0730725X1600028X	25	750	6	MRI	28
SUID	2020	https://ieee-dataport.org/open-access/suid-synthetic-underwater-image-dataset#files	30	900	4	Underwater	50

2.2 No Reference Image Quality Assessment (NR-IQA)

NR-IQA is an objective assessment which automatically predicts the subjective quality of distorted images with respect to human perception without the information about the reference images. NR-IQA is the most suitable IQA metric in practical applications where the reference image is difficult to obtain or unavailable. Several NR-IQA algorithms have been developed by training Support Vector Machine (SVM) with natural images from LIVE database (H.R. Sheikh et al., 2006), namely Blind/Referenceless Image Spatial Quality Evaluator (BRISQUE) (Mittal et al., 2012), Blind Image Integrity Notator using DCT-Statistics (BLIINDS) (Saad, Bovik, & Charrier, 2012), Distortion Identification-based Image Verity and Integrity Evaluation (DIIVINE) (Moorthy & Bovik, 2011), Complex Extension of DIIVINE (C-DIIVINE) (Y. Zhang, Moorthy, Chandler, & Bovik, 2014), DIIVINE- Generalized Gaussian scale mixtures (GGSM) (Gupta, Moorthy, Soundararajan, & Bovik, 2018), Hierarchical Feature Degradation- Blind Image Quality Assessment (HFD-BIQA) (Wu, Zeng, Dong, Shi, & Lin, 2019) and ContourletQA (C. Li et al., 2021).

The DIIVINE metric is generated by modelling a set of neighbouring wavelet coefficients using the Gaussian scale mixture (GSM) model. The GSM model has been used to model the marginal and joint statistics of the wavelet coefficients of natural images. Next, statistical features were extracted from the distorted image using the steerable pyramid decomposition. The steerable pyramid decomposition was computed in two scales and six orientations and these forms 12 sub-bands. Eighty-eight (88) features were extracted from the natural images and the details of the features are shown in Table 2.2. Then, the extracted features and subjective scores of natural images in LIVE database were used to train SVM. The SVM model then predicts the quality score and the predicted score is the DIIVINE score (Moorthy & Bovik, 2011).

Table 2.3: Details of Features Extracted to Model DIIVINE Metric

Features	Description of the features	Computations
f_1-f_{12}	Variance of sub-band coefficients	Fitting a generalized Gaussian to sub-band coefficients
f_{13}-f_{24}	Shape parameter of sub-band coefficients	Fitting a generalized Gaussian to sub-band coefficients
f_{25}-f_{31}	Shape parameter across sub-band coefficients	Fitting a generalized Gaussian to orientation sub-band coefficients
f_{32}-f_{43}	Correlations across scales	Computing windowed structural correlation between filter response
f_{44}-f_{73}	Spatial correlation across sub-bands	Fitting a polynomial to the correlation function
f_{74}-f_{88}	Across orientation statistics	Computing windowed structural correlation between adjacent orientations at same scale

The BLIINDS metric is a fast single-stage framework that relies on a statistical model of local discrete cosine transform (DCT) coefficients. Firstly, 2-D DCT coefficient is computed from an image. This is performed by partitioning the image into equally sized *n x n* blocks, which is referred to as local image patches, then computing a local 2-D DCT on each of the blocks. Then, feature extraction is performed in the local frequency (DCT) domain from the 2D DCT coefficients computed previously. Twenty-four features were extracted over three scales. Then, the extracted features and subjective scores of natural images in LIVE database were used to train SVM. The SVM model then predicts the quality score and the predicted score is the BLIINDS score (Saad et al., 2012). BLIINDS metric is better than DIIVINE metric as DIIVINE uses a dense complex representation of images in the wavelet domain and extracts a large number of features to train the algorithm compared to BLIINDS (Saad et al., 2012). However, it requires nonlinear sorting of block based NSS features, which slows it considerably. Moreover, the image has to be transformed to DCT domain as well. Therefore, BRISQUE metric has been introduced.

The BRISQUE model used a spatial approach. First, a locally normalized luminance, also known as Mean Subtracted Contrast Normalized (MSCN) is computed. The MSCN coefficients were then fitted to Generalized Gaussian Distribution (GGD) and Asymmetric Generalized Gaussian Distribution (AGGD). There are two parameters computed for the GGD where α represents the shape of the distribution and σ^2 represents the variance. While, four parameters were computed for AGGD, namely υ which represents the shape of the distribution, σ_l^2 and σ_r^2 which represent the left- and right-scale parameters, respectively, and η. The four parameters of AGGD: $\eta, v, \sigma_l^2, \sigma_r^2$ are calculated along four orientations of the neighbourhood pixels of LIVE images. In total, 18 parameters of GGD and AGGD where 2 parameters of GGD and 16 parameters of AGGD were computed for LIVE images. The 18 features are explained in Table 2.4. The 18 parameters were then computed at two scales and this forms 36 parameters which represents the features of LIVE images. These 36 features and subjective scores of LIVE images are used to train the SVR. The SVM model then predicts the quality score and the predicted score is the BRISQUE score (Mittal et al., 2012).

Table 2.4: Explanation of 18 parameters

Features	Description	Computation Procedures
$f_1 - f_2$	α and σ^2	Fit GGD to MSCN coefficients
$f_3 - f_6$	υ, η, σ_l^2 and σ_r^2	Fit AGGD to horizontal (H) pairwise products
$f_7 - f_{10}$	υ, η, σ_l^2 and σ_r^2	Fit AGGD to vertical (V) pairwise products
$f_{11} - f_{14}$	υ, η, σ_l^2 and σ_r^2	Fit AGGD to diagonal (D_1) pairwise products
$f_{15} - f_{18}$	υ, η, σ_l^2 and σ_r^2	Fit AGGD to diagonal (D_2 pairwise products

The C-DIIVINE is the extension of DIIVINE metric which blindly assesses image quality based on the complex Gaussian scale mixture model corresponding to the complex version of the steerable pyramid wavelet transform. Three distribution models were used to fit the statistics of the wavelet coefficients: (1) the complex Generalized Gaussian distribution is used to model the wavelet coefficient magnitudes, (2) the Generalized Gaussian distribution is used to model the coefficients' relative magnitudes, and (3) the wrapped Cauchy distribution is used to model the coefficients' relative phases. All these distributions have characteristic shapes that are consistent across different natural images but change significantly in the presence of distortions. Complex wavelet structural similarity index was used to measure degradation of the correlations across image scales, which serves as an important indicator of the sub-bands' energy distribution and the loss of alignment of local spectral components contributing to image structure. The complex steerable pyramid decomposition was computed in six orientations over 3 scales and this forms 18 sub-bands in total. Three types of features, namely magnitude based features, phase based features and across-scale correlation features were extracted from LIVE images. These features and subjective scores of LIVE images are used to train the SVR. The SVM model then predicts the quality score and the predicted score is the C-DIIVINE score (Y. Zhang et al., 2014). Although, the performance of C-DIIVINE is slightly better than BRISQUE, C-DIIVINE runs slower than BRISQUE. This is mainly because of the divisive normalization, a relatively time- consuming process required for computing the magnitude-based features (Y. Zhang et al., 2014).

The GGSM-DIIVINE is a statistical model proposed for the image wavelet coefficients by generalizing the Gaussian Scale Mixtures (GSM) model for natural images. The GGSM model is suitable for the wavelet coefficients of both natural and distorted images. The Kotz-type distribution, a multivariate elliptical distribution, where zero mean zero-mean Multivariate Generalized Gaussian (MVGG) were incorporated into the GGSM model. Both the GSM and the GGSM represent infinite (scale) mixtures of Multivariate Gaussian and MVGG vectors, respectively. An iterative approach to estimate the normalizer were used, while matching the statistics of the normalized coefficients to that of the underlying MVGG distribution. Next, the 88 statistical features of DIIVINE were extracted in the wavelet domain after divisive normalization under the GGSM model (Gupta et al., 2018). The performance of the GGSM-DIIVINE were compared with BRISQUE using LIVE database and the result shows that BRISQUE outperforms the GGSM-DIIVINE metric.

The CounterletQA is a new NR-IQA model that operates on natural scene statistics in the contourlet domain. Before applying the contourlet transform, two preprocessing steps are performed to create more information-dense, low-entropy representations. Firstly, the image is converted into the CIELAB color space and gradient magnitude map. Then, 80 'quality-aware' features were computed in the contourlet transform domain: the energy of the sub-band coefficients within scales, and the energy differences between scales, as well as measurements of the statistical relationships of pixels across scales. The 80 features are described in Table 2.5. These features were then fed to SVR model which learns to predict image quality (C. Li et al., 2021). The performance of the CounterletQA were compared with GGSM-DIIVINE and BRISQUE using LIVE database and the result shows that CounterletQA outperforms the GGSM-DIIVINE metric. However, the features extraction computation for CounterletQA takes more time compared to BRISQUE as only 36 features are extracted from the image for BRISQUE while 80 features are extracted for CounterletQA.

Table 2.5: Explanation of 80 'quality aware' features (C. Li et al., 2021)

Features	Description	Computation Procedures
$f_1 - f_{24}$	Energy within scales	Sub-band image coefficients by contourlet transform
$f_{25} - f_{48}$	Energy differences across scales	Compute the energy differences across scales along 8 orientations
$f_{49} - f_{80}$	Neighboring Energy Statistics across scales	Fit GGD to neighboring pairs, R1 and R5 after

Features	Description	Computation Procedures
		merging all orientations at the second and third scales

On the other hand, there several researchers have proposed Convolution Neural Network (CNN) based NR-IQA metric such as Deep Neural Network IQA (deepIQA) and Deep Bilinear Convolution Neural Network (DB-CNN). deepIQA is trained end to-end and involves 10 convolutional layers, 5 pooling layers for feature extraction and 2 fully connected layers for regression (Bosse, Maniry, Müller, Wiegand, & Samek, 2018) while DB-CNN is trained by two sets of features namely, CNN for synthetic distortions (S-CNN) and VGG-16, that are bi-linearly pooled to predict the quality of the image (W. Zhang, Ma, Yan, Deng, & Wang, 2018). However, CNN based NR-IQA model requires a very large training database as limited number of labelled training data often leads to overfitting problem in CNN (W. Zhang et al., 2018).

CHAPTER 3: APPLICATION OF IMAGE QUALITY ASSESSMENT MODULE TO MOTION-BLURRED WOOD IMAGES FOR WOOD SPECIES IDENTIFICATION SYSTEM

3.1 Introduction

The objective of this chapter is to classify tropical wood species based on motion-blurred wood texture images. Despite tighter conservation regulations, demand for timber products has continued to increase due to growing population. Normally, experts identify the wood species based on the pattern of the wood surface texture. However, manual inspection on wood texture is tedious, time-consuming, impractical and cost-ineffective for a human to analyze a large number of timber species. Therefore, a reliable automatic wood recognition system is needed in order to classify the wood species efficiently. The proposed system includes image acquisition, image quality assessment module (IQA), image deblurring, feature extraction and classification. In this research, the wood images are motion-blurred due to imperfections in the imaging and capturing process. Hence, an IQA module is proposed to monitor the quality of images before proceeding to the next stage which is the feature extraction process. The IQA module will determine whether the image has to undergo the image deblurring process based on the image quality value. If the image is of low quality based on the image quality value obtained, then the image will be deblurred before the feature extraction procedure. A reliable motion deblurring technique, which is based on Lucy–Richardson algorithm, is employed to enhance the motion-blurred images before proceeding to the next stage, which is the feature extraction process. Then, a statistical feature extraction technique is proposed to extract 24 features from each wood image. Finally, a support vector machine is used to classify the 20 tropical wood species. This chapter also proves the important of IQA module to increase the rate of wood species recognition or identification system.

3.2 Background of the Study

Increasing forestry to supply more timber is a long-term commitment and as such must be well planned and the forests well managed in order to maximize their broad and far-reaching benefits. Nowadays, the machine vision and image processing industries are vast, ever-expanding and on the cutting edge of technology. Researches on wood based on image analysis have been implemented in various applications, such as wood species classification systems (Bremananth R. ; Nithya B. ; Saipriya R., 2009; Esteban et al., 2017; Ibrahim et al., 2017; Yusof et al., 2013; Zamri et al., 2018), wood defect classification (Gu, Andersson, & Vicen, 2010), health assessment of tree trunk (Qin et al., 2018), determining the influence of bark on the mapping of mechanical strain (Dahle 2017), hyperspectral mapping of wood to determine fit-for-purpose usage (Defoirdt et al., 2017), strain measurement on a tree subjected to mechanical load (Sebera et al. 2014), wood fingerprint recognition (Pahlberg et al. 2015) and automatic bark detection (Denzler et al. 2013).

The features and characteristics of timbers vary widely, which makes classifying wood species an important practical problem in timber industry. In order to manage timber resources efficiently, the supervisory agencies have to verify the correct timber species traded by the timber industry. The inspection of wood species is vital for timber-exporting countries to curb fraudulent labeling of timber species at custom checkpoints. Hence, a reliable wood species recognition system based on image analysis is crucial in order to perform wood inspection process at custom checkpoints to ease the timber trading verification process. In order to perform the image recognition tasks, good quality of wood images is important. A low-quality image may cause misclassification of wood species. In previous works (Bremananth R. ; Nithya B. ; Saipriya R., 2009; Esteban et al., 2017; Ibrahim et al., 2017; Yusof et al., 2013; Zamri et al., 2018), the quality of wood images was not assessed before the preprocessing and recognition stage. This means that some of the images may be enhanced even though they were already of good quality. In this case, the enhancement or deblurring is redundant and contributes to additional computational process. If the images were assessed beforehand, images with low quality could be identified, and corrective actions could be taken to obtain higher-quality images to be used for recognition tasks. Therefore, an image quality assessment (IQA) module is proposed in this research to assess the quality of wood images captured in order to aid the classification process. If the initial image obtained is of low quality, the IQA module will direct the image to undergo the image deblurring process before proceeding to the feature extraction stage.

When an image is captured in low-light conditions or of a fast moving object, motion blur can cause significant degradation of the image. This is caused by the movement of the object relative to the sensor in the camera during the time the shutter is open. Both the object moving and camera shake contribute to this blurring. There are several techniques that can be used to remove motion blur that can be split roughly into the following categories: (1) hardware in the optical system of the camera to stabilize the image, (2) preprocessing of the image to remove motion blur by estimating the camera's motion and (3) a hybrid approach that measures the camera's motion during image capture. Motion-blurred wood images may cause the wood features to be degraded. Image of wood samples must be at acceptable quality before recognition can be done, to avoid misclassifications. Thus, the image is evaluated using IQA module first, and if the quality score generated from the IQA module shows the image is of low quality, then the image will be deblurred. Hence, this study proposed the implementation of motion deblurring technique on wood images to enhance the feature representation of the wood texture images to aid the classification process effectively.

In previous works, the wood images are preprocessed using homomorphic filters (Bremananth R. ; Nithya B. ; Saipriya R., 2009; Esteban et al., 2017; Ibrahim et al., 2017; Yusof et al., 2013; Zamri et al., 2018). Homomorphic filtering utilizes a linear filter to do a nonlinear mapping to a different domain. The algorithm of homomorphic filtering is explained in more detail in Woods and Gonzalez (2008). However, homomorphic filtering technique does not work well on motion-blurred images. Unlike previous works by (Bremananth R. ; Nithya B. ; Saipriya R., 2009; Esteban et al., 2017; Ibrahim et al., 2017; Yusof et al., 2013; Zamri et al., 2018), this research focuses on classifying tropical wood species based on motion-blurred wood texture images. Therefore, a more reliable denoising technique which is based on Lucy–Richardson (LR) algorithm is proposed to overcome the limitation of previous works and improve the image representation of the wood texture. Lucy–Richardson algorithm has been shown to be effective in enhancing motion-blurred images in various applications such as in satellite image restoration (Aouinti, Nasri, Moussaoui, & Bouali, 2018), animal PET imaging (Angelis, Gillam, Kyme, Fulton, & Meikle, 2018), thyroid cancer treatment (Barrack, Scuffham, & McQuaid, 2018) and inversion of light scattering data (Buccini, Donatelli, & Ferri, 2018). Generally, an automated wood species recognition system is comprised of four basic modules which are image acquisition, image preprocessing, feature extraction and classification. To the best of the authors' knowledge, previous works on automated wood species recognition system only focused on classifying wood species based on non-motion-blurred images and do not employ any IQA module to access the quality of the input wood images. Hence, this research focuses on applying IQA module to access the quality of input images before feature extraction and analyzing wood texture images for classification of tropical wood species.

3.3 Methodology

This section explains the image acquisition of the wood surface texture. This section also describes the image quality assessment (IQA) module which is proposed in this research to evaluate the quality of wood images before transferring the image to the next process, which is the feature extraction process. Image deblurring using the Lucy–Richardson technique will be also explained in this section.

3.3.1 Image Acquisition

The first step in the proposed wood species recognition system is the image acquisition of the wood surface texture. One of the characteristics that remains unique to each wood species even after undergoing the chemical procedures is the surface texture. The wood samples were in cubic form (approximately 25.4 mm by 25.4 mm in size). The treatment of the wood samples was done by sanding the wood surfaces. This research was performed on 20 tropical wood species. A specially designed portable camera was used to capture wood surface images at 10X magnification. The portable camera is suitable for on-field testing thanks to its portability and embedded white LED lights to ensure controlled environment. The camera is equipped with a systematic focusing function, whereby the distance between the camera and the wood sample is fixed to 10 cm. The housing of the camera is made of a tube based on theoretical optimal object distance, and hence, the object is just required to be laid against the camera housing. The “tube function” is made in opaque material in order to cut all ambient light and its fluctuations. The size of each image is 768 × 576 pixels. The wood images were obtained from Forest

Research Institute Malaysia (FRIM). Figure 3.1 shows the sample of 10 tropical wood species used in this study.

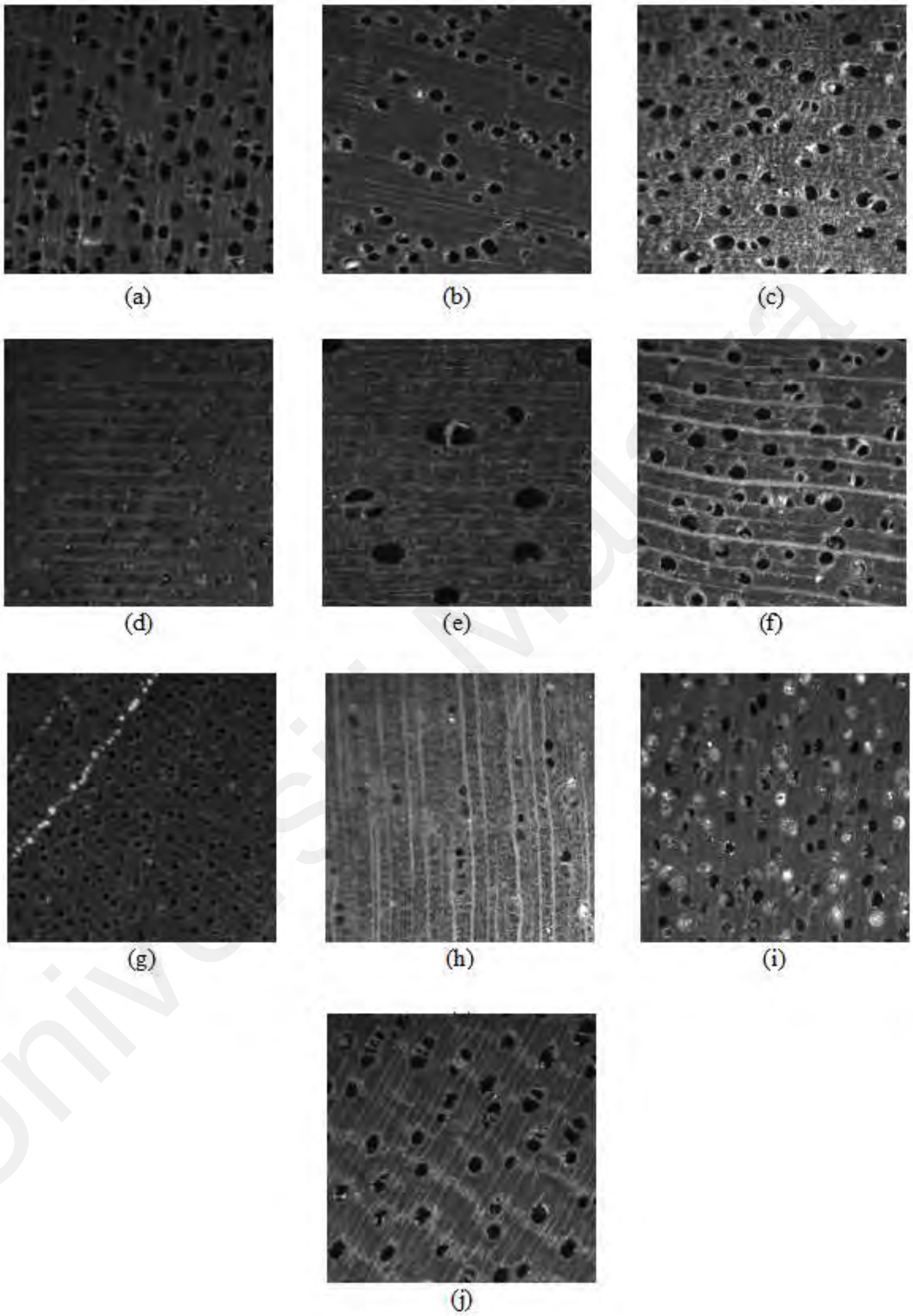

Figure 3.1: Ten Reference Wood Images: a) Balau, b) Bintangor, c) Bitis, d) Chengal, e) Durian, f) Gerutu, g) Giam, h) Jelutong, i) Kapur, j) Kekatong

3.3.2 The proposed image quality assessment (IQA) module

An image quality assessment (IQA) module is proposed in this research to evaluate the quality of wood images before transferring the image to the next process, which is the feature extraction process. There are five full reference image quality analysis (FR-IQA) metrics employed as the IQA module in this research, which are Structural Similarity Index (SSIM) (Zhou Wang et al., 2003), Multiscale SSIM (MS-SSIM) (Zhou Wang et al., 2003), Feature SIMilarity (FSIM) (L. Zhang et al., 2011), Information Weighted SSIM (IW-SSIM) (Zhou Wang & Li, 2011) and Gradient Magnitude Similarity Deviation (GMSD) (Xue et al., 2014). These FR-IQA metrics were explained in Section 2.1.

The threshold for the IQA module is 0.9 for MSSIM, SSIM, FSIM and IWSSIM, while threshold is 0.1 for GMSD. If the initial image obtained is of low quality (below 0.9 for MSSIM, SSIM, FSIM and IWSSIM and above 0.1 for GMSD), the IQA module will direct the image to undergo the image deblurring process before proceeding to the feature extraction stage. If the initial image is of good quality (above 0.9 for MSSIM, SSIM, FSIM and IWSSIM and below 0.1 for GMSD), then the image will directly proceed to the feature extraction process. The flowchart of the proposed IQA module is presented in Figure 3.2.

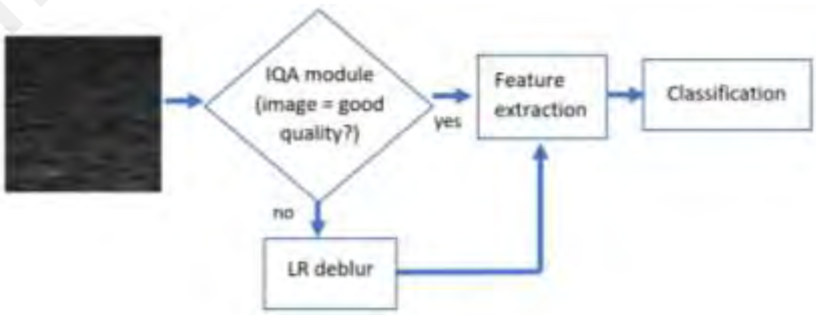

Figure 3.2: Flowchart of the proposed IQA module in wood species recognition system

3.3.3 Image Deblurring

Due to imperfections in the imaging and capturing process, the recorded image invariably represents a degraded version of the original scene. These images obtained lower MSSIM, SSIM, FSIM and IWSSIM and higher GMSD scores due to the low quality of the image. The degradation results in image blur, affecting identification and extraction of the useful information in the images. It can be caused by relative motion between the camera and the original scene or by optical aberration. Lucy–Richardson (LR) algorithm is an iterative image restoration technique. LR algorithm is developed based on Bayesian framework by maximizing the likelihood probability function iteratively as follows (Abang, Ramli, & Halim, 2018)

$$p(F|G) = p(G|F)\frac{p(F)}{p(G)} \tag{3.1}$$

where $p(G|F)$ is the likelihood probability, $p(F|G)$ is the posterior probability, $p(F)$is a model of the original image, and $p(G)$ is a model of the degraded image. The example of motion-blurred image and deblurred image using Lucy Richardson technique is shown in Figure 3.3.

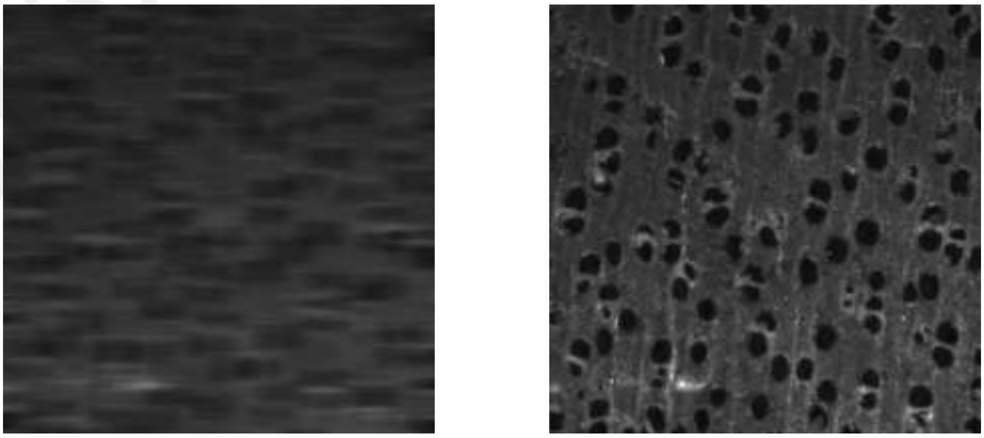

(a) (b)

Figure 3.3: Wood sample of species Shorea laevis (a) motion-blurred image, (b) de-blurred image using LR technique

3.3.4 Feature Extraction

The most important step in texture classification is the feature extraction stage where the challenge is to represent textures mathematically and accurately. The most significant features used by experts to identify the wood species are the pore appearances. This is because pores are exclusive for every species. Therefore, this research will focus on size of pores, quantity of pores, types of pores and arrangement of pores on the wood texture. Basically, the statistical feature extraction process consists of two steps, namely pore extraction and fuzzy pore management as shown in Figure 3.4. The statistical features will only allow distinct pores to be acknowledged as characteristics of a wood species. Then, a support vector machine (SVM) classifier is used to classify the wood species based on the statistical wood features.

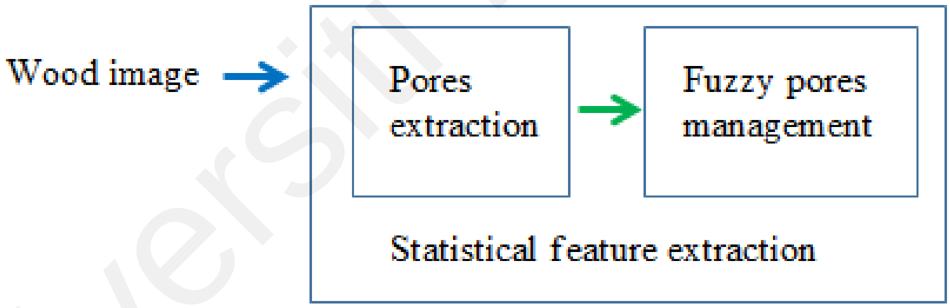

Figure 3.4: The flowchart of the statistical feature extraction process (Zamri et al., 2018)

In the statistical feature extraction process, the area of a region is detected and measured by pixels, which means the number of pixels inside a region was used to represent the area of region. The components in an image are classified to convert a binary image into a label matrix to compute region descriptors. The binary images are created by using the default binarization based on Otsu's method for optimal threshold selection. A threshold filter displays each pixel of an image in only one of the two states, black or white. That state is set according to a particular threshold value. If the pixel's brightness is greater than the threshold, the pixel is colored white, if less, then black. This thresholding technique stores the intensities of the pixels in an array. The threshold is calculated by using total mean and variance. Based on this threshold value, each pixel is set to either 0 or 1. The pore extraction process extracted the statistical properties of pores from both binary images for each wood image. The second step in the proposed statistical feature extraction is the fuzzy management process. Fuzzy if-else rules are employed to categorize the pores from both binary images into several features such as sizes of pores, types of pores and pore arrangements. The total number of statistical features extracted from each wood image is 24 features. The extracted features are 12 features from black pore image and 12 features from white pore image. The 12 features extracted from each binary image are quantity of small vessels, medium vessels, large vessels, solitary vessels, pair vessels and multiple vessels, and vessel arrangements between small vessel with small vessel, medium vessel with medium vessel, large vessel with large vessel, small vessel with medium vessel, small vessel with large vessel and medium vessel with large vessel. The detail algorithm on the proposed statistical feature extraction technique is explained in (Zamri et al., 2018). The next step after feature extraction is the classification process, where the wood species are classified into its own species based on the statistical features.

3.3.5 Classification

Classifying data is the key to determine the features or characteristics of its desired group. This is performed by training a classifier model that works by analyzing features and assigning each sample to a certain class (Iglesias, Anjos, Martínez, Pereira, & Taboada, 2015) . Support vector machine (SVM) is a useful tool as a learning algorithm in analyzing and recognizing data. In SVM, the input training data are mapped into a high dimensional space using radial basis function kernel (RBF), where the optimal hyperplane is determined (Chang, Chih-Chung and Lin, 2011). SVM classifier has been widely used in solving various problems, such as solid waste level classification (Aziz et al., 2018), moisture content recognition for wood chips (Daassi-Gnaba et al., 2018), wood defect classification (Gu et al., 2010) and image analyses on beef tenderness forecasting (Konda Naganathan et al., 2016). The classification process was performed by using LIBSVM toolbox implemented in MATLAB. The optimum value of penalty parameter of the error term, C and kernel parameter, gamma (γ), was obtained by using grid search method using the training data. The algorithm of LIBSVM is explained in more detail in (Chih-Wei Hsu, Chih-Chung Chang, 2016). Cross-validation and grid search were applied to find the satisfactory parameters for RBF kernel.

3.4 Results and Discussions

There are a total of 1400 wood images used in this research, which were obtained from 20 tropical wood species. The experiments were done in two phases: training phase and testing phase. For each wood species, 70 images were captured, where 40 images were used as training database, while 30 images were used as testing images to evaluate the performance of the proposed system. Several experiments were performed to evaluate the performance of the proposed system: (1) image quality assessment for motion-blurred images, (2) image quality assessment for deblurred images and (3) classification of wood species.

3.4.1 Image quality assessment for motion-blurred images

Figure 3.5 shows the average of image quality values for 20 wood species based on motion-blurred images. There are five different IQA techniques employed in this research to evaluate the quality of wood images such as MSSIM, SSIM, FSIM, IWSSIM and GMSD for comparison purposes.

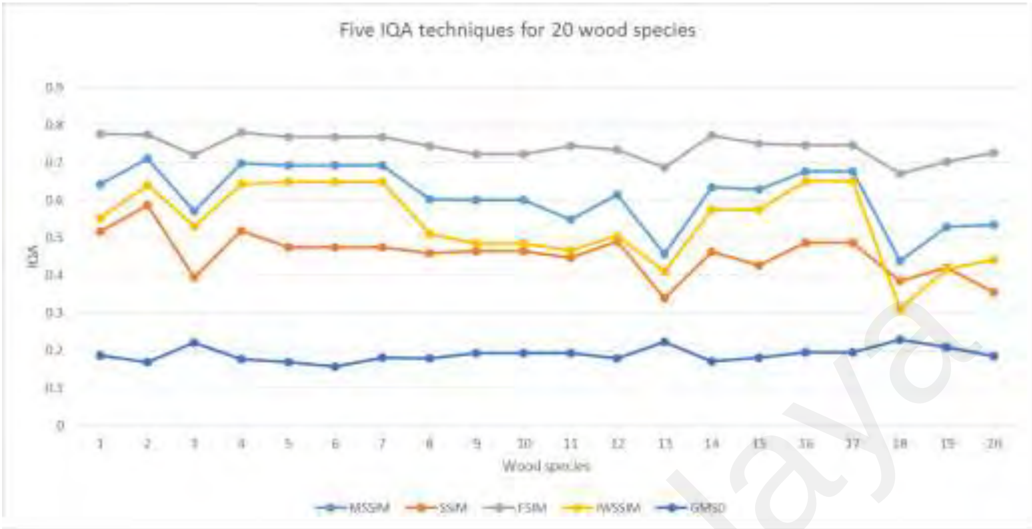

Figure 3.5: The average of image quality values for motion-blurred images from 20 wood species by using five different IQA techniques.

Based on the results obtained, it can be seen that the value of image quality for blurred images is below 0.8 for all four IQA techniques (MSSIM, SSIM, FSIM, IWSSIM) and above 0.1 for GMSD. A good quality image will have IQA value nearing to 1.0 for MSSIM, SSIM, FSIM, IWSSIM while value nearing to 0 for GMSD. This means that the blurred image has low image quality. Hence, these low quality images will have to undergo the LR deblur process as presented in Figure 3.2 to improve the image quality before proceeding to the feature extraction process. Figure 3.6 shows the example of motion-blurred wood images used in this work and quality scores obtained from the IQA modules.

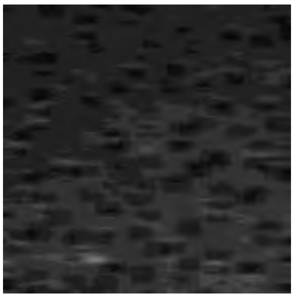

(a)
MSSIM: 0.626
SSIM: 0.497
FSIM: 0.764
IWSSIM: 0.540
GMSD: 0.179

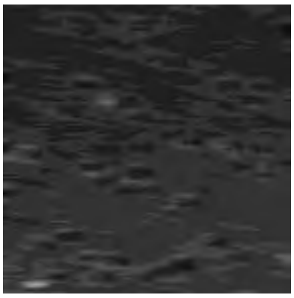

(b)
MSSIM: 0.707
SSIM: 0.574
FSIM: 0.760
IWSSIM: 0.622
GMSD: 0.160

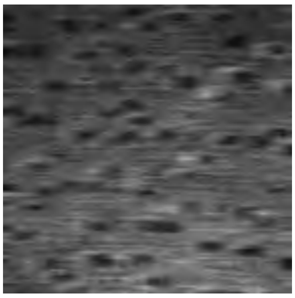

(c)
MSSIM: 0.567
SSIM: 0.385
FSIM: 0.713
IWSSIM: 0.516
GMSD: 0.211

(d)
MSSIM: 0.687
SSIM: 0.509
FSIM: 0.792
IWSSIM: 0.634
GMSD: 0.160

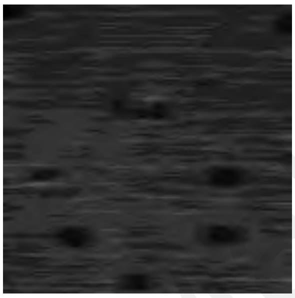

(e)
MSSIM: 0.693
SSIM: 0.475
FSIM: 0.769
IWSSIM: 0.649
GMSD: 0.173

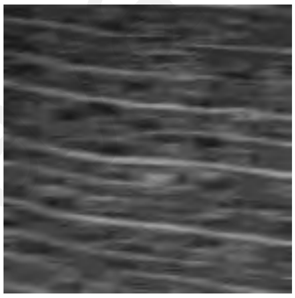

(f)
MSSIM: 0.733
SSIM: 0.529
FSIM: 0.772
IWSSIM: 0.703
GMSD: 0.181

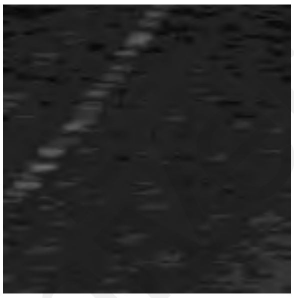

(g)
MSSIM: 0.603
SSIM: 0.458
FSIM: 0.745
IWSSIM: 0.511
GMSD: 0.178

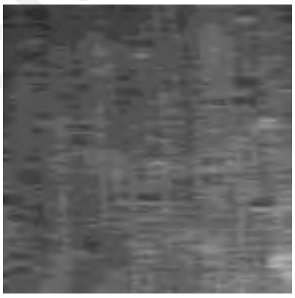

(h)
MSSIM: 0.476
SSIM: 0.410
FSIM: 0.687
IWSSIM: 0.353
GMSD: 0.223

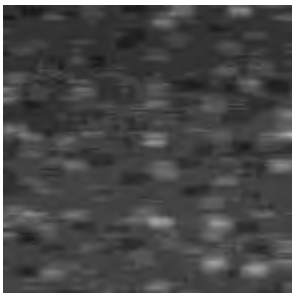

(i)
MSSIM: 0.602
SSIM: 0.466
FSIM: 0.723
IWSSIM: 0.486
GMSD: 0.194

Figure 3.6: Samples of motion-blurred wood images from wood species (a) Shorea laevis, (b) Calophyllum kunstleri, (c) Palaquium stellatum, (d) Neobalanocarpas heimii, (e) Durio spp, (f) Parashorea globose, (g) Hopea spp, (h) Dyera costulata, (i) Drybala

From Figure 3.6, it is found that all the blurred images have lower MSSIM, SSIM, FSIM, IWSSIM scores (lower than 0.8) and GMSD scores greater than 0.1. This also shows that the images are of lower quality. In addition, the features of the pores on the wood texture could not be distinctively differentiate, as a result of low value of image quality as tabulated in Figure 3.5. This will further contribute to the misclassification of the wood species since the feature extractor will not be able to extract distinctive features from the wood texture images effectively. Therefore, IQA module is useful in order to assess the quality of the images before the feature extraction process.

3.4.2 Image quality assessment for deblurred images

It is an important task to faithfully evaluate the perceptual quality of input images in many applications, such as image restoration. A good image quality assessment (IQA) model should deliver high quality prediction accuracy to aid the classification process. Figure 3.7 tabulates the average of image quality values for 20 wood species based on motion-deblurred images. Based on the results obtained, it can be seen that the value of image quality for deblurred images is above 0.9 for MSSIM, SSIM, FSIM, IWSSIM IQA techniques and below 0.1 for GMSD technique. This proves that the deblurrred images are of good quality since the IQA value nearing to 1.0 for MSSIM, SSIM, FSIM, IWSSIM while IQA value nearing to 0 for GMSD. Figure 3.8 shows the example of motion-deblurred wood images used in this work. The features of the pores on the wood texture could now be differentiate distinctively. This will further contribute to higher classification rate of the wood species since the feature extractor will be able to extract distinctive features from the wood texture images effectively.

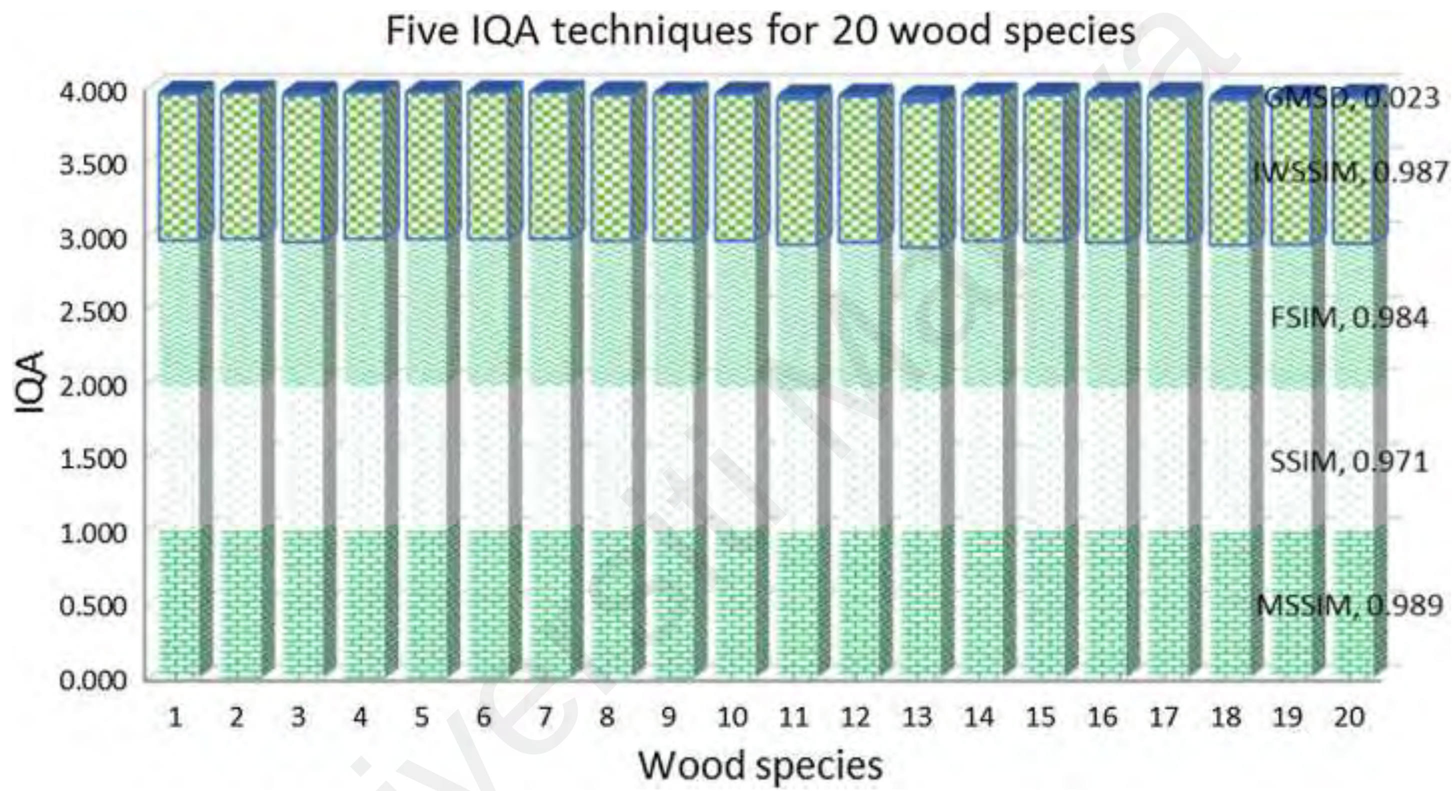

Figure 3.7: The average of image quality values for deblurred images from 20 wood species by using five different IQA techniques

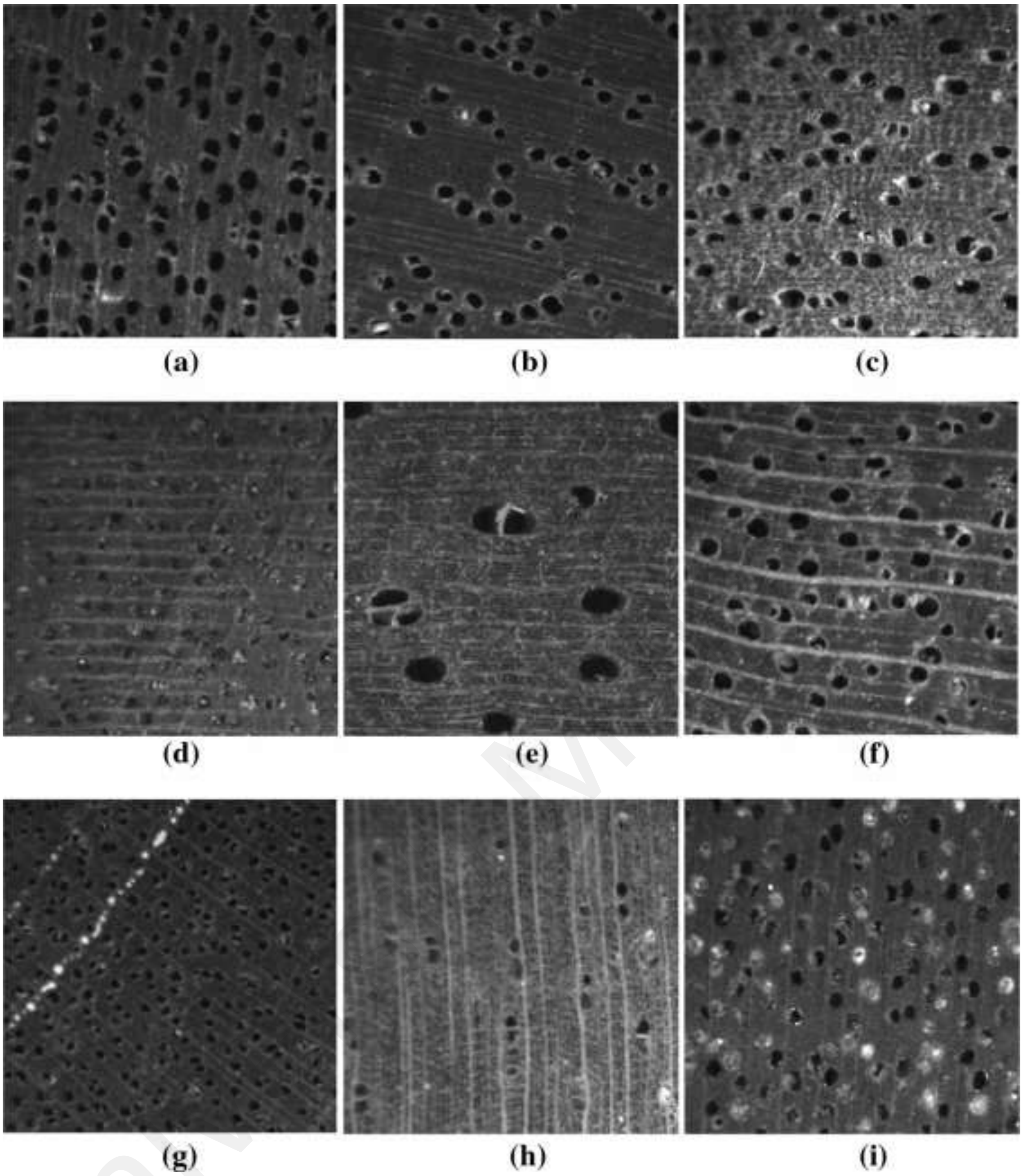

Figure 3.8: Samples of de-blurred wood images from wood species (a) Shorea laevis, (b) Calophyllum kunstleri, (c) Palaquium stellatum, (d) Neobalanocarpas heimii, (e) Durio spp, (f) Parashorea globose, (g) Hopea spp, (h) Dyera costulata, (i) Drybalanops aromatic.

3.4.3 Classification of wood species

This experiment was done to evaluate the capability of the proposed system to classify the test samples accurately based on the trained wood database. In order to examine the classification performance for each wood species, a confusion matrix is tabulated as shown in Table 3.1. The confusion matrix shows how the predictions are made by the proposed wood species recognition system. There were 30 test samples used for each wood species. As shown in Table 3.1, this study focused on classifying motion-blurred images by employing Lucy–Richardson algorithm to enhance the images and IQA module to assess the quality of images, which results in 89.3% classification accuracy for 20 wood species.

The proposed system is benchmarked with previous works as shown in Table 3.2. The previous works focused on enhancing the images by using homomorphic filtering technique, and none of the previous works implemented the IQA module in their system. Homomorphic filtering technique is one of the important ways used for digital images, especially when the input image suffers from poor illumination conditions. Albeit the accuracy of the system proposed by previous works was more than 90%, the accuracy dropped to 50% when the homomorphic filtering technique was employed on the current motion blurred wood database. Hence, the employment of a homomorphic filtering technique is inadequate when dealing with motion-blurred images since this technique only works well for enhancing details in blurry images and is sensitive to noise. This is because the homomorphic filtering method boosts high-frequency data of the images, and the noise which is part of that data will be increased as well (Woods and Gonzalez 2008).

This shows that the employment of IQA module and Lucy–Richardson algorithm in classifying motion-blurred wood images based on statistical features is more reliable compared to previous works. Finally, the proposed system is also tested on 30 test samples for each species using non motion-blurred images. Based on the results, it can be seen that the classification accuracy for non-motion-blurred images is higher by approximately 6% compared to classifying the motion-blurred images. For future works, a more efficient feature extraction approach and classification technique can be proposed to improve the performance of the proposed system.

Table 3.1: Confusion matrix of 30 wood species for 30 test samples for each species

Wood species	Correctly classified	Misclassified
Shorea laevis	26	4
Calophyllum kunstleri	27	3
Palaquium stellatum	28	2
Neobalanocarpas heimii	27	3
Durio spp	27	3
Parashorea globosa	26	4
Hopea spp	27	3
Dyera costulata	28	2
Drybalanops aromatic	26	4
Cynometra malaccensis	27	3
Madhuca utilis	26	4
Hevea brasiliensis	28	2
Pometia ridleyi	27	3
Artocarpus dadah	26	4
Dialum kingie	26	4
M. quadrifida	27	3
Kokoona sessilis	27	3
Dehaasia curtisii	28	2
Sp of lauraceacae	26	4
Pentace curtisii	26	4

Table 3.2: The comparison of classification accuracy and test samples used for testing between the proposed system and previous works

Previous works	Test samples are motion blurred ?	Image pre-processing technique	Classification accuracy (%)
GLCM feature extraction by Khalid et al. (2008)	No	Homomorphic filter	95.0 %
BGLAM feature extraction by Zamri et al. (2016)	No	Homomorphic filter	98.0%
BGLAM and statistical features by Yusof et al. 2013b	No	Homomorphic filter	93.0%
Statistical feature extraction by Ibrahim et al. (2018)	No	Homomorphic filter	89.3 %
The proposed system with IQA module	No	Lucy Richardson algorithm	95.0%

3.5 Chapter Conclusion

In conclusion, the image quality assessment (IQA) module has been adopted to measure the quality of the motion-blurred wood images before proceeding to the feature extraction process. If the wood image is of poor quality, the image will be enhanced by using Lucy–Richardson (LR) deblurring technique. The deblurred image will then be passed to the feature extraction stage and finally to the classification stage. The mean of IQA values for each wood species has been computed by using five different IQA approaches for comparison purposes. Then, the classification accuracy of the proposed system is computed based on the deblurred images. The results are also compared with previous works, which implemented homomorphic filtering. Based on the results obtained, the proposed IQA module and LR deblurring technique gives better performance in denoising the motion-blurred wood texture images.

CHAPTER 4: SUBJECTIVE AND OBJECTIVE ASSESSMENT ON WOOD IMAGES

4.1 Introduction

The objective of this chapter is to perform both subjective and objective assessment of Full Reference Image Quality Assessment (FR-IQA) for wood images. The wood images are distorted with two distortion types that may occur during image acquisition process. There is a total of 190 wood images which consists of 180 distorted images. The distorted images are derived from ten reference images by using two types of distortion which are Gaussian White Noise and Motion Blur. The wood images are evaluated by thirty human subjects, eleven staff from Tapak Semaian Mantin, Jabatan Perhutanan Negeri Sembilan, nineteen students and staff from Department of Electrical and Electronic Engineering, Manipal International University (MIU), Nilai. The subject ratings are converted to Mean Opinion Score (MOS).

This study also produces a set of MOS data related to these distorted wood images. The MOS values are compared with five FR-IQA metrics: Structural Similarity Index (SSIM) (Zhou Wang et al., 2003), Multiscale SSIM (MS-SSIM) (Zhou Wang et al., 2003), Feature SIMilarity (FSIM) (L. Zhang et al., 2011), Information Weighted SSIM (IW-SSIM) (Zhou Wang & Li, 2011) and Gradient Magnitude Similarity Deviation (GMSD) (Xue et al., 2014). These FR-IQAs were tested on several natural images database such as TID2008, CSIQ and LIVE and are suitable to evaluate images distorted with Gaussian White Noise and Motion Blur. We use Pearson Linear Correlation Coefficient (PLCC) and Root Mean Square Error (RMSE) to validate the correlation between MOS and all the five FR-IQA. High correlation is found between MOS and all the five FR-IQAs for all the two types of distortions.

4.2 Background of the Study

The demand for wood is increasing day by day where it is used for many purposes mainly for construction of building, paper, furniture, cooking utensils and sports equipment (Shivashankar, 2018). Every wood species has their unique physical properties such as knot, colour, structure and density which determines its usage and price (Barmpoutis et al., 2018; Funck et al., 2003; Longuetaud et al., 2012; Shivashankar, 2018; Zamri et al., 2018). For example, mahogany is used mainly for fine furniture crafting as it is a medium-dense hardwood. It is essential to choose the right wood for construction of building to ensure the safety and durability of the building. Therefore, selection of wood should be made carefully.

To rectify this issue, manufacturers have made efforts to appoint certified personnel to identify quality of wood via manual inspection (Gazo et al., 2018; Yusof et al., 2013). However, manual inspection takes longer time, hectic work and subjective (Gazo et al., 2018; Shivashankar, 2018). Hence, wood image processing such as wood slice recognition and wood texture analysis are performed to judge the physical properties and economic value of different wood species correctly (Guang-sheng & Peng, 2012; Pan & Kudo, 2011). In addition, wood slice recognition and wood texture analysis could detect wood species accurately and this could decrease the economic losses due to mislabeling of a good quality wood with a lower quality.

However, in order to perform these image processing and recognition tasks, good quality wood images are needed. A low-quality image may produce an inaccurate result from the wood slice recognition and texture analysis. However, it may not be possible to obtain a perfect image due to the dusty, high temperature and poor illumination environment in the timber factories (Ratnasinga et al., 2011). Therefore, a feedback system prior to image processing and recognition tasks must be implemented to avoid wood species misclassification. If the initial image obtained is of low quality, the feedback system will automatically inform the operator either to acquire a new image after taking the corrective action such as cleaning the camera lens, station and wood surface.

Prior studies on wood slice recognition based on image processing can be found in work of (Barmpoutis et al., 2018; Khalid et al., 2008; Venkatachalapathy & Sudhakar, 2014; Zamri et al., 2018). In Khalid et al., Venkatachalapathy & Sudhakar and Zamri et al., the wood images were enhanced before performing the recognition tasks in order to obtain clearer texture properties from the images. However, the wood images quality was not assessed before the pre-processing and recognition tasks. This means that some of the images may be enhanced even though they were already of good quality. In this case, the enhancement is redundant and contributes to additional computational process. Furthermore, enhancement process ignores the dynamical information of image channels (Barmpoutis et al., 2018). If the images were assessed beforehand, images with low quality could be identified, and corrective actions could be taken to obtain higher quality images to be used for recognition tasks. Hence, the recognition rate can be increased than the one obtained without quality assessment**.**

There are two types of image quality assessment (IQA) which are objective and subjective evaluations. Subjective evaluation is the scores given by human subjects based on their judgment on the image quality while objective assessment is a method defined mathematically to assess images (L.S. Chow et al., 2016). Subjective evaluation is often assumed as the benchmark or gold standard in the image quality assessment. However, subjective evaluation is not practical as it is time consuming. Therefore, objective assessment is used as an alternative to the subjective evaluation. The aim of the objective assessment is to be consistent and in close agreement with subjective evaluation (H.R. Sheikh et al., 2006). In this study, Full Reference Image Quality Analysis (FR-IQA) is chosen as an objective assessment to evaluate the wood images. FR-IQA evaluates an image by comparing the image with its reference image where the reference image has to be a distortion free image (Chandler, 2013; Gulame et al., 2013).

4.3 Methodology

This section explains the reference wood images chosen and the two types of image distortions applied to the reference wood images. The procedures involved in subjective evaluation and the processing of the subjective scores are explained in this section. This section also describes performance metrics used to evaluate the correlation between MOS values and all the five FR-IQA metrics for different types of distortions.

4.3.1 Reference Images

Ten wood images from ten wood species encountered in the lumber industry which are economically important, namely *Turraeanthus africanus* (Avodire), *Ochroma pyramidale* (Balsa), *Cordia spp.* (Bocote), *Juglans cinerea* (Butternut), *Tilia Americana* (Basswood), *Vouacapoua americana* (Brownheart), *Cornus florida* (Dogwood), *Cordia spp.* (Laurel Blanco), *Swartzia Cubensis* (Katalox), *and Dipterocarpus spp* (Keruing). The images were obtained from a public wood database: https://www.wood-database.com/ (Meier, 2007). The ten wood images are shown in Figure 4.1. The images were converted to grayscale and the pixel values were normalized to the range 0 - 255 for ease of applying the same levels of distortion across all the reference images. The images consisted of a matrix of 600 x 600 pixels, corresponding to resolution of 360000 and an image area of 9525 cm^2. The ten reference images are from ten different wood species and have varying grain and texture pattern and characteristics. The details of the reference images are shown in Table 4.1. These ten reference wood images were the distorted by Gaussian white noise and motion blur, which represent image distortions typically encountered in the industrial setting. Gaussian white noise often arises in during acquisition of wood images due to sensor noise (Rahman, Haque, Rozario, & Uddin, 2014) caused by poor illumination and high ambient temperature in the lumber mill (Ratnasinga et al., 2011). On the other hand, wood images are subjected to motion blur when there is a relative motion between the camera and the wood slice (Guang-sheng & Peng, 2012). The Gaussian white noise with standard deviation, σ_{GN} and motion blur with standard deviation, σ_{MB} were applied to the reference images at nine levels of distortion of the reference images, i.e.: σ_{GN} = 10, 20, 30, 40, 50, 60, 70, 80 and 90 for Gaussian white noise and σ_{MB} = 2, 4, 6, 8, 10, 12, 14, 16 and 18 for motion blur.

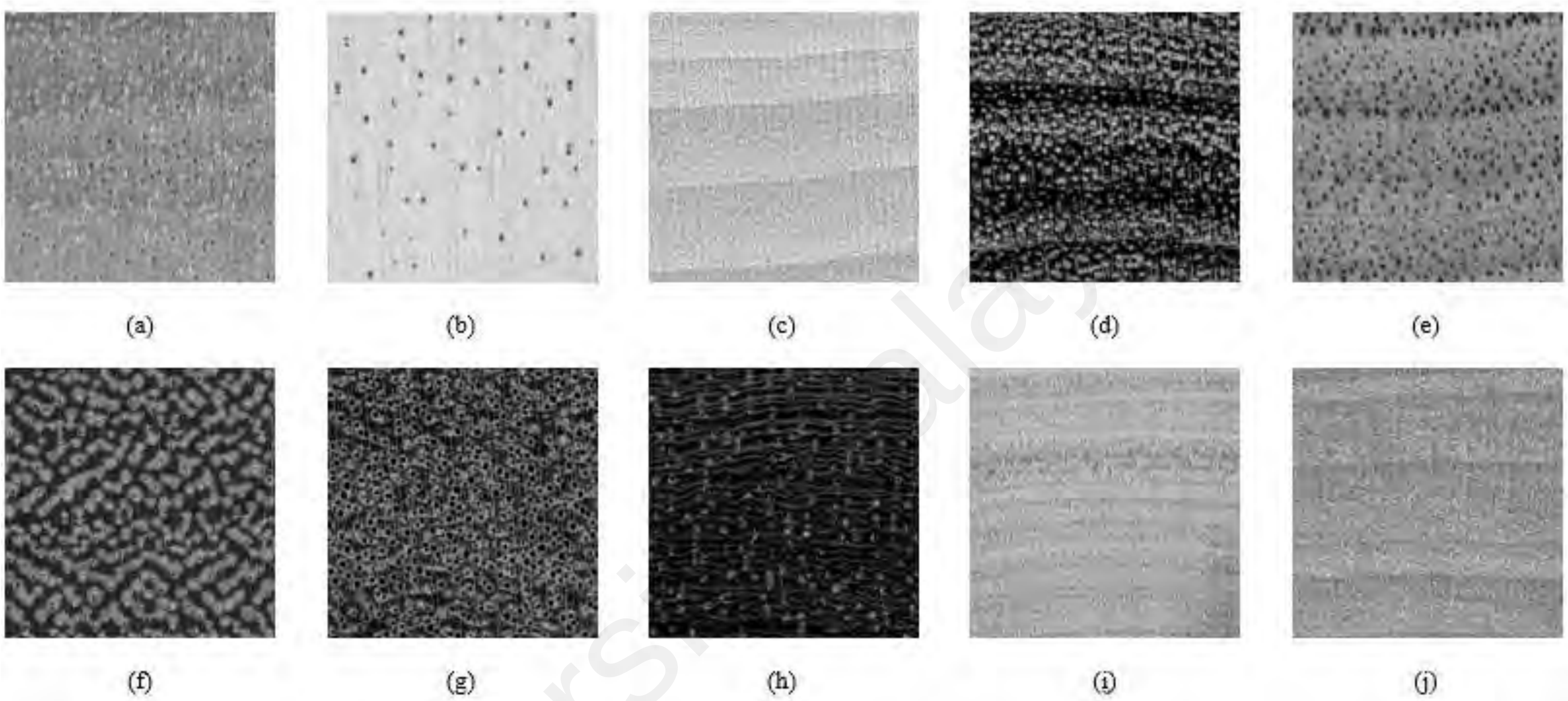

Figure 4.1: Ten reference wood images (a) *Turraeanthus africanus*, (b) *Ochroma pyramidale*, (c) *Tilia americana*, (d) *Cordia spp*., (e) *Juglans cinerea*, (f) *Vouacapoua americana*, (g) *Dipterocarpus spp*., (h) *Swartzia Cubensis*, (i) *Cordia spp*., (j) *Cornus florida*

Table 4.1: Details of Reference Images

No	Image	Wood Name	Colour	Intensity	Grain and Texture	Usage
1	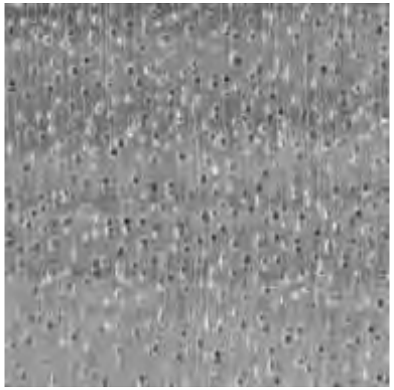	Turraeanthus africanus	Pale yellow or cream.	32-255	Grain can be straight, wavy, or irregular and interlocked. Texture is fine, with a high natural luster.	Veneer, cabinetry, furniture, millwork, and plywood.
2	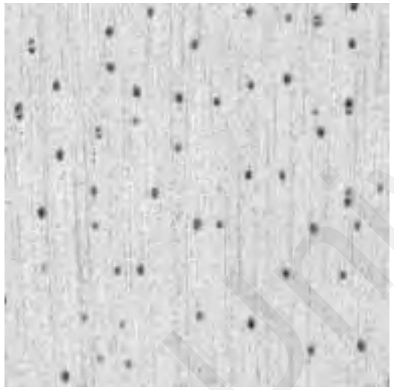	Ochroma pyramidale	White to off-white or tan color	50-255	Balsa has a straight grain with a medium to coarse texture and low natural luster.	Buoys, rafts, surfboards, model airplanes, musical instruments, packing/transport cases, core stock in sandwich laminations, and fishing lures.

No	Image	Wood Name	Colour	Intensity	Grain and Texture	Usage
3	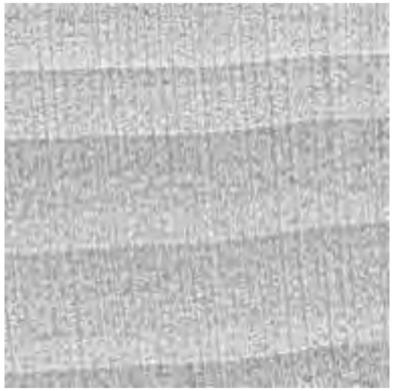	Tilia americana	Pale white to light brown color	126-255	Grain is straight, with a fine, even texture and moderate natural luster.	Carvings, lumber, musical instruments (electric guitar bodies), veneer, plywood, and wood pulp and fiber products
4	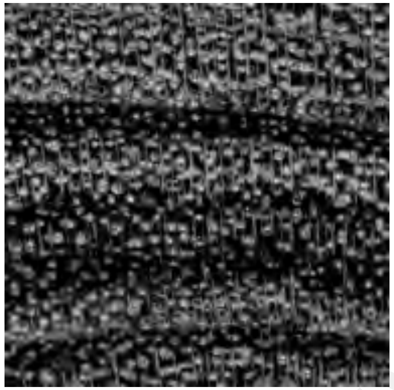	Cordia spp.	Yellowish brown body with dramatic dark brown to almost black stripes.	0-255	Grain is interlocked. Medium uniform texture. Good natural luster.	Fine furniture, cabinetry, flooring, veneer, boatbuilding, musical instruments, gunstocks, turned objects, and other small specialty wood items

No	Image	Wood Name	Colour	Intensity	Grain and Texture	Usage
5	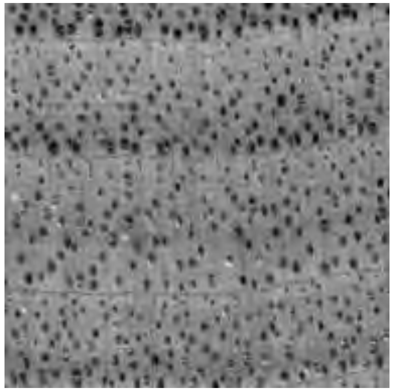	Juglans cinerea	Light to medium tan with a reddish tint.	8-255	Grain is typically straight, with a medium to coarse texture. Silky natural luster.	Veneer, carving, furniture, interior trim, boxes, and crates
6	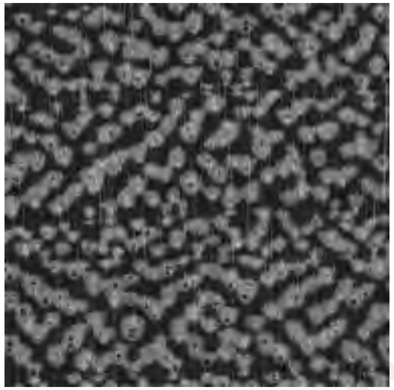	Vouacapoua americana	Medium to dark brown with a reddish hue.	8-255	Grain is straight to slightly irregular, with a uniform medium texture and moderate natural luster	Flooring, heavy construction, turned objects, furniture, and cabinetry

No	Image	Wood Name	Colour	Intensity	Grain and Texture	Usage
7	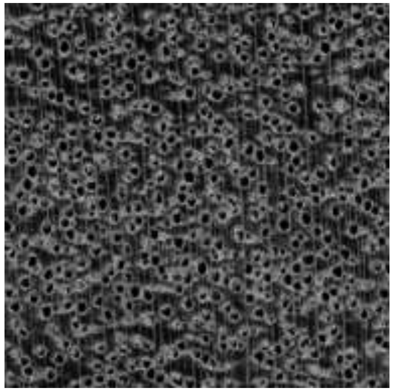	Dipterocarpus spp.	Light to medium yellowish brown to a darker reddish brown.	0-255	Grain is generally straight to slightly interlocked. Medium to coarse texture and moderate natural luster	Furniture, flooring, trailer decks, and utility lumber
8	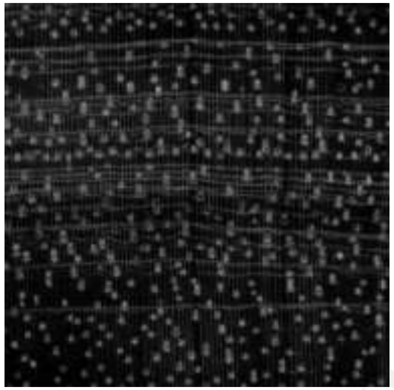	Swartzia Cubensis	Medium reddish brown to purplish black, with darker contrasting stripes.	0-255	The grain is usually straight, but can also be irregular or interlocked. With a fine even texture and good natural luster	Inlays, fine furniture and cabinetry, parquet flooring, turnings, and other small specialty items

No	Image	Wood Name	Colour	Intensity	Grain and Texture	Usage
9	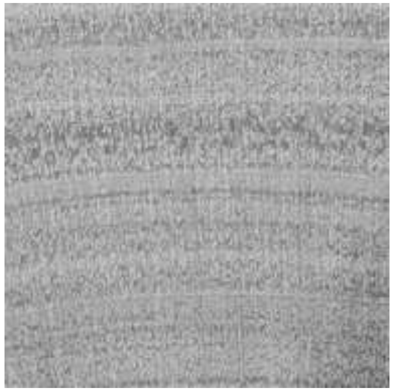	Cordia spp.	Light yellowish to medium brown, with darker streaks.	54-255	Grain is straight to shallowly interlocked. Texture can vary from fine to coarse. Good natural luster	Veneer, furniture, turned objects, cabinetry, boatbuilding, and millwork
10	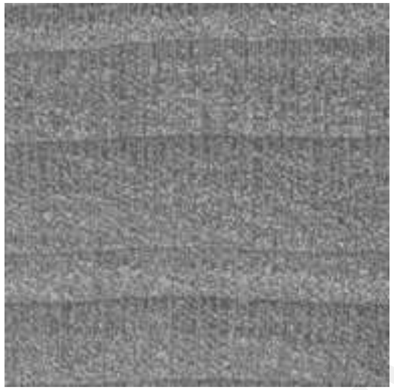	Cornus florida	Reddish brown.	70-255	Grain is interlocked, with a fine, uniform texture. Moderate natural luster.	Golf club heads, textile shuttles, bows (archery), mallets, pulleys, and turned objects

4.3.2 Types of Image Distortion

The ten reference images were distorted using two types of distortions each at nice different levels as summarized in Table 4.2. The Gaussian white noise with standard deviation, σ_{GN} and motion blur with standard deviation, σ_{MB} were applied to the reference images. The distortion level is determined by the standard deviation where higher standard deviation produces higher distortion.

Table 4.2: Summary of all types of distortions applied to the reference wood images.

Distortion type	Description	Distortion levels
Gaussian White Noise	Gaussian White Noise distribution with standard deviation, σ_{GN}.	σ_{GN}: 10, 20, 30, 40, 50, 60, 70, 80 and 90
Motion Blur	Applies linear motion of a camera with the length of the motion, σ_{MB}.	σ_{MB} = 2, 4, 6, 8, 10, 12, 14, 16 and 18

Gaussian white noise and motion blur were selected as these artifacts often occur in wood images. Gaussian noise often occurs during image acquisition which arises in images due to sensor noise (Rahman et al., 2014) caused by poor illumination and high temperature in the timber factory (Ratnasinga et al., 2011). On the other hand, wood images are subjected to motion blur when there is a relative motion between the camera and the wood slice (Guang-sheng & Peng, 2012). Figure 4.2 show one reference images with two types of distorted images with nine levels of distortions each.

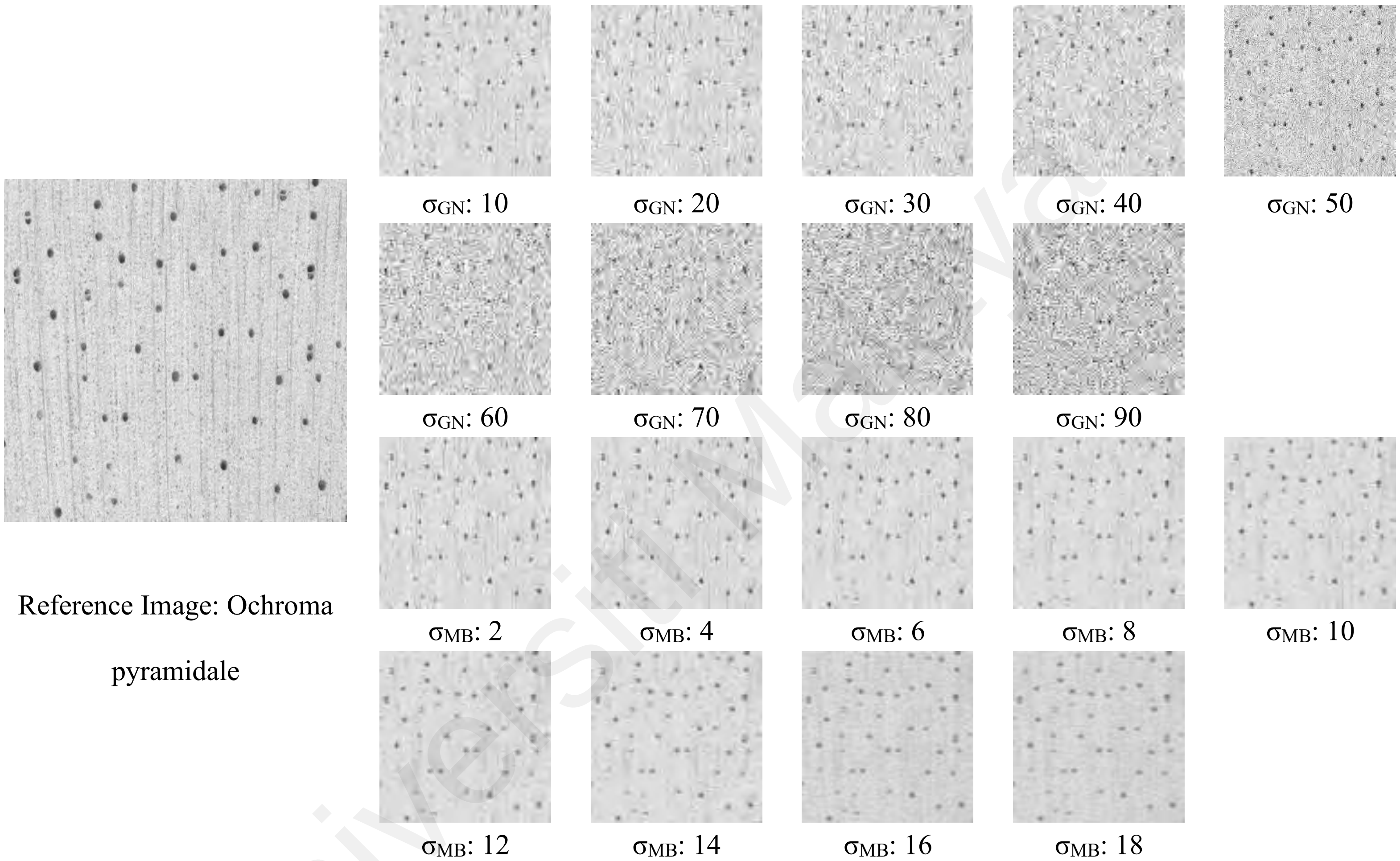

Figure 4.2: Reference image with two types of distorted images with nine levels of distortions each

4.3.3 Subjective Evaluation

Thirty subjects, eleven staff from Tapak Semaian Mantin, Jabatan Perhutanan Negeri Sembilan, nineteen students and staff from Department of Electrical and Electronic Engineering, Manipal International University (MIU), Nilai, Malaysia were chosen to evaluate the wood images. The age of the subjects is between 20 to 50 years old. The evaluation was performed based on the procedures suggested in Rec. ITU-R BT.500-11 and Chow et al. (L.S. Chow et al., 2016; Recommendation, 2000). The evaluation was performed in an office environment using a 21 inch LED monitor with a resolution of 1920 x 1080 pixels. The subjects' near vision acuity was checked using Snellen Chart before the subjective evaluation to ensure that the subject is fit to perform the evaluation task. The Snellen Chart is shown in Appendix A.

Simultaneous Double Stimulus for Continuous Evaluation (SDSCE) methodology was implemented for the subjective evaluation (L.S. Chow et al., 2016; Recommendation, 2000). The reference and distorted images are displayed on the monitor screen side by side where the reference image is displayed on the left, and the distorted image is displayed on the right. Each subject evaluates the distorted image by comparing the quality of the images (right side) with its reference image (left side). Figure 4.3 shows an example of the monitor display during the evaluation session.

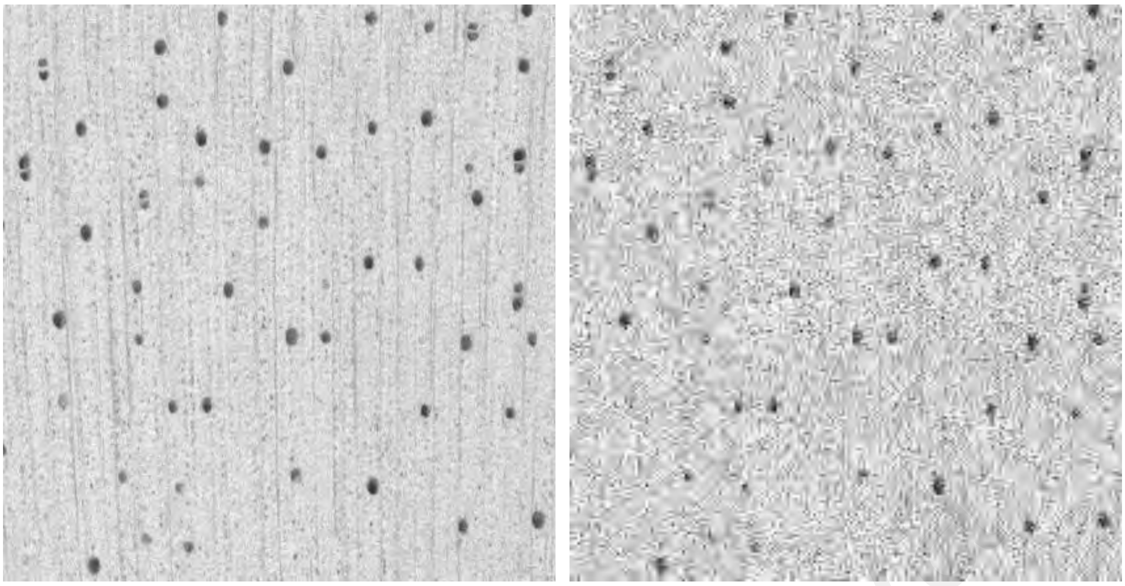

Reference Image: Ochroma pyramidale

Image Distorted by Gaussian White Noise, σ_{GN}: 50

Figure 4.3: Monitor display during the evaluation session. Left is the Reference Image and right is the Distorted Image.

The subject rates either 5 (Excellent), 4 (Good), 3 (Fair), 2(Poor) or 1(Bad) for each image displayed. These numerical scores were not revealed to the subjects as it could cause biasness by the subjects (Bindu, Ganpati, & Sharma, 2012).

Firstly, written instructions on the evaluation procedures were given to each subject prior to evaluation of the wood images. The written instructions are printed in Appendix B. Then, a demonstration session was conducted with a few examples of distorted images corresponding to a recommended quality rating. A mock test was also performed where the subjects evaluated two sets of wood images (two reference images with thirty-six test images). In the case where two similar reference images were shown on the screen, if the subject did not rate it as 'Excellent' quality, this subject would not do the rest of the image evaluation. The subjective evaluation period should take less than 30 minutes for each subject to avoid fatigue. There was no time constraint for the subjective assessment. The subjects took an average of 45 minutes for each session.

The subjective evaluation was conducted virtually using Google Form for staff from Tapak Semaian Mantin, Jabatan Perhutanan Negeri Sembilan to facilitate smooth evaluation without interrupting their daily work. The sample of google form is attached in Appendix C. Figure 4.4 shows the picture taken during evaluation by four of the staff from Tapak Semaian Mantin, Jabatan Perhutanan Negeri Sembilan.

Figure 4.4: Four of the subjects (staff from Tapak Semaian Mantin, Jabatan Perhutanan Negeri Sembilan) performing subjective evaluation

4.3.4 Processing of Subjective Scores

The ratings obtained from the subjects were used to calculate MOS using Eq. (4.1) where the average of the scores obtained from all the thirty human subjects were calculated:

$$\text{MOS (k)} = \frac{1}{N}\sum_{i=1}^{N} S_{ik} \qquad (4.1)$$

where S_{ik} is the score given by i^{th} subject for k^{th} image and N is the number of human subject. In this study, N = 30 as we have thirty human subjects.

Next, five FR-IQA metrics were calculated using the original reference image and each distorted images. The chosen FR-IQA metrics are Structural Similarity Index (SSIM) (Zhou Wang et al., 2003), Multiscale SSIM (MS-SSIM) (Zhou Wang et al., 2003), Feature SIMilarity (FSIM) (L. Zhang et al., 2011), Information Weighted SSIM (IW-SSIM) (Zhou Wang & Li, 2011) and Gradient Magnitude Similarity Deviation (GMSD) (Xue et al., 2014). These FR-IQA metrics were explained in Section 2.1.

4.3.5 Performance Metrics

We use two types of performance metrics to validate the MOS values in this study: Root Mean Square Error (RMSE) (Chai & Draxler, 2014) , logistic regression (H.R. Sheikh et al., 2006; Xue et al., 2014; L. Zhang et al., 2011) and correlation coefficient, Pearson Linear Correlation Coefficient (PLCC). The formulas for these performance metrics are listed in Table 4.3. In Table 4.3, *M* denotes the MOS values, *Q* denotes the original objective scores calculated from the FR-IQA metrics, and Q_r denotes the objective scores after regression.

RMSE is a standard statistical metric used to evaluate the performance of a model and the consistency of the prediction. A nonlinear regression for the objective scores is constructed using a logistic regression function. It provides nonlinear mapping between the objective and subjective scores (Rohaly, A. M., Corriveau, P. J., Libert, J. M., Webster, A. A., Baroncini, V., Beerends, J., ... & Winkler, 2000). The nonlinear mapping is plotted on a graph for visual inspection and comparison between the subjective data points and computed objective values.

Table 4.3: Performance Metrics

No	IQA Algorithm	Description
1	Logistic Regression	$Q_r = \beta_1\left(\frac{1}{2} - \frac{1}{1+\exp\left(\beta_2(Q-\beta_3)\right)}\right) + \beta_4 Q + \beta_5$ (4.2) where $\beta_1, \beta_2, \beta_3, \beta_4, \beta_5$ are the regression model parameters. Optimal parameters, β are obtained using nonlinear least squares.
2	PLCC	$PLCC(Q_r, M) = \frac{\sum_i^n (Q_{r_i} - \overline{Q_r}) \sum_i^n (D_i - \bar{D})}{\sqrt{\sum_i^n (Q_{r_i} - \overline{Q_r})^2}\sqrt{\sum_i^n (D_i - \bar{D})^2}}$ (4.3) where $\overline{Q_r}$ and $\bar{M}$ are the means for dataset Q_r and M respectively.
5	RMSE	$RMSE(Q_r, M) = \sqrt{\frac{\sum_i^n (Q_{r_i} - D_i)^2}{n}}$ (4.4) where n is the total number of data pairs.

Relationship between two datasets can be measured statistically using correlation coefficient. According to Taylor R. (Taylor, 1990), two datasets are said to have high correlation if the correlation coefficient values are between 0.68 to 1.0. The correlation coefficients, PLCC was used in this study to measure the relationship between the subjective score (MOS) and objective (FR-IQA) scores. PLCC, also known as Pearson product-moment correlation coefficient, is used to evaluate the accuracy of the prediction.

4.4 Results and Discussions

In order to evaluate the performance of the proposed system, a 190 wood images which consists of 10 reference images from 10 wood species and 180 distorted images are produced by applying distortions to the 10 reference images.

4.4.1 Relationship Between MOS and Different Distortion Levels

The variation on the subjective evaluation with the increasing distortion level for Gaussian White Noise and Motion Blur is shown in Figure 4.4 (a) and (b), respectively. Higher standard deviation in Gaussian White Noise and Motion Blur, σ_{GN} and σ_{MB} produces poorer quality of distorted images, where the MOS values are lower. Based on scatter plot in Figure 4.4 (a) and (b), the MOS value decreases as the distortion level increases. This means that human subjects could differentiate images distorted with different levels of Gaussian white noise and motion blur. This is due to less perceptibility of the low contrast entity after the image is subjected to Gaussian White Noise. Hence, the visual quality of the wood images will be affected (L.S. Chow et al., 2016). On the other hand, Motion Blur could cause the camera movement to be visible resulting the image quality to be affected (Kurimo et al., 2009).

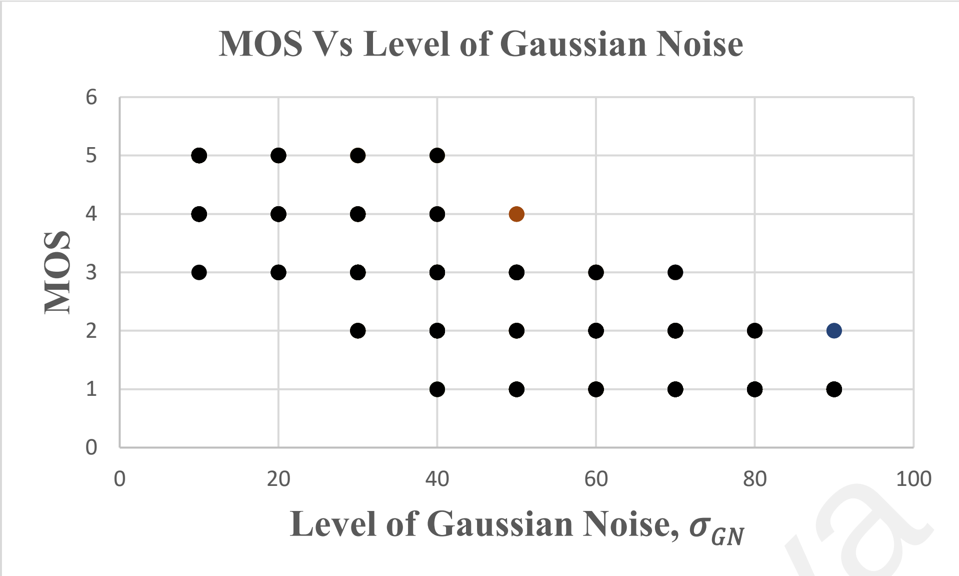

(a)

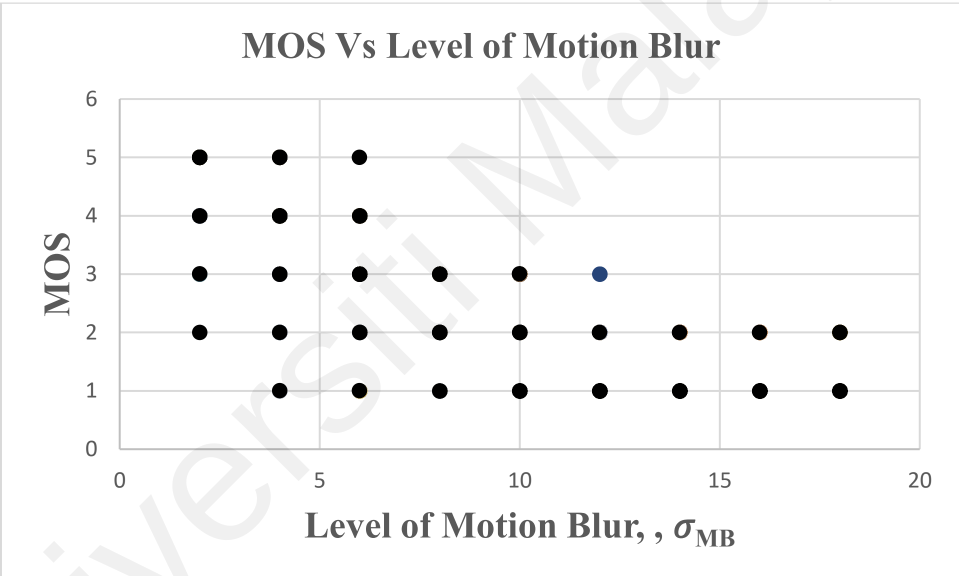

(b)

Figure 4.5: Scatter Plot of MOS versus distortion levels of (a) Gaussian White Noise and (b) Motion Blur

4.4.2 Relationship Between MOS and FR-IQAs

The MOS values obtained from the subjective evaluation were compared with five FR-IQAs: Structural Similarity Index (SSIM) (Zhou Wang et al., 2003), Multiscale SSIM (MS-SSIM) (Zhou Wang et al., 2003), Feature SIMilarity (FSIM) (L. Zhang et al., 2011), Information Weighted SSIM (IW-SSIM) (Zhou Wang & Li, 2011) and Gradient Magnitude Similarity Deviation (GMSD) (Xue et al., 2014). PLCC and RMSE were calculated between MOS and the five FR-IQA metrics. The nearer the PLCC values to 1, the closer the relationship between MOS and the FR-IQA metric, which means that the FR-IQA agrees with the MOS values. Table 4.4 shows the PLCC and RMSE values between MOS and five FR-IQAs. The PLCC values for Gaussian White Noise, Motion Blur and overall images are close to 1. This means that the correlation between MOS and all the five FR-IQAs is high for Gaussian White Noise (Taylor, 1990). In addition, the PLCC values between MOS and FSIM for Gaussian White Noise, Motion Blur and overall images are the highest compared to the other four FR-IQA metrics.

Lower RMSE values signify closer relationship between MOS and the FR-IQA metric. Both PLCC and RMSE values in Table 4.4 gives similar findings where MOS is close to all the five FR-IQAs. The PLCC and RMSE values in Table 4.3 also show that FSIM is the closest FR-IQA metric to MOS for the overall images.

Table 4.4: PLCC and RMSE values between MOS and five FR-IQAs

		MSSIM	SSIM	FSIM	IWSSIM	GMSD
PLCC	GWN	0.823	0.908	**0.955**	0.923	0.919
	MB	0.908	0.873	**0.951**	0.913	0.924
	All	0.855	0.824	**0.953**	0.913	0.913
RMSE	GWN	0.723	0.643	**0.423**	0.667	0.512
	MB	0.637	0.734	**0.408**	0.567	0.615
	All	0.672	0.702	**0.414**	0.626	0.554

The MOS values versus the FR-IQAs: MSSIM, SSIM, FSIM, IWSSIM and GMSD were plotted for Gaussian White Noise, Motion Blur and overall images in Figures 4.5 – 4.9 (a) – (c), respectively. The fitted curves using non-linear regression were overlaid with the data points on the same graphs. The trend of Figures 4.5 - 4.8 are as expected, where a better image quality is represented by a larger MOS score corresponding to all the FR-IQA values closer to 1. In contrast, the trend of Figure 4.9 is a better image as represented by a larger MOS score corresponding to GMSD values closer to 0. The characteristics of the curve fitting in Figures 4.5 – 4.9 (a) – (c) differs for every FR-IQA metric due to different data distribution and inconsistent relationship between the FR-IQAs and MOS to evaluate the wood images for lower Gaussian Noise and Motion Blur. Based on the results as tabulated in Table 4.4, we found that MOS close to the FR-IQAs for wood images distorted with Gaussian White Noise and Motion Blur. Therefore, MOS is valid and the MOS values calculated in our study are applicable to model a new NR-IQA method.

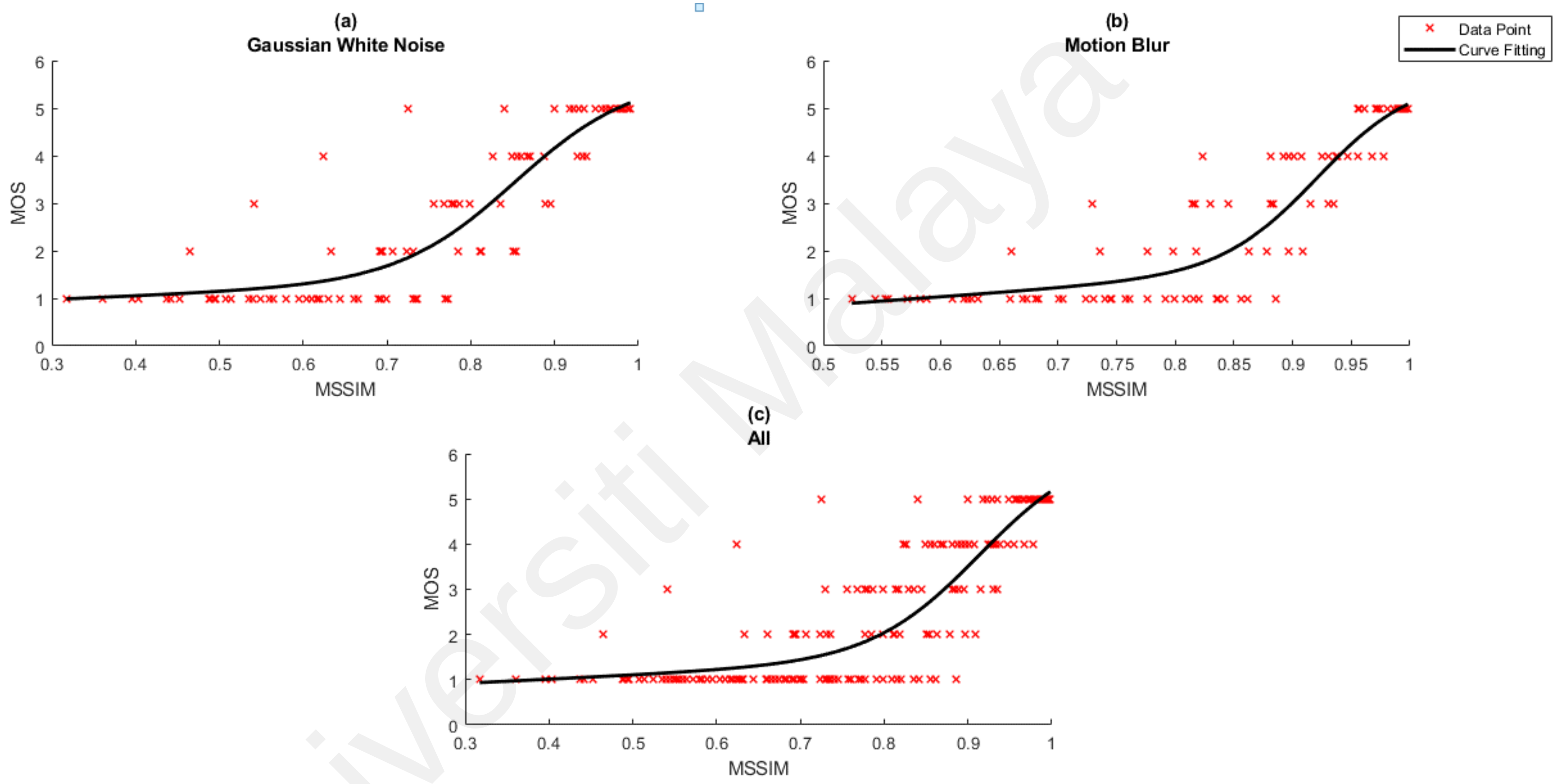

Figure 4.6: MOS versus MSSIM for a) Gaussian White Noise, b) Motion Blur, c) Overall Images

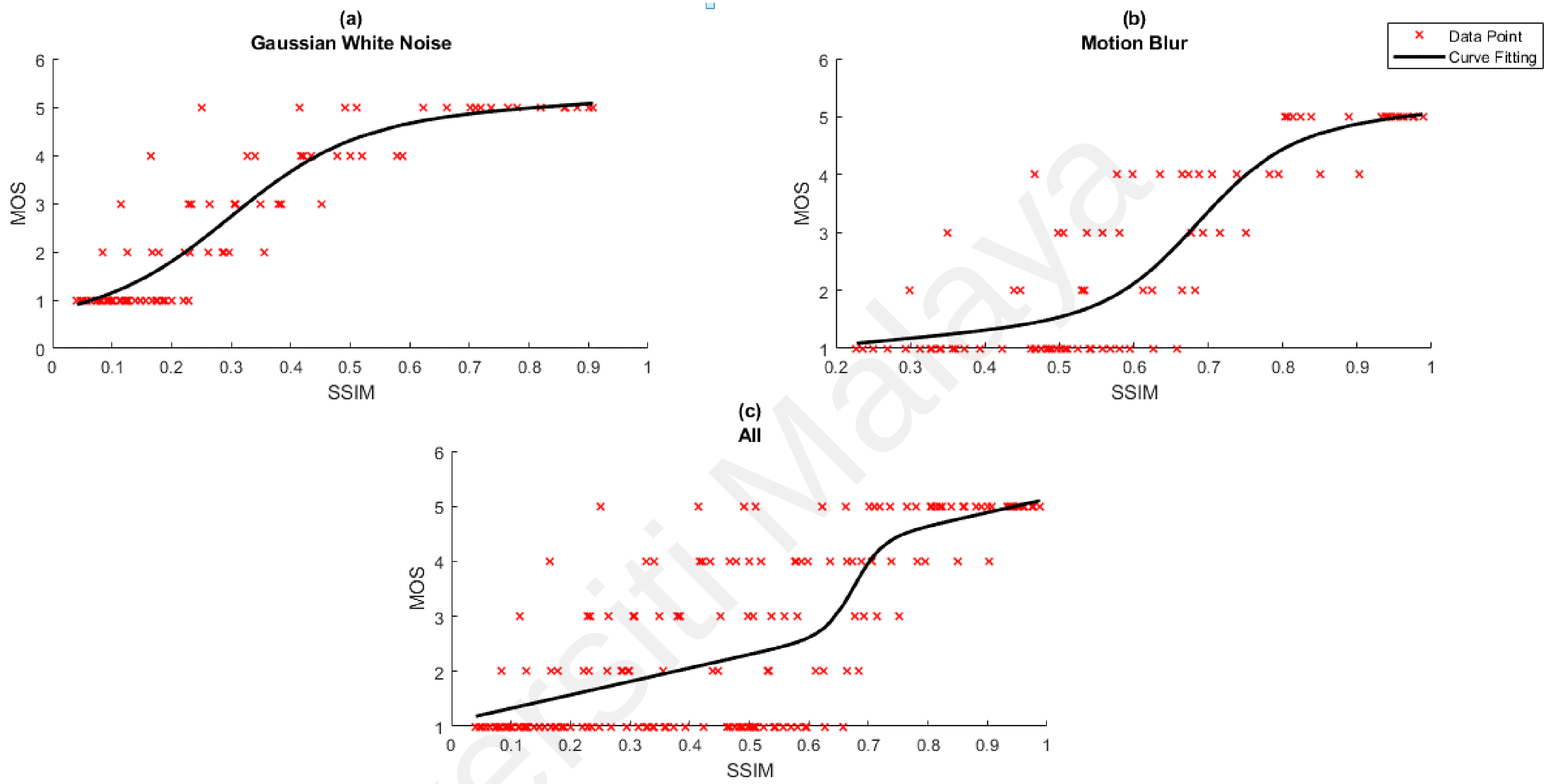

Figure 4.7: MOS versus SSIM for a) Gaussian White Noise, b) Motion Blur, c) Overall Images

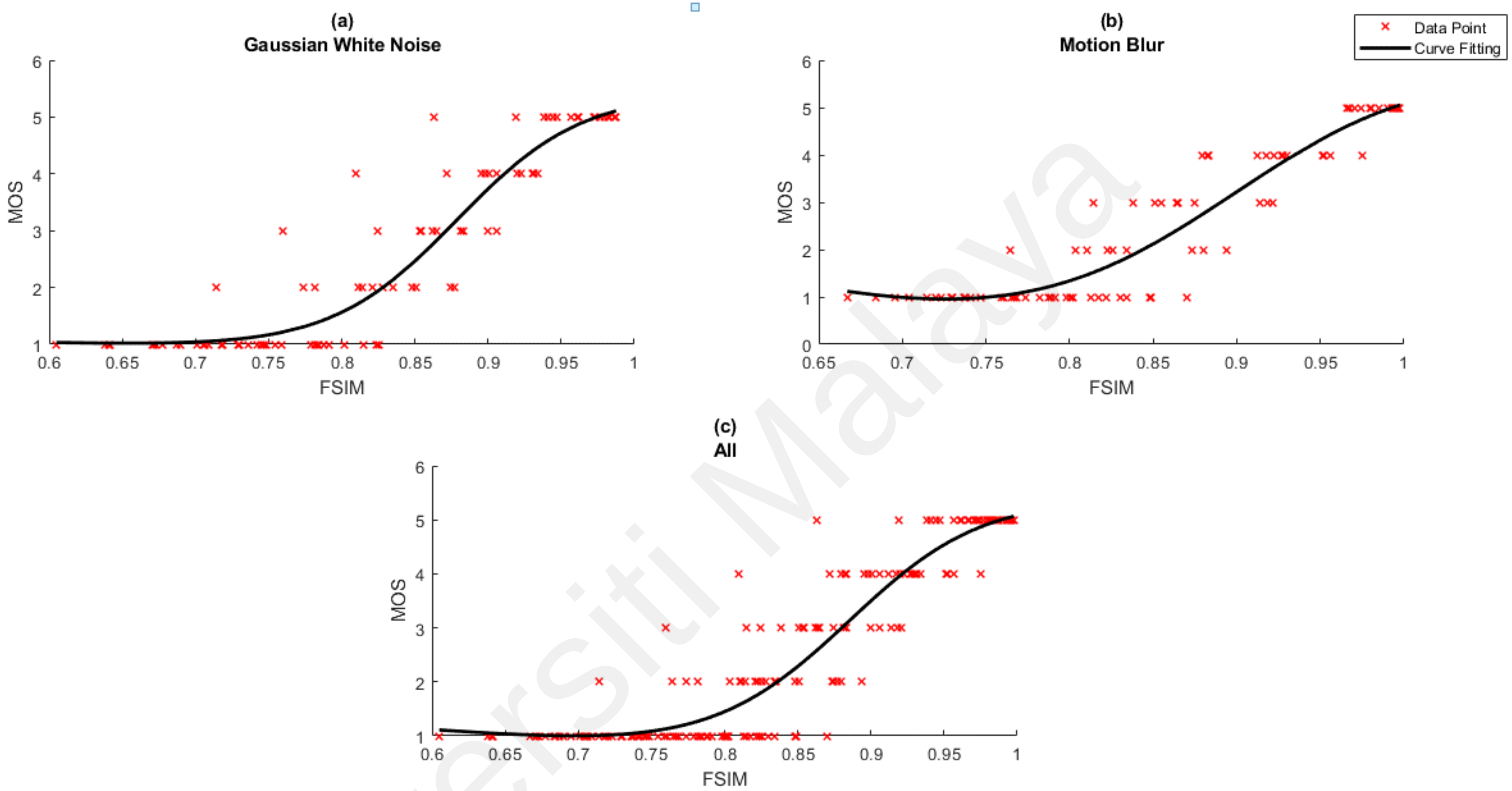

Figure 4.8: MOS versus FSIM for a) Gaussian White Noise, b) Motion Blur, c) Overall Images

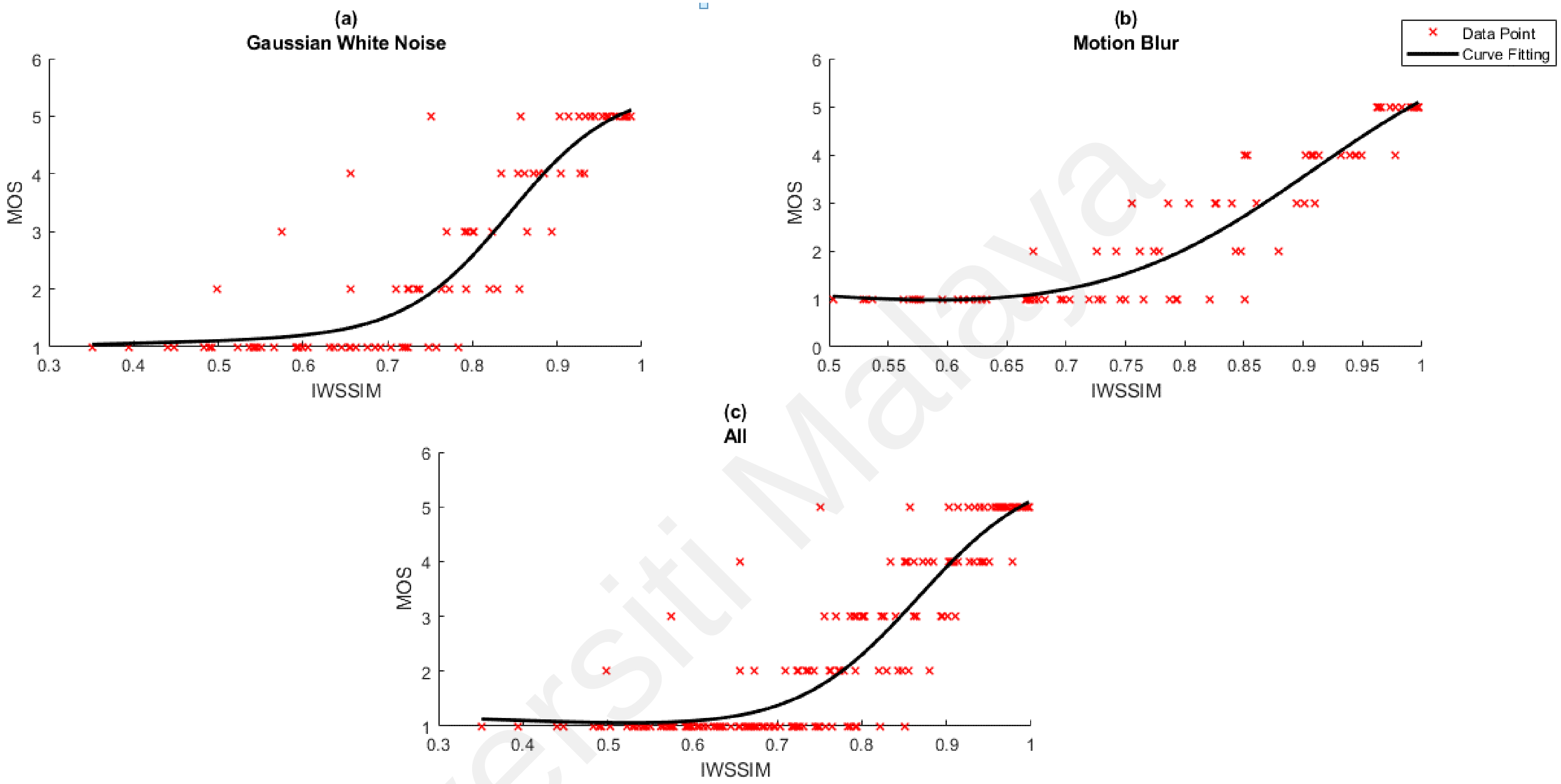

Figure 4.9: MOS versus IWSSIM for a) Gaussian White Noise, b) Motion Blur, c) Overall Images

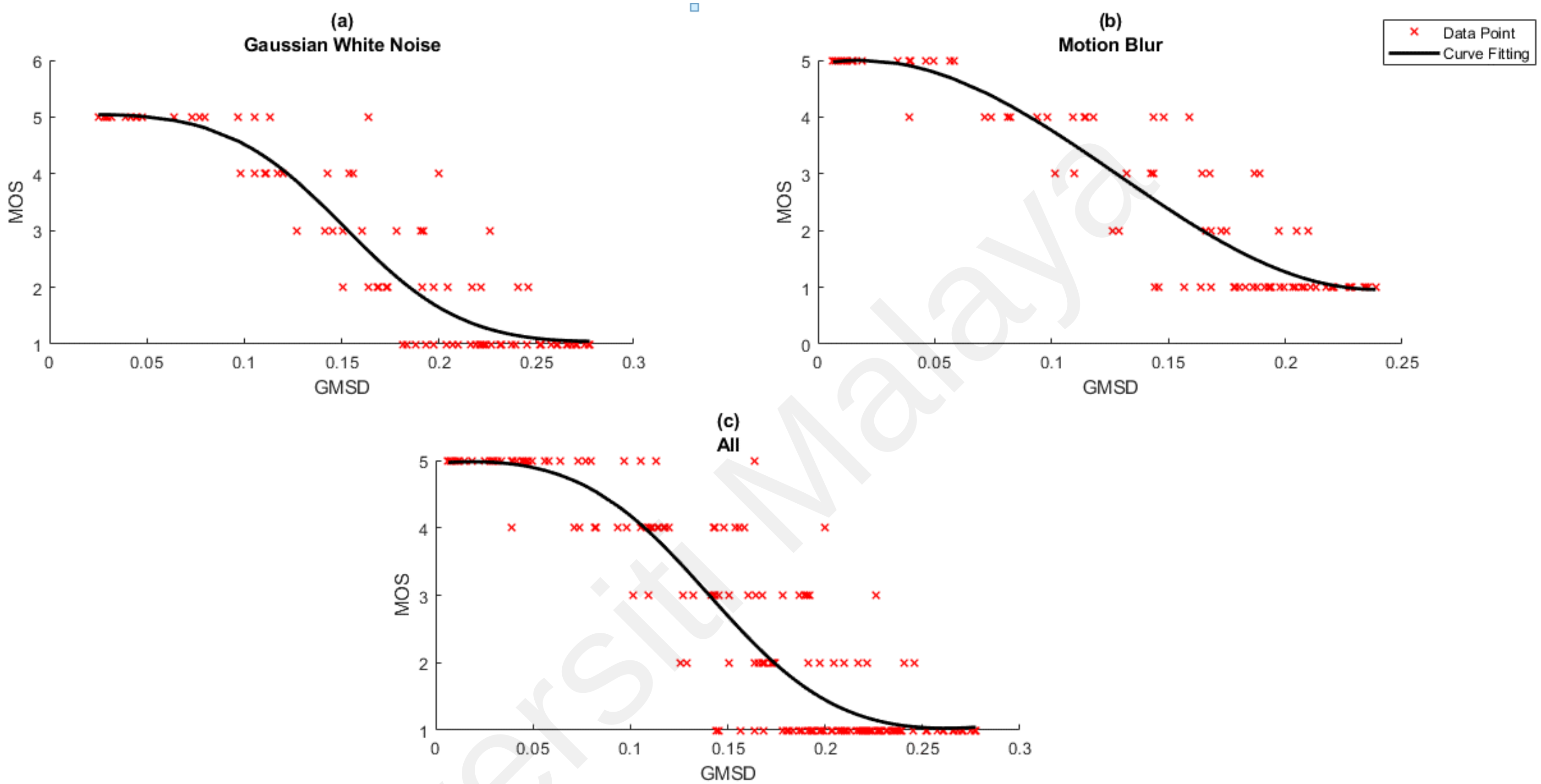

Figure 4.10: MOS versus GMSD for a) Gaussian White Noise, b) Motion Blur, c) Overall Images

4.5 Chapter Conclusion

190 wood images (10 reference and 180 distorted images) was generated in this study. The reference images were distorted with Gaussian White Noise and Motion Blur which commonly occur during the acquisition of wood images. The study also contains the subjective MOS and five types of objective FR-IQAs evaluation. The relationship between the subjective MOS and objective FR-IQAs are examined using performance metrics namely PLCC and RMSE. Both performance metrics showed that MOS is close to all the FR-IQAs. Hence, the MOS values calculated in our study are applicable to model a new NR-IQA method which will be explained in the next chapter.

CHAPTER 5: MODIFIED BRISQUE WOOD IMAGE QUALITY ASSESSMENT FOR WOOD IMAGES

5.1 Introduction

The objective of this chapter is to propose a No Reference Image Quality Assessment (NR-IQA) method for accessing the image quality of wood images. This is achieved by modifying a widely-used NR-IQA, the Blind/Referenceless Image Spatial Quality Evaluator (BRISQUE) model (Mittal et al., 2012). This NR-IQA metric is known as Modified BRISQUE Wood Image Quality Assessment, MBW-IQA. Modification of the BRISQUE model for wood analysis is required, as it was designed to evaluate natural images.

Similar to the original BRISQUE model, the proposed NR-IQA quantifies the deviations in the wood image that arises due to the distortion by using the locally normalized luminance coefficients. The locally normalized luminance coefficients are used to calculate the image features. The Support Vector Machine (SVM) Regression (SVR) was trained with the Mean Opinion Score (MOS) and the locally normalized luminance coefficients to develop the MBW-IQA metric. The locally normalized luminance coefficients are calculated for the wood images.

The efficiency of MBW-IQA metric is compared with BRISQUE, Deep Neural Network IQA (deepIQA), Deep Bilinear Convolution Neural Network (DB-CNN) and five types of established FR-IQA metrics, i.e. Structural Similarity Index (SSIM) (Zhou Wang et al., 2003), Multiscale SSIM (MS-SSIM) (Zhou Wang et al., 2003), Feature Similarity (FSIM) (L. Zhang et al., 2011), Information Weighted SSIM (IW-SSIM) (Zhou Wang & Li, 2011) and Gradient Magnitude Similarity Deviation (GMSD) (Xue et al., 2014) using PLCC and RMSE values.

5.2 Background of the Study

Wood is a plant tissue with a characteristic porous and fibrous structure, which is widely used for furniture, millwork, flooring, building construction, paper production, and as a source of energy (Shivashankar, 2018). There are thousands of wood producing tree species, yielding materials of distinct physical characteristic such as structure, density, colour and texture (Barmpoutis et al., 2018), which can define their preferred usages and monetary values (Zamri et al., 2018). While timber production at high latitudes is based on a small number of species, there is great diversity in tropical forests. For example, conifers of the genus Pine are widespread in the northern hemisphere, producing a moderately priced wood of high resin content that is widely used for indoor furniture. Bocote (*Cordia gerascanthus*), which can be found in a native of central America, is used to produce expensive hardwood that is suitable for high quality furniture and cabinetry, as its oily surface gives it a naturally glossy finish. Rosewood (*Dalbergia* sp.) is another expensive wood, sought after for instrument making and flooring due to it high strength and density. Since each wood species has a different price and characteristics, misclassification could lead to financial losses. Therefore, it important to identify correctly the different wood species.

Traditionally, the recognition of wood species is done by human (Gazo et al., 2018). However, this is time consuming and involves high cost to the lumber industry. Hence, many algorithms have been developed for automatic recognition of wood samples (Barmpoutis et al., 2018; Guang-sheng & Peng, 2012; Shivashankar, 2018; Venkatachalapathy & Sudhakar, 2014). There is scope for improving the accuracy of automatic wood recognition systems through use of high quality microscopy images, which are sometimes pre-processed to enhance their recognition. However, image enhancement processes bring an extra requirement for time, and may impart a checkerboard artefact to the wood images (Xiao, Tang, Jiang, Li, & Wang, 2018). Furthermore, the environment in timber factories is encumbered by dust, poor illumination, and heat (Ratnasinga et al., 2011), which risk degrading the image quality. Hence, a suitable image quality assessment (IQA) metric is needed to evaluate captured images before proceeding in the pipeline for recognition algorithms.

As mentioned in Chapter 2, IQA can be divided into two categories, namely subjective and objective evaluations. Subjective evaluation occurs when the images are evaluated by human, who provide scores based on their perception on the image quality, whereas objective evaluation uses mathematical algorithms to calculate quality score for the images.

There are three types of objective evaluation, namely Full-Reference-IQA (FR-IQA), Reduced Reference-IQA (RR-IQA) and No-Reference/Blind IQA (NR-IQA) (Chandler, 2013; Gulame et al., 2013). FR-IQA evaluates an image by comparing the image with its reference image, while NR-IQA evaluates an image without using a reference image. On the other hand, RR-IQA assesses an image using partial information from reference images. NR-IQA is the most suitable metric to assess wood images, given the impediments to obtaining high quality images in the environment of lumber mills. Hence, an NR-IQA procedure motivated from a widely-used NR-IQA, the Blind/Referenceless Image Spatial Quality Evaluator (BRISQUE) model, MBW-IQA is proposed. BRISQUE is an IQA model, which considers the luminance and image features of the natural images and it is not a distortion-specific model (Mittal et al., 2012). The BRISQUE model is trained with subjective scores to enable emulation of human judgement on the quality of the images. BRISQUE is trained to evaluate natural images. Therefore, it is not optimal to assess wood images. Hence, a NR-IQA, MBW-IQA is proposed to assess wood images specifically.

5.3 Training and Testing Database

The BRISQUE model was trained to assess natural images by using Support Vector Machine (SVM) Regression (SVR), which was trained with subjective Difference Mean Opinion Scores (DMOS) and 36 features calculated for natural images: four features of Generalized Gaussian Distribution (GGD) and 32 features of Asymmetric Generalized Gaussian Distribution (AGGD) (Mittal et al., 2012). Similar to the BRISQUE approach, the MBW-IQA model was trained to assess wood images by using SVR in conjunction with Generalized Gaussian Distribution (GGD) and Asymmetric Generalized Gaussian Distribution (AGGD) features calculated for wood images and the subjective MOS from subjective evaluation.

The SVM model is used widely in modelling IQA metric as it is capable to handle high-dimensional data exist along with a corresponding lack of knowledge of the underlying distribution. Even with a relatively small sample size, SVMs have the benefit of not being constrained by distributional assumptions, other than that the data are independent and identically distributed (Wilson, 2008).

5.3.1 Wood Images

The same ten wood images from ten wood species, namely *Turraeanthus africanus* (Avodire)*, Ochroma pyramidale* (Balsa), *Cordia spp.* (Bocote), *Juglans cinerea* (Butternut)*, Tilia Americana* (Basswood), *Vouacapoua americana* (Brownheart), *Cornus florida* (Dogwood), *Cordia spp.* (Laurel Blanco)*, Swartzia Cubensis* (Katalox)*, and Dipterocarpus spp* (Keruing) as mentioned in Section 4.3.1 were chosen. The Gaussian white noise with standard deviation, σ_{GN} and motion blur with standard deviation, σ_{MB} were applied to the reference images at nine levels of distortion of the reference images, i.e.: σ_{GN} = 10, 20, 30, 40, 50, 60, 70, 80 and 90 for Gaussian white noise and σ_{MB} = 2, 4, 6, 8, 10, 12, 14, 16 and 18 for motion blur.

5.3.2 GGD and AGGD Features

First, Mean Subtracted Contrast Normalized (MSCN), $\hat{I}(m,n)$ is calculated using Eq. (5.1) (Mittal et al., 2012):

$$\hat{I}(m,n) = \frac{I(m,n) - \mu(m,n)}{\sigma(m,n) + 1} \tag{5.1}$$

Where *I(m,n)* denotes an image, *μ(m,n)* denotes the local mean of *I(m,n)*, $\sigma(m,n)$ is the local variance of *I(m,n),* $\in 1,2,\ldots,M, n \in 1,2,\ldots,N$ are spatial indices, M and N are the height and width of image, *I(m,n)* respectively.

The local mean, *μ(m,n)* and local variance, *σ(m,n)* are calculated using Eq. (5.2) and Eq. (5.3), respectively (Mittal et al., 2012):

$$\mu(m,n) = \sum_{k=-K}^{K} \sum_{l=-L}^{L} w_{k,l} I_{k,l}(m,n) \tag{5.2}$$

$$\sigma(m,n) = \sqrt{\sum_{k=-K}^{K} \sum_{l=-L}^{L} w_{k,l} \left(I_{k,l}(m,n) - \mu(m,n)\right)^2} \tag{5.3}$$

where $w = \{w_{k,l} | k = -K, \ldots, K,\ l = -L, \ldots, L\}$ denotes a 2-dimension (2D) circularly-symmetric Gaussian weighting function that is sampled out to three standard deviations and rescaled to unit volume, and where K and L are the window sizes. The MSCN, local mean and local variance on the wood images are shown in Figure 4.1 to depict the effect of the contrast normalization. Figure 5.1 (d) shows that the local variance field, σ only highlights the boundary of the pores, and Figure 5.1 (e) shows that the MSCN coefficients highlights key elements of the wood images such as pores and grains, with few low-energy residual object boundaries.

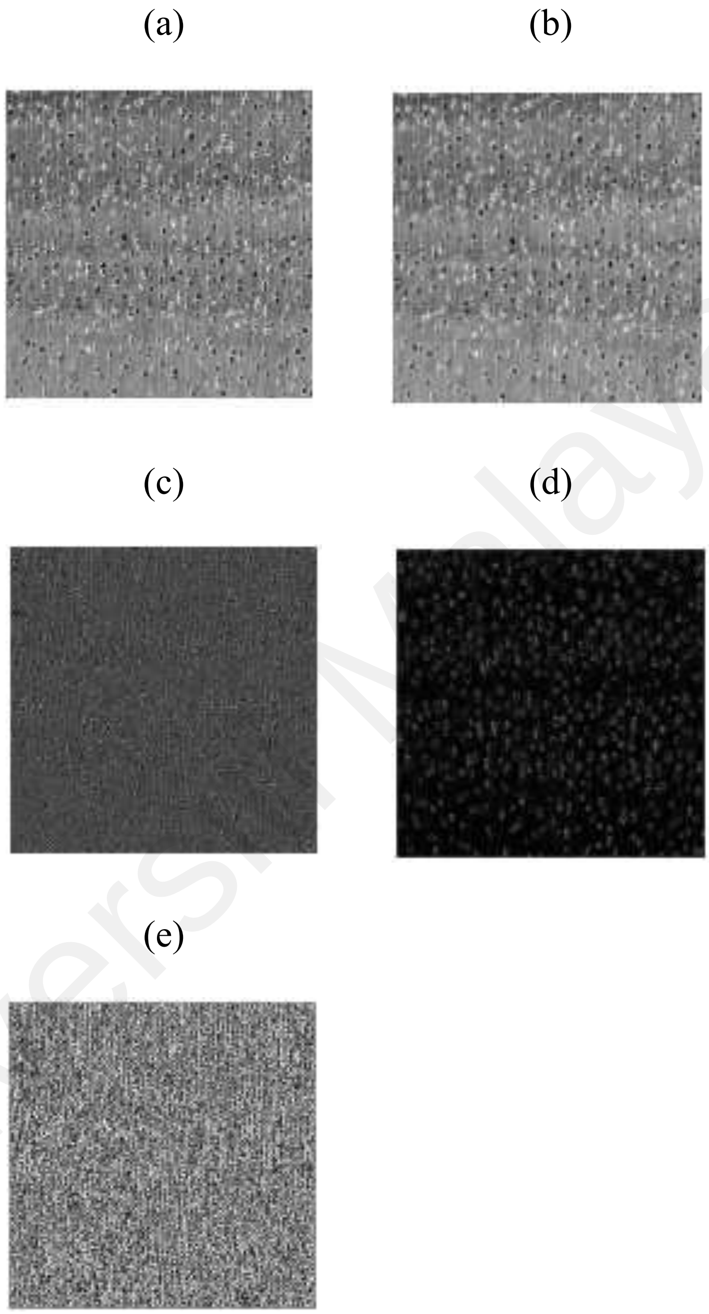

Figure 5.1: The effect of the image normalization procedure. Results are presented for the representative case of to Swartzia Cubensis: (a) Original image I, (b) Local mean field, μ, (c) I − μ, (d) Local variance field, σ and (e) MSCN coefficients

According to Mittal et al., the characteristics of MSCN coefficients varies with the occurrence of the distortions (Mittal et al., 2012). Therefore, the MSCN coefficients were plotted for the reference image and images distorted with Gaussian white noise and motion blur in Figure 5.2 to depict resultant changes in the coefficients. Figure 5.2 shows that the reference images exhibit Gaussian distribution, while the distribution of the images distorted with Gaussian white noise and motion blur have different tail behaviours.

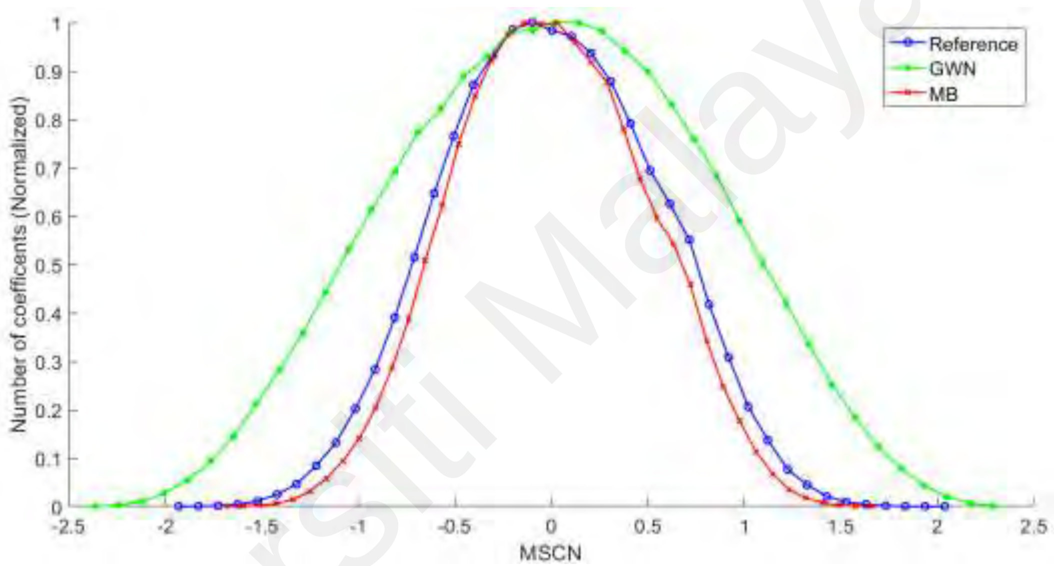

Figure 5.2: Histogram of MSCN coefficients for reference image and distorted images with: Gaussian white noise (GWN) and motion blur (MB)

Two types of Gaussian distribution functions were incorporated in this study to accommodate the varying characteristics of MSCN coefficients: Generalized Gaussian Distribution (GGD) and Asymmetric Generalized Gaussian Distribution (AGGD) (Mittal et al., 2012). There are two parameters computed for the GGD, where α represents the shape of the distribution and σ^2 represents the variance. These two parameters are calculated for wood images using the moment-matching principle. The GGD is computed using Eq. (5.4) (Sharifi & Leon-Garcia, 1995):

$$f(x;\alpha,\sigma^2) = \frac{\alpha}{2\beta\Gamma\left(\frac{1}{\alpha}\right)} \exp\left(-\left(\frac{|x|}{\beta}\right)^{\alpha}\right) \tag{5.4}$$

where

$$\beta = \sigma\sqrt{\frac{\Gamma\left(\frac{1}{\alpha}\right)}{\Gamma\left(\frac{3}{\alpha}\right)}} \tag{5.5}$$

$$\Gamma(a) = \int_0^{\infty} t^{a-1}\, e^{-t}\, dt, a > 0 \tag{5.6}$$

There are four parameters computed for AGGD, namely υ, which represents the shape of the distribution, σ_l^2 and σ_r^2 which represent the left- and right-scale parameters, respectively, and η. The AGGD is computed using Eq. (5.7) (Lasmar, Stitou, & Berthoumieu, 2009):

$$f(x;v,\sigma_l^2,\sigma_r^2) = \begin{cases} \frac{v}{(\beta_l+\beta_r)\Gamma\left(\frac{1}{v}\right)} \exp\left(-\left(\frac{-x}{\beta_l}\right)^{v}\right) & x < 0 \\ \frac{v}{(\beta_l+\beta_r)\Gamma\left(\frac{1}{v}\right)} \exp\left(-\left(\frac{x}{\beta_r}\right)^{v}\right) & x \geq 0 \end{cases} \tag{5.7}$$

where

$$\beta_l = \sigma_l\sqrt{\frac{\Gamma\left(\frac{1}{v}\right)}{\Gamma\left(\frac{3}{v}\right)}} \tag{5.8}$$

$$\beta_r = \sigma_r\sqrt{\frac{\Gamma\left(\frac{1}{v}\right)}{\Gamma\left(\frac{3}{v}\right)}} \tag{5.9}$$

The parameters $(\eta, v, \sigma_l^2, \sigma_r^2)$ of the best AGGD fit are computed using the similar moment-matching approach used for GGD and η is calculated using Eq. (5.10) (Mittal et al., 2012):

$$\eta = (\beta_r - \beta_l)\frac{\Gamma\left(\frac{2}{v}\right)}{\Gamma\left(\frac{1}{v}\right)} \tag{5.10}$$

The four parameters of AGGD: $\eta, v, \sigma_l^2, \sigma_r^2$ are calculated along various orientations of the neighbourhood pixels of wood images, as illustrated in Figure 5.3.

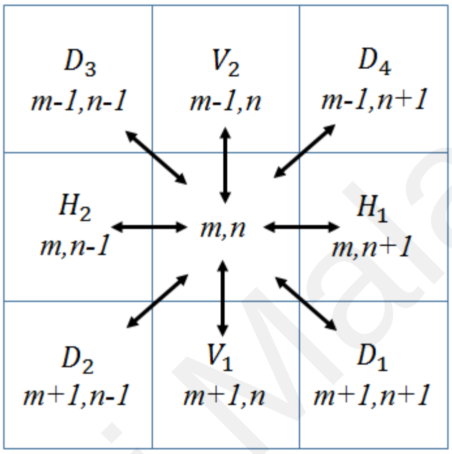

Figure 5.3: Eight orientations of neighbourhood pixels of wood images: horizontal (H_1 and H_2), vertical (V_1 and V_2) and diagonal (D_1, D_2, D_3 and D_4)

The pairwise products of MSCN coefficients are computed along eight orientation, namely horizontal (H_1 and H_2), vertical (V_1 and V_2), and diagonal (D_1, D_2, D_3 and D_4) as shown in Figure 5.3 using Eqs. (5.11) – (5.18) (Mittal et al., 2012):

$$H_1(m,n) = \hat{I}(m,n)\hat{I}(m,n+1) \tag{5.11}$$

$$H_2(m,n) = \hat{I}(m,n)\hat{I}(m,n-1) \tag{5.12}$$

$$V_1(m,n) = \hat{I}(m,n)\hat{I}(m+1,n) \tag{5.13}$$

$$V_2(m,n) = \hat{I}(m,n)\hat{I}(m-1,n) \tag{5.14}$$

$$D_1(m,n) = \hat{I}(m,n)\hat{I}(m+1,n+1) \tag{5.15}$$

$$D_2(m,n) = \hat{I}(m,n)\hat{I}(m+1,n-1) \tag{5.16}$$

$$D_3(m,n) = \hat{I}(m,n)\hat{I}(m-1,n-1) \tag{5.17}$$

$$D_4(m,n) = \hat{I}(m,n)\hat{I}(m-1,n+1) \tag{5.18}$$

where $m \in 1,2,\dots,M$, $n \in 1,2,\dots,N$ and M and N are the height and width of the image.

The histogram of the pairwise products of MSCN coefficients along all eight orientations is shown in Figure 5.4. The difference between pairwise products of MSCN coefficients along H_1 and H_2, V_1 and V_2, D_1 and D_3, and D_2 and D_4 were calculated, which indicates that $H_1 = H_2$, $V_1 = V_2$, $D_1 = D_3$, and $D_2 = D_4$. Hence, four orientations, namely H_1, V_1, D_1 and D_2 were chosen. The η, v, σ_l^2, and σ_r^2 parameters of AGGD are calculated along these four orientations. In total, we thus calculated 18 parameters of GGD and AGGD for the wood images, i.e. two parameters of GGD and 16 parameters of AGGD. According to Mittal et al., an IQA considering multi-scale information of an image can assess images accurately (Mittal et al., 2012). Therefore, the 18 parameters are computed at two scales (original image scale and image reduced by a factor of 0.5). Hence, the full procedure produces 36 parameters to represent the features of wood images, all of which are used to train the SVR. Only two scales were used, as Mittal et al. has shown that performance of the metric in unimproved when more scales are incorporated (Mittal et al., 2012). Moreover, the computation time will increase with increasing number of scales.

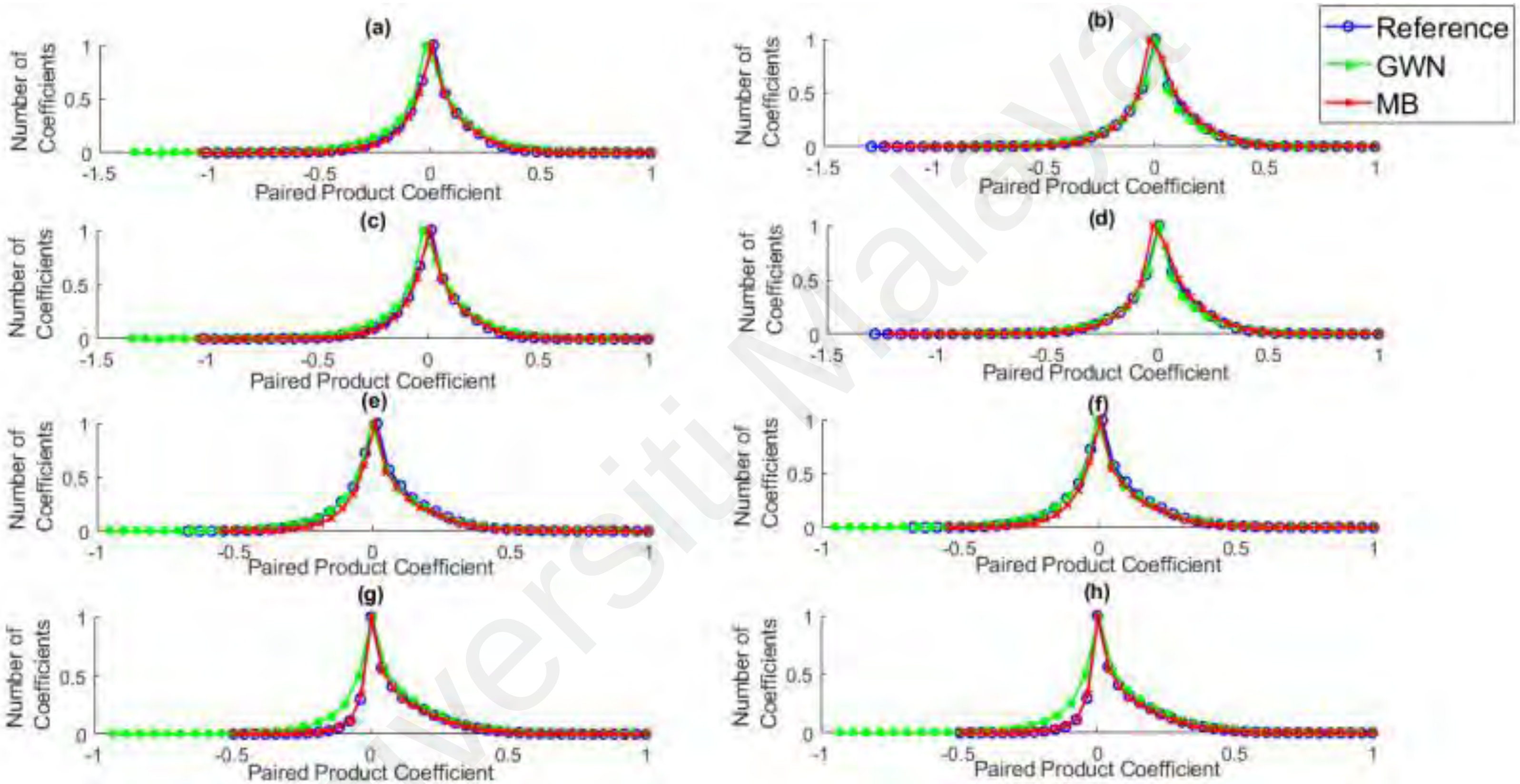

Figure 5.4: Histogram of pairwise products of MSCN coefficients in eight directions: (a) D_1 (b) D_2 (c) D_3 (d) D_4 (e) H_1 (f) H_2 (g) V_1 (h) V_2 for the Reference image and images distorted with: Gaussian white noise (GWN) and motion blur (MB)

5.3.3 MOS

The same MOS values obtained from the subjective evaluation obtained for wood images as explained in Section 4.3.3 were used to train SVR.

5.3.4 Regression Module

Similar to BRISQUE, an $\in -$SVR model (Chang, Chih-Chung and Lin, 2011) was used to design MBW-IQA. As noted above, the $\in -$SVR is trained using MOS and 36 GGD and AGGD features of wood images. The 36 image features calculated for the wood images are mapped to the MOS values of the respective wood images. The 36 features and MOS of wood images were divided randomly into two sets, where one set is used for training and the other set for testing the system: 80% of the 36 features and MOS values were used to train the SVR model and remaining 20% were used to test the model. The training and testing datasets were permutated randomly to avoid any biasness while training and testing of the model (Mittal et al., 2012).

Several experiments were performed on the training and testing data split (70% for training and 30% for testing, 80% for training and 20% for testing and 90% for training and 10% for testing). The PLCC and RMSE were calculated for these data splits and the result is shown in Table 5.1.

Table 5.1: PLCC and RMSE for Data Splits for One Iteration

Percentage of Training Data (%)	Percentage of Testing Data (%)	PLCC	RMSE	Computation time (second)
70	30	0.953	0.792	**18**
80	20	0.985	0.245	**30**
90	10	0.987	0.238	**50**

When a higher percentage of data (90%) for training procedure was tested, the model performance only increased slightly. However, the computation time is longer. A lower percentage of data (70%) for training procedure was tested but the performance of the model decreased. Hence, 80% of data was used for training and 20% of data was used for testing the model. There was no overlap between the training and testing data to ensure a fair prediction of quality scores.

The difference between the BRISQUE and the MBW-IQA metric is, BRISQUE is made to assess natural images where the SVR model was trained with DMOS, 36 GGD and AGGD features of natural images, while the MBW-IQA is trained with MOS, 36 GGD and AGGD features of wood images. The flow diagram of the MBW-IQA metric is shown in Figure 5.5. Pearson's Linear Correlation Coefficient (PLCC) (Song, 2007) and Root Mean Square Error (RMSE) (Chai & Draxler, 2014) between the MOS values and the quality score obtained from the MBW-IQA were calculated to evaluate the performance of the system. Higher PLCC and lower RMSE values indicate that the system is accurate, since the quality scores obtained from the MBW-IQA are close in magnitude to the MOS values. The training and testing of the system were iterated 1000 times and the PLCC and RMSE values were recorded for every iteration. The optimized cost parameter, C, and width parameter, g, of the SVR model is chosen based on the median of the PLCC and RMSE values. In this study, C = 512 and g = 0.25 were used to form the optimized SVM model.

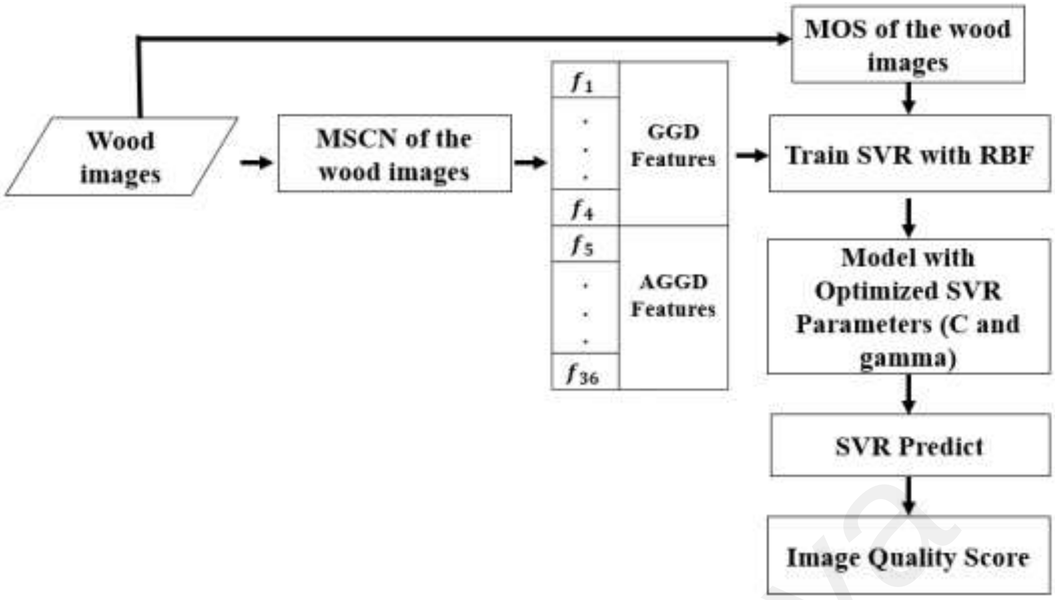

Figure 5.5: Flow diagram of the MBW-IQA Metric

5.3.5 Performance Evaluation

The MBW-IQA is compared with five FR-IQA metrics: Structural Similarity Index (SSIM) (Zhou Wang et al., 2003), Multiscale SSIM (MS-SSIM) (Zhou Wang et al., 2003), Feature Similarity (FSIM) (L. Zhang et al., 2011), Information Weighted SSIM (IW-SSIM) (Zhou Wang & Li, 2011) and Gradient Magnitude Similarity Deviation (GMSD) (Xue et al., 2014). In addition, the MBW-IQA is also compared with BRISQUE, deepIQA, DB-CNN which are an established NR-IQA. PLCC and RMSE (L.S. Chow et al., 2016) values between these FR-IQAs, BRISQUE, deepIQA, DB-CNN and MBW-IQA are calculated in order to evaluate the performance of the MBW-IQA, BRISQUE, deepIQA, DB-CNN and FR-IQAs.

5.4 Results and Discussions

Second dataset were created to evaluate the performance of the MBW-IQA metric. The MBW-IQA metric is compared with the five FR-IQAs, BRISQUE, deepIQA and

DB-CNN obtained for the second dataset. This dataset was generated using 10 'perfect' reference images obtained from ten different wood species namely, *Julbernardia pellegriniana* (Beli), *Dalbergia cultrate* (Blackwood), *Dalbergia retusa* (Cocobolo), *Dalbergia cearensis* (Kingwood), *Guaiacum officinale* (Lignum), *Swartzia spp.* (Queenwood), *Dalbergia spruceana* (Rosewood), *Dalbergia sissoo* (Sisso), *Swartzia benthamiana* (Wamara) and *Euxylophora paraensis* (Yellowheart). These images are shown in Figure 5.6. These images were obtained from the same wood image database (Meier, 2007). These images were distorted with Gaussian white noise with σ_{GN} = 10, 20, 30, 40, 50, 60, 70, 80 and 90 and motion blur with σ_{MB} = 2, 4, 6, 8, 10, 12, 14, 16 and 18 to form 180 images. In total, this dataset comprises of 190 wood images.

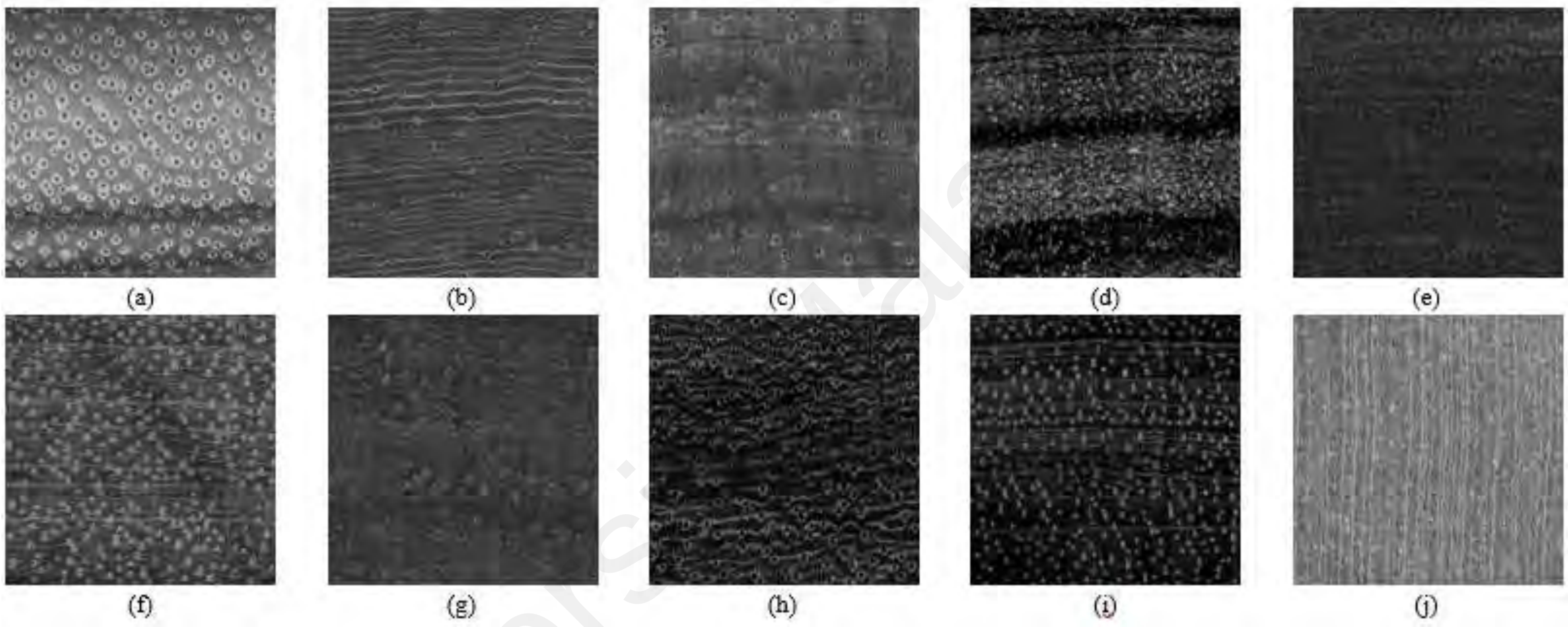

Figure 5.6: Ten reference wood images in the second dataset (a) *Julbernardia pellegriniana,,* (b) *Dalbergia cultrate,* (c) *Dalbergia retusa,* (d) *Dalbergia cearensis*, (e) *Guaiacum officinale,* (f) *Swartzia spp.,* (g) *Dalbergia spruceana,* (h) *Dalbergia sissoo,* (i) *Swartzia benthamiana* and (j) *Euxylophora paraensis*

5.4.1 Relationship Between MOS and Different Distortion Levels

The relationship between MOS and different distortion levels of Gaussian white noise and motion blur is shown in Figure 5.7 (a) and (b). Higher MOS values indicates higher image quality, and higher distortion levels generate lower image quality. Hence, the MOS values for images with higher distortion levels will be lower. Based on scatter plot in Figure 5.7 (a) and (b), the MOS value decreases as the distortion level increases. This means that human subjects could differentiate images distorted with different levels of Gaussian white noise and motion blur.

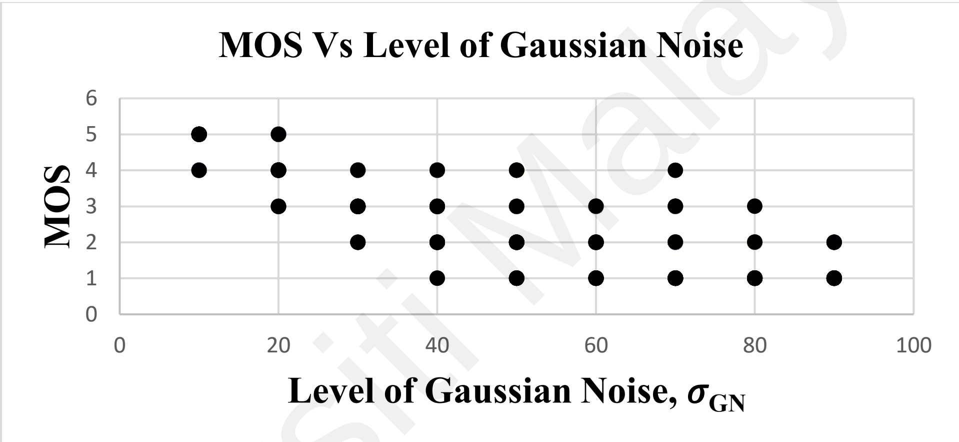

(a)

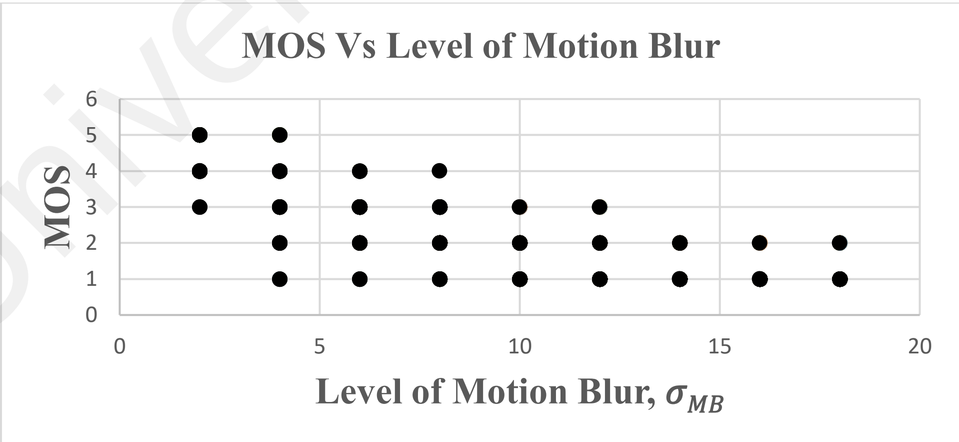

(b)

Figure 5.7: Scatter Plot of MOS versus distortion levels of (a) Gaussian White Noise and (b) Motion Blur

5.4.2 Relationship between MOS and MBW-IQA Metric, BRISQUE, FR-IQAs

The calculated PLCC and RMSE values between MOS and the MBW-IQA, BRISQUE and the five FR-IQA metrics are shown in Table 5.2. PLCC values close to 1 indicates that the MOS correlates well with the IQA metric, whereas lower RMSE values indicate that the MOS correlates with the IQA metric. Table 5.2 shows that the PLCC values for Gaussian white noise, motion blur and the overall images obtained for the MBW-IQA metric are the highest compared to BRISQUE and five FR-IQAs. Furthermore, Table 5.2 also shows that the lowest PLCC values is for BRISQUE, meaning that the MBW-IQA metric outperforms BRISQUE, SSIM, MS-SSIM, FSIM, IW-SSIM and GMSD. This is also indicated by the MBW-IQA having the lowest RMSE values and BRISQUE having the highest RMSE values. The PLCC and RMSE were illustrated in histogram form in Figures 5.8 and 5.9 to show the difference in the PLCC and RMSE values between MOS and the MBW-IQA metric, BRISQUE and the five FR-IQA metrics clearly.

Table 5.2: PLCC and RMSE values between MOS and MBW-IQA, deepIQA, DB-CNN, BRISQUE, FR-IQAs

		MBW-IQA	BRISQUE	deepIQA	DB-CNN	MSSIM	SSIM	FSIM	IWSSIM	GMSD
PLCC	GWN	**0.935**	0.585	0.542	0.527	0.847	0.865	0.903	0.855	0.914
	MB	**0.954**	0.563	0.513	0.538	0.845	0.805	0.912	0.902	0.915
	All	**0.942**	0.594	0.528	0.529	0.843	0.836	0.914	0.879	0.910
RMSE	GWN	**0.462**	1.126	1.256	1.457	0.675	0.627	0.558	0.633	0.542
	MB	**0.335**	0.957	1.134	1.386	0.564	0.643	0.487	0.502	0.475
	All	**0.400**	1.028	1.248	1.365	0.614	0.629	0.526	0.552	0.510

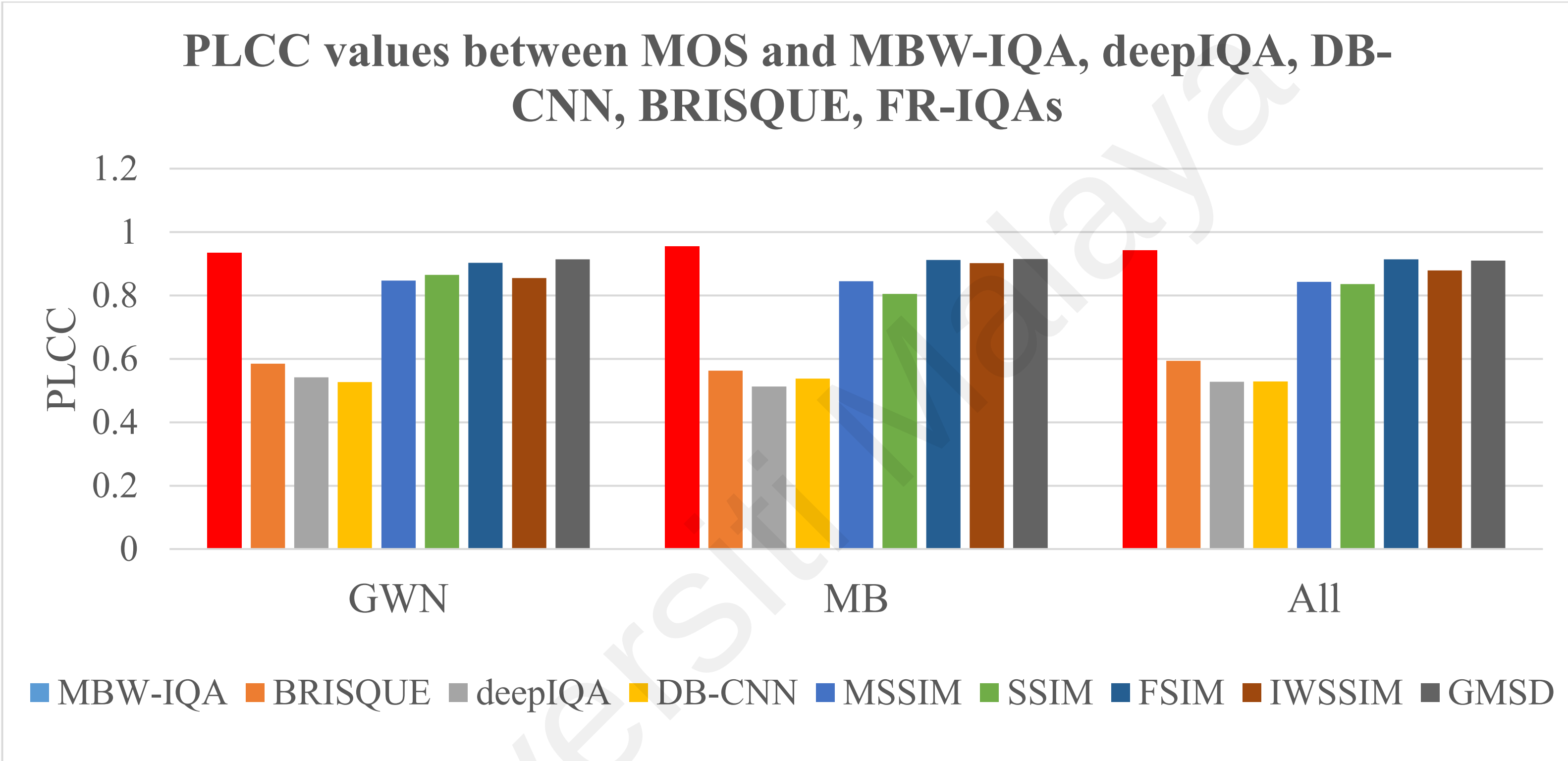

Figure 5.8: PLCC between MOS and MBW-IQA, deepIQA, DB-CNN, BRISQUE, FR-IQAs

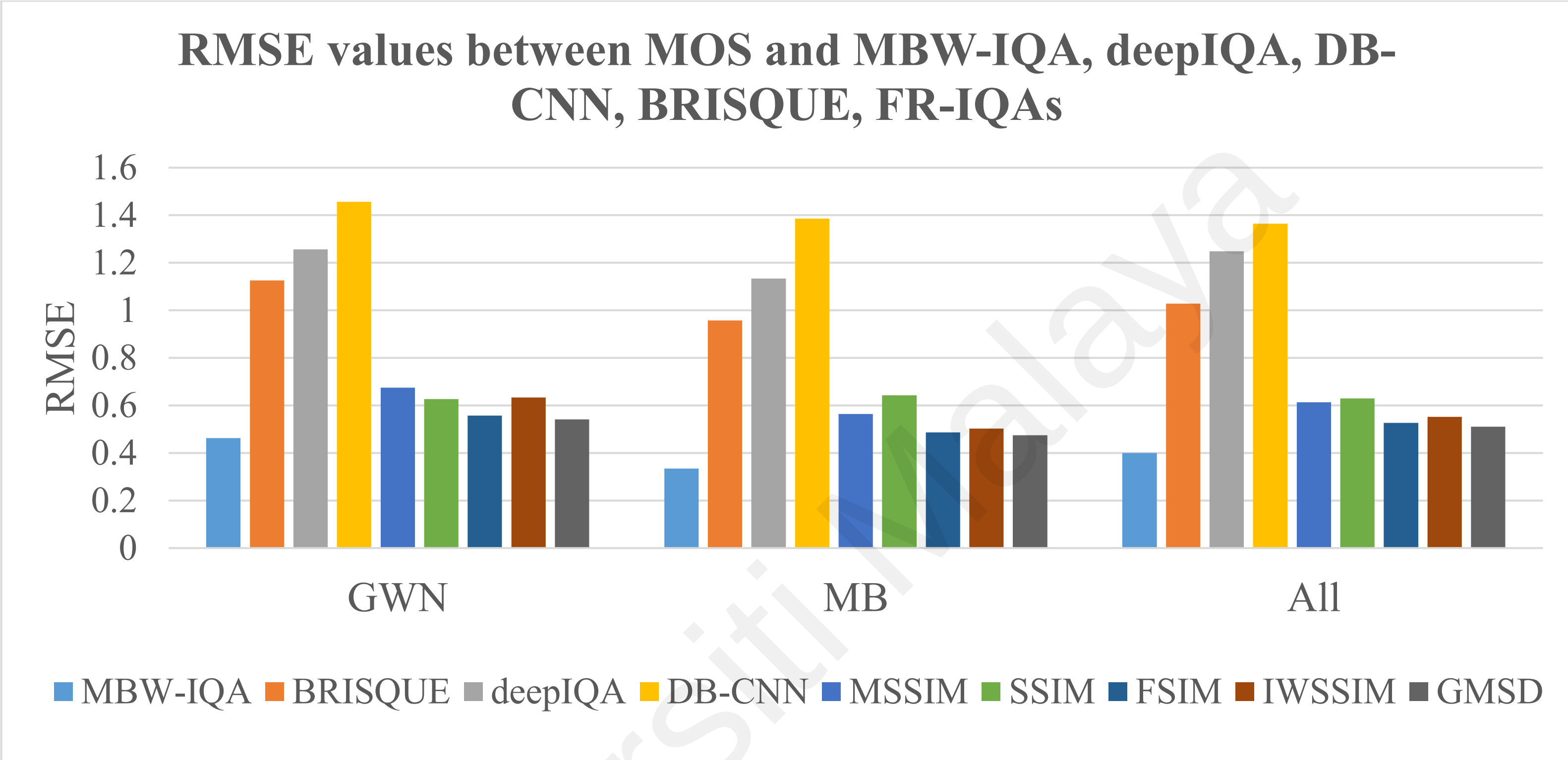

Figure 5.9: RMSE between MOS and MBW-IQA, deepIQA, DB-CNN, BRISQUE, FR-IQAs

5.5 Chapter Conclusion

In this chapter, we proposed a No-Reference Image Quality Assessment (NR-IQA) metric, MBW-IQA to evaluate wood images prior to species classification. The MBW-IQA metric was produced by modifying BRISQUE, one of the established NR-IQA methods. Some modification is required as BRISQUE was trained to assess natural images and is therefore not optimal to assess wood images. Therefore, the MBW-IQA metric was trained using MOS and a set of features calculated for wood images. The performance of the MBW-IQA metric was evaluated by comparing the correlation between MOS, MBW-IQA, deepIQA, DB-CNN, BRISQUE and five FR-IQA metrics, whereas PLCC and RMSE were calculated in order to determine the relationship between MOS, the MBW-IQA metric, deepIQA, DB-CNN, BRISQUE and a range of FR-IQAs. PLCC and RMSE values both showed that the MBW-IQA metric outperforms BRISQUE, deepIQA, DB-CNN and the five FR-IQAs. The MBW-IQA gives a sensitive and accurate assessment of the quality of wood images, which should serve for selecting images suitable for entry into the wood recognition algorithm. In timber industry, it is impossible to obtain a perfect image due to the nature of the industry itself such as dust, poor illumination, hot environment and motion blur caused by relative motion between the camera and the wood slice. Notably, our quality assessment does not require a perfect reference image in order to evaluate the quality of the test wood images.

CHAPTER 6: GLCM AND GABOR FEATURES BASED NO-REFERENCE IMAGE QUALITY ASSESSMENT FOR WOOD IMAGES

6.1 Introduction

The objective of this chapter is to propose GLCM and Gabor features based No Reference Image Quality Assessment (NR-IQA) method to evaluate the quality of wood images. This method is known as GLCM and Gabor Wood Image Quality Assessment (GGW-IQA) metric. The GGW-IQA metric is proposed to improvise the MBW-IQA metric by incorporating widely used GLCM and Gabor features in wood species recognition system (Bremananth R. ; Nithya B. ; Saipriya R., 2009; Khalid et al., 2008; Tou, Tay, & Lau, 2009; Venkatachalapathy & Sudhakar, 2014). The high efficiency of the wood recognition algorithm which uses these features (Bremananth R. ; Nithya B. ; Saipriya R., 2009; Khalid et al., 2008; Tou et al., 2009; Venkatachalapathy & Sudhakar, 2014) shows that they reflects the unique characteristics of wood images such as knot and pores. The GGW-IQA is compared with the Blind/Referenceless Image Spatial Quality Evaluator (BRISQUE), Deep Neural Network IQA (deepIQA), Deep Bilinear Convolution Neural Network (DB-CNN), Modified BRISQUE Wood Image Quality Assessment (MBW-IQA) (as explained in Chapter 5) and five types of established FR-IQA metrics, i.e. Structural Similarity Index (SSIM) (Zhou Wang et al., 2003), Multiscale SSIM (MS-SSIM) (Zhou Wang et al., 2003), Feature Similarity (FSIM) (L. Zhang et al., 2011), Information Weighted SSIM (IW-SSIM) (Zhou Wang & Li, 2011) and Gradient Magnitude Similarity Deviation (GMSD) (Xue et al., 2014). The relative efficiency of the proposed two NR-IQA methods: MBW-IQA, GGW-IQA, deepIQA, DB-CNN, BRISQUE and FR-IQAs are determined based on the correlation between the human mean opinion scores (MOS) and the metrics using Pearson Linear Correlation Coefficient (PLCC) and Root Mean Squared Error (RMSE) (L.S. Chow et al., 2016).

6.2 Background of the Study

In this study, GLCM and Gabor features were used to develop the NR-IQA metric. These two features are widely used in wood species recognition system (Bremananth R. ; Nithya B. ; Saipriya R., 2009; Khalid et al., 2008; Tou et al., 2009; Venkatachalapathy & Sudhakar, 2014). The GLCM depicts second order statistic of an image by calculating how frequent pairs of pixel with specific values and in a specified spatial relationship occur in an image (Abd Latif, MH, Md. Yusof, H, Sidek, S.N, Rusli, 2015). There are four texture statistics in the GLCM matrix and they are contrast, correlation, energy and homogeneity. The 2D Gabor function which represents the spatial summation properties of simple cells in the visual cortex (Rubiyah Yusof, Nenny Ruthfalydia Rosli, 2010). There are seven parameters in the Gabor features, $x, y; \lambda, \theta, \psi, \sigma, \gamma$, where x and y represents the image, λ is the wavelength of the sinusoidal factor, θ is the orientation of the normal to the parallel stripes of a Gabor function, ψ is the phase offset, σ is the standard deviation of the Gaussian envelope and γ is the spatial aspect ratio. These features are calculated in four orientations, 0°, 45°, 90° and 135° which represents the similar 4 orientations in GGD and AGGD features calculation as explained in Section 5.3.2.

6.3 Materials and Methods

6.3.1 Training and Testing Database

A SVR model is trained with the GLCM and Gabor features calculated for normalized wood images with the subjective MOS obtained from subjective evaluation for wood images to design the GGW-IQA metric. These GLCM and Gabor features and MOS are used as the training and testing database for the SVR model.

6.3.2 Wood Images

The same ten wood images from ten wood species, namely *Turraeanthus africanus* (Avodire)*, Ochroma pyramidale* (Balsa), *Cordia spp.* (Bocote), *Juglans cinerea* (Butternut)*, Tilia Americana* (Basswood), *Vouacapoua americana* (Brownheart), *Cornus florida* (Dogwood), *Cordia spp.* (Laurel Blanco)*, Swartzia Cubensis* (Katalox)*, and Dipterocarpus spp* (Keruing) as mentioned in Section 4.3.1 were chosen. The Gaussian white noise with standard deviation, σ_{GN} and motion blur with standard deviation, σ_{MB} were applied to the reference images at nine levels of distortion of the reference images, i.e.: σ_{GN} = 10, 20, 30, 40, 50, 60, 70, 80 and 90 for Gaussian white noise and σ_{MB} = 2, 4, 6, 8, 10, 12, 14, 16 and 18 for motion blur.

6.3.3 GLCM and Gabor Features

First, Mean Subtracted Contrast Normalized (MSCN), $\hat{I}(m, n)$ as explained in Section 5.3.2 is calculated (Mittal et al., 2012). Next, two types of features GLCM and Gabor features were incorporated in this study.

6.3.3.1 GLCM Features

GLCM is one of the most popular feature extraction method. The GLCM characterize second order statistic of an image by computing how often pairs of pixel with specific values and in a specified spatial relationship occur in an image. The matrix contains the conditional joint probabilities of all pair wise combinations of gray levels given at particular displacement distance, d and orientation, θ. The displacement distance, d is also known as inter-pixel distance. The probability, P_{ij} can be defined as Eq. (6.1) (Abd Latif, MH, Md. Yusof, H, Sidek, S.N, Rusli, 2015)

$$P_{ij} = \{C_{ij} | (d, \theta)\} \tag{6.1}$$

where

$$C_{ij} = \frac{P_{ij}}{\sum_{i,j=1}^{G} P_{ij}} \tag{6.2}$$

Where C_{ij} denotes the number of occurrences of gray level in row, i and column, j, P_{ij} denotes the probability value from the GLCM and G represents the total number of gray levels. Four texture statistics, contrast, correlation, energy and homogeneity were extracted from the GLCM matric.

Contrast measures the local variations in the gray-level co-occurrence matrix and is defined as Eq. (6.3).

$$\text{Contrast} = \sum_{i,j} |i - j|^2 p(i,j) \tag{6.3}$$

Correlation measures the joint probability occurrence of the specified pixel pairs and is defined as Eq. (6.4).

$$\text{Correlation} = \sum_{i,j} \frac{(i-\mu i)(j-\mu j)p(i,j)}{\sigma_i \sigma_j} \tag{6.4}$$

Energy provides the sum of squared elements in the GLCM. And it is also known as uniformity or the angular second moment. The energy parameter is computed as Eq. (6.5)

$$\text{Energy} = \sum_{i,j} p(i,j)^2 \tag{6.5}$$

Homogeneity measures the closeness of the distribution of elements in the GLCM to the GLCM diagonal and is computed as Eq. (6.6).

$$\text{Homogeneity} = \sum_{i,j} \frac{p(i,j)}{1+|i-j|} \tag{6.6}$$

These four parameters were computed at four directions, 0°, 45°, 90° and 135° and these forms sixteen GLCM features.

6.3.3.2 Gabor Features

The two- dimensional Gabor function to model the spatial summation properties of simple cells in the visual cortex is defined as Eq. (6.7)

$$g(x, y; \lambda, \theta, \psi, \sigma, \gamma) = exp\left(-\frac{x'^2+\gamma^2 y'^2}{2\sigma^2}\right) cos\left(2\pi\frac{x'}{\lambda}+\psi\right) \quad (6.7)$$

Where $x' = x\ cos\ \theta + y\ sin\ \theta$ and $y' = -x\ sin\ \theta + y\ cos\ \theta$ (6.8)

λ denotes the wavelength of the sinusoidal factor, θ denotes the orientation of the normal to the parallel stripes of a Gabor function, ψ represents the phase offset, σ represents the standard deviation of the Gaussian envelope and γ represents the spatial aspect ratio and it specifies the ellipticity of the support of the Gabor function. The computational models of such 2D Gabor filters are as in Eq. (6.9) and (6.10):

$$h_e = g(x, y) cos\big(2\pi f(x\cos\theta + y\sin\theta)\big) \quad (6.9)$$

$$h_o = g(x, y) sin\big(2\pi f(x\cos\theta + y\sin\theta)\big) \quad (6.10)$$

Where h_e and h_o represents the even symmetric and odd symmetric Gabor filters while $g(x, y)$ represents the isotropic Gaussian function as in Eq. (6.11):

$$g(x, y) = \frac{1}{\sqrt{2\pi\sigma^2}} exp\left(-\frac{x'^2+y'^2}{2\sigma^2}\right) \quad (6.11)$$

And the spatial frequency response of the Gabor functions is as shown in Eq. (6.12):

$$f = N/P \quad (6.12)$$

Where N denotes the size of the kernel and P denotes period in pixel.

In this study, wavelength, λ was in increasing powers of two starting from $4/\sqrt{2}$ up to the hypotenuse length of the input image (Jain, Anil K., 1991) and four orientation, 0°, 45°, 90° and 135° were used. This forms twenty-eight features Gabor features. In total, the sixteen GLCM and twenty-eight Gabor features were combined and this forms forty-four features in total. These forty-four features were calculated for the normalized wood images.

6.3.4 MOS

The same MOS values obtained for wood images as explained in Section 4.3.3 were also used to train SVR.

6.3.5 Regression Module

The $\in -$SVR is trained using MOS and forty-four GLCM and Gabor features of wood images to design GGW-IQA metric. The forty-four image features calculated for the wood images are mapped to the MOS values of the respective wood images. The forty-four features and MOS of wood images were divided randomly into two sets, where one set is used for training and the other set for testing the system: 80% of the forty-four features and MOS values were used to train the SVR model and remaining 20% were used to test the system. The training and testing datasets were permutated randomly to avoid any biasness while training and testing of the system (Mittal et al., 2012). The flow diagram of the GGW-IQA metric system is shown in Figure 6.1.

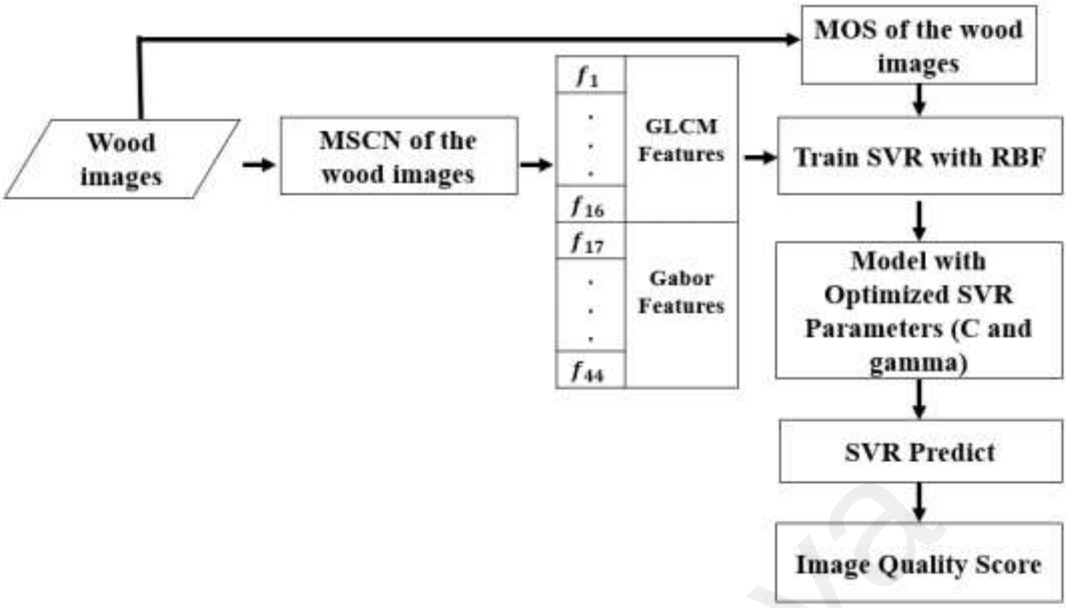

Figure 6.1: Flow diagram of the GGW-IQA Metric

The performance of the GGW-IQA metric were evaluated using Pearson's Linear Correlation Coefficient (PLCC) (Song, 2007) and Root Mean Square Error (RMSE) (Chai & Draxler, 2014) calculated between the MOS values and the quality score obtained from the GGW-IQA metric. Higher PLCC and lower RMSE values indicate that the quality metric is in close agreement with the MOS values. The training and testing of the system were iterated 1000 times and the PLCC and RMSE values were recorded for every iteration. The optimized cost parameter, C, and width parameter, g, of the SVR model is chosen based on the median of the PLCC and RMSE values obtained for all the 1000 iterations. In this study, C = 32768 and g = 0.125 were used to form the optimized SVM model.

6.3.6 Performance Evaluation

The GGW-IQA metric is compared with five FR-IQA metrics (Rajagopal, H., Khairuddin, A.S.M., Mokhtar, 2019): Structural Similarity Index (SSIM) (Zhou Wang et al., 2003), Multiscale SSIM (MS-SSIM) (Zhou Wang et al., 2003), Feature Similarity (FSIM) (L. Zhang et al., 2011), Information Weighted SSIM (IW-SSIM) (Zhou Wang &

Li, 2011) and Gradient Magnitude Similarity Deviation (GMSD) (Xue et al., 2014). In addition, the GGW-IQA metric is also compared with MBW-IQA metric deepIQA, DB-CNN and BRISQUE. PLCC and RMSE (L.S. Chow et al., 2016) values between these FR-IQAs, BRISQUE, deepIQA, DB-CNN and the two proposed metrics, GGW-IQA and MBW-IQA are calculated in order to evaluate the performance of the proposed GGW-IQA and MBW-IQA metrics, BRISQUE, deepIQA, DB-CNN and FR-IQAs.

6.4 Results and Discussions

The same second dataset as explained in Section 5.4 were used to evaluate the efficiency of the proposed metric. The GGW-IQA metric is compared with the five FR-IQAs, BRISQUE, deepIQA and DB-CNN obtained for the second dataset. This dataset was produced using the same ten 'perfect' reference images as explained in Section 5.4.1. These images were distorted with Gaussian white noise with σ_{GN} = 10, 20, 30, 40, 50, 60, 70, 80 and 90 and motion blur with σ_{MB} = 2, 4, 6, 8, 10, 12, 14, 16 and 18 to form 180 images. In total, this dataset comprises of 190 wood images.

In addition, the efficiency of the proposed metric was also tested with third dataset which is generated using wood images obtained from Forest Research Institute Malaysia (FRIM). Ten reference wood images were obtained from ten different wood species. The gaussian white noise with standard deviation, σ_{GN} and motion blur with standard deviation, σ_{MB} were applied to the reference images. For each type of the distortions, there were nine levels of distortion applied to the reference images where the standard deviation takes the value of 10, 20, 30, 40, 50, 60, 70, 80 and 90. This dataset comprises of ten reference and 180 distorted wood images. The GGW-IQA metric is compared with the five FR-IQAs, BRISQUE, deepIQA and DB-CNN obtained for the second dataset.

6.4.1 Relationship between MOS and GGW-IQA, MBW-IQA, BRISQUE, FR-IQAs

The calculated PLCC and RMSE values between MOS and the GGW-IQA, MBW-IQA, deepIQA, DB-CNN, BRISQUE and the five FR-IQA metrics for second and third dataset are shown in Tables 6.1-6.2, respectively. PLCC values close to 1 indicates that the MOS correlates well with the IQA metric, whereas lower RMSE values indicate that the MOS correlates with the IQA metric. Tables 6.1-6.2 shows that the PLCC values for Gaussian white noise, motion blur and the overall images obtained for the GGW-IQA are the highest compared to the MBW-IQA, deepIQA, DB-CNN, BRISQUE and five FR-IQAs. This shows that the GGW-IQA outperforms MBW-IQA, deepIQA, DB-CNN, BRISQUE, SSIM, MS-SSIM, FSIM, IW-SSIM and GMSD. GGW-IQA is the best metric compared to other seven metrics as it is designed by using Gabor and GLCM features and these features are widely used as it reflects the unique characteristics of wood images such as the knot and pores. This is also indicated by the GGW-IQA metric having the lowest RMSE values compared to MBW-IQA, BRISQUE and FR-IQAs. The PLCC and RMSE values for second and third dataset were illustrated in histogram form in Figures 6.2 - 6.5, respectively to show the difference in the PLCC and RMSE values between MOS and the GGW-IQA, MBW-IQA, deepIQA, DB-CNN, BRISQUE and the five FR-IQA metrics clearly. Sample of wood images with the MOS and quality scores values of GGW-IQA, MBW-IQA, deepIQA, DB-CNN, BRISQUE and the five FR-IQA metrics is shown in Figure 6.6.

Table 6.1: PLCC and RMSE values between MOS and GGW-IQA, MBW-IQA, BRISQUE and five FR-IQAs for second dataset

		GGW-IQA	MBW-IQA	BRISQUE	deepIQA	DB-CNN	MSSIM	SSIM	FSIM	IWSSIM	GMSD
PLCC	GWN	**0.982**	0.935	0.585	0.542	0.527	0.847	0.865	0.903	0.855	0.914
	MB	**0.987**	0.954	0.563	0.513	0.538	0.845	0.805	0.912	0.902	0.915
	All	**0.985**	0.942	0.594	0.528	0.529	0.843	0.836	0.914	0.879	0.910
RMSE	GWN	**0.253**	0.462	1.126	1.256	1.457	0.675	0.627	0.558	0.633	0.542
	MB	**0.217**	0.335	0.957	1.134	1.386	0.564	0.643	0.487	0.502	0.475
	All	**0.206**	0.400	1.028	1.248	1.365	0.614	0.629	0.526	0.552	0.510

Table 6.2: PLCC and RMSE values between MOS and GGW-IQA, MBW-IQA, BRISQUE and five FR-IQAs for third dataset

		GGW-IQA	MBW-IQA	BRISQUE	deepIQA	DB-CNN	MSSIM	SSIM	FSIM	IWSSIM	GMSD
PLCC	GWN	**0.971**	0.957	0.629	0.514	0.517	0.954	0.963	0.959	0.955	0.944
	MB	**0.962**	0.933	0.623	0.525	0.519	0.575	0.664	0.646	0.689	0.650
	All	**0.968**	0.927	0.615	0.518	0.513	0.869	0.589	0.743	0.887	0.867
RMSE	GWN	**0.283**	0.306	1.026	1.224	1.209	0.364	0.327	0.345	0.361	0.401
	MB	**0.225**	0.325	1.002	1.138	1.228	0.550	0.502	0.513	0.486	0.511
	All	**0.219**	0.315	0.938	1.236	1.216	0.504	0.823	0.682	0.469	0.507

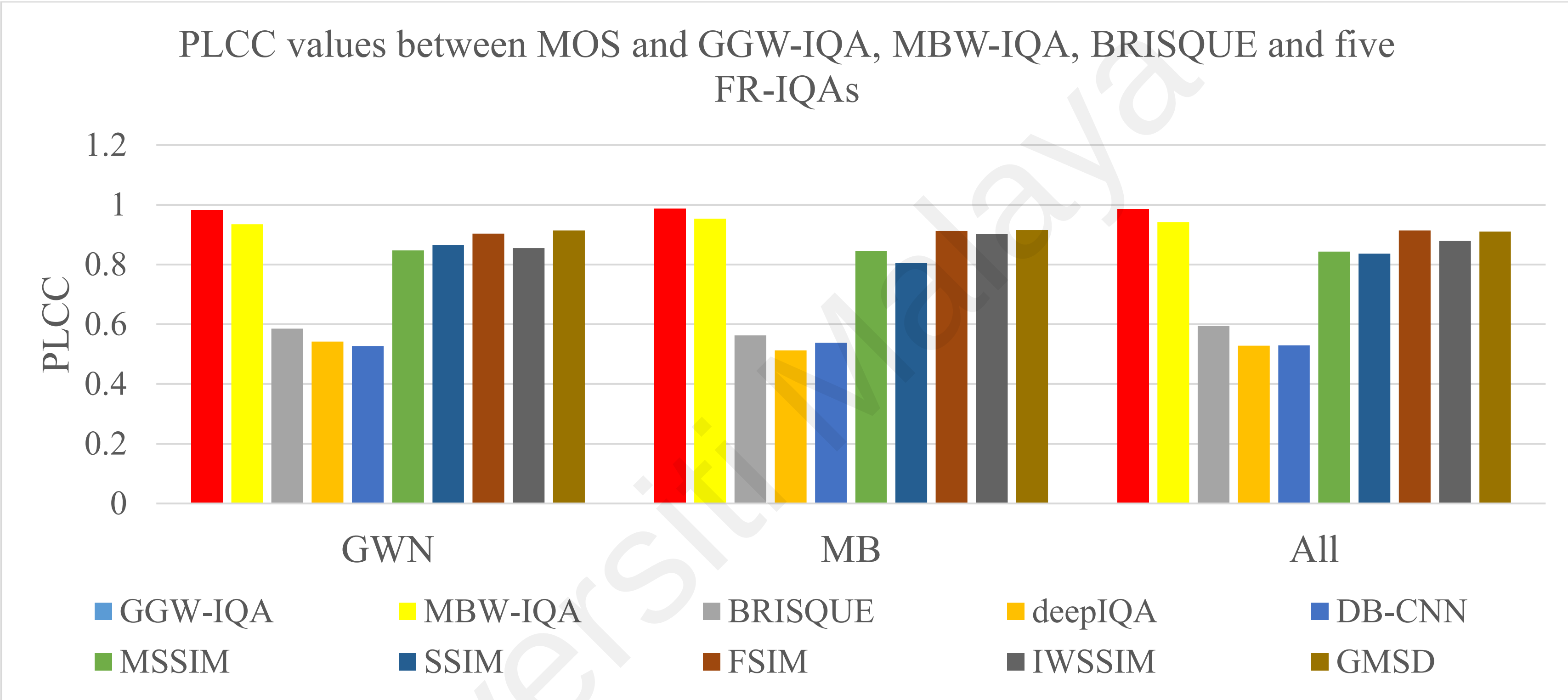

Figure 6.2: PLCC values between MOS and GGW-IQA, MBW-IQA, deepIQA, DB-CNN, BRISQUE and five FR-IQAs for second dataset

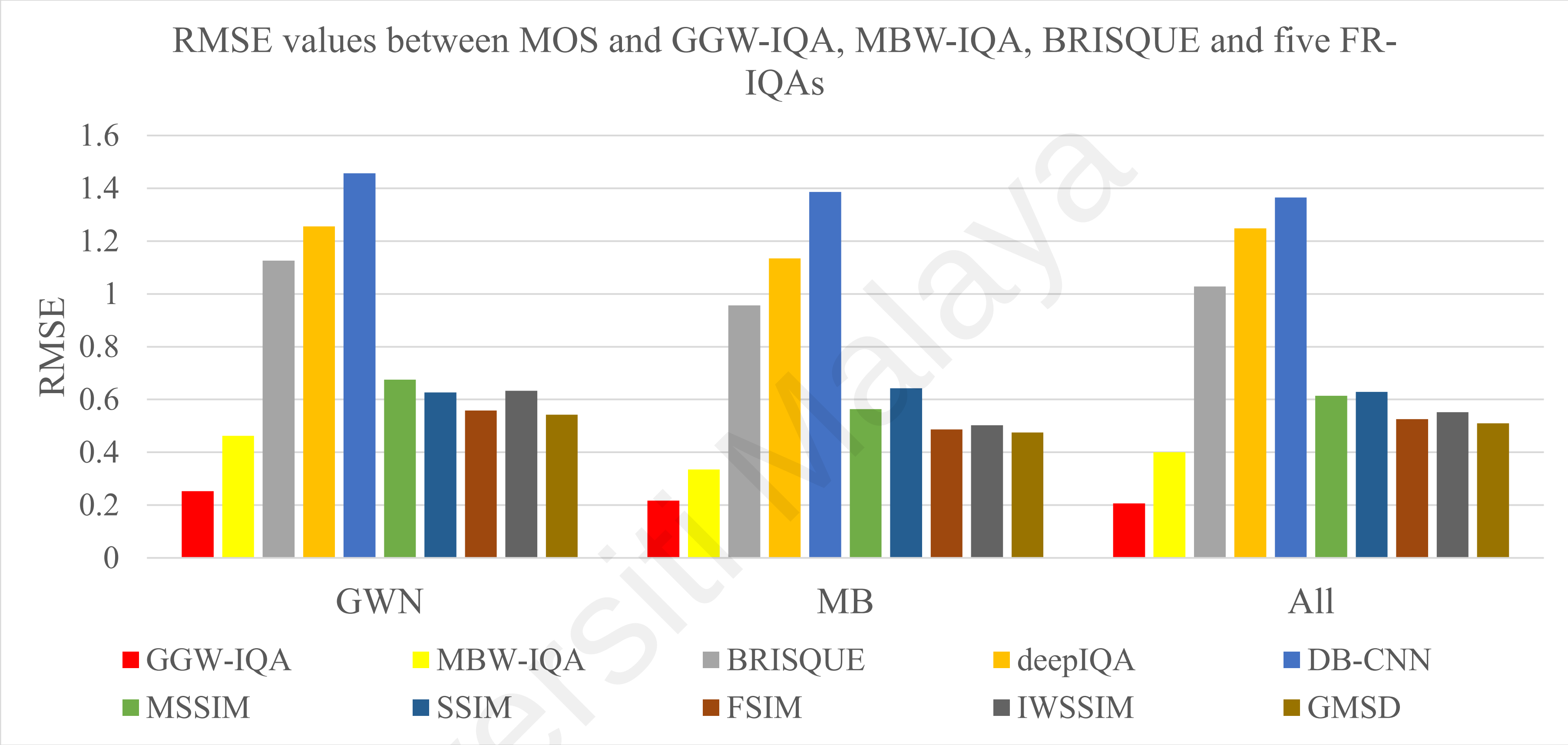

Figure 6.3: RMSE values between MOS and GGW-IQA, MBW-IQA, deepIQA, DB-CNN, BRISQUE and five FR-IQAs for second dataset

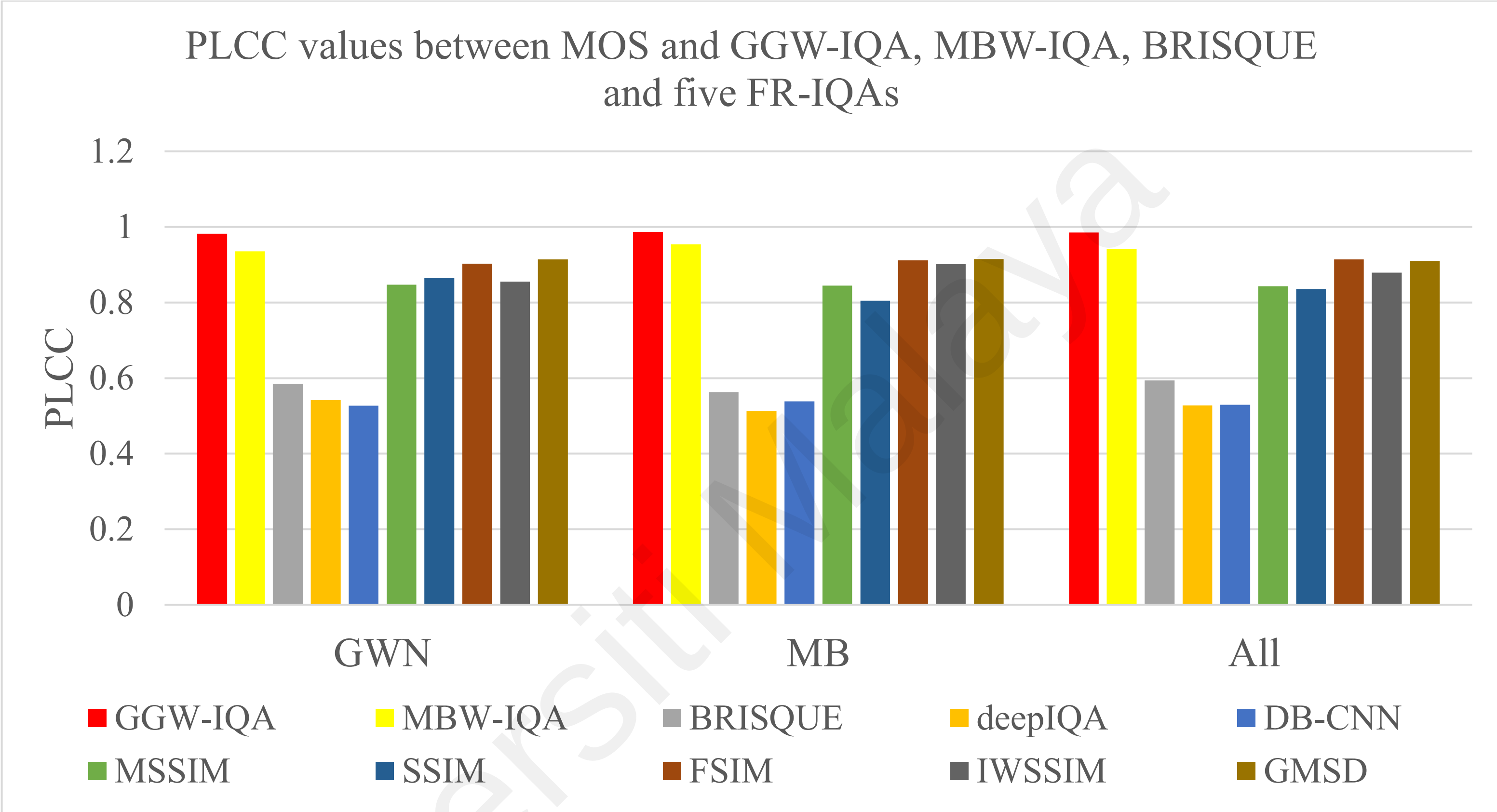

Figure 6.4: PLCC values between MOS and GGW-IQA, MBW-IQA, deepIQA, DB-CNN, BRISQUE and five FR-IQAs for third dataset

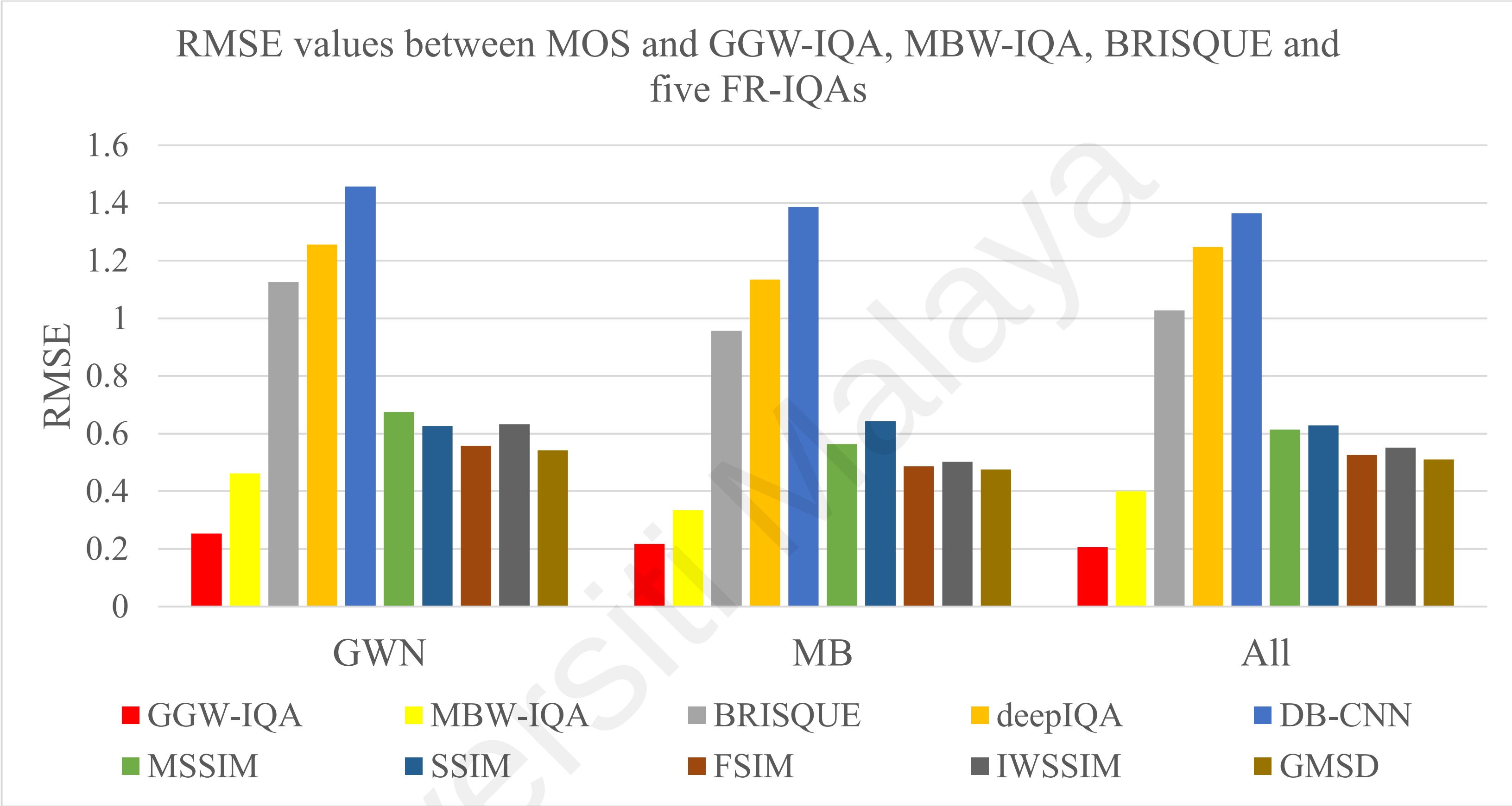

Figure 6.5: RMSE values between MOS and GGW-IQA, MBW-IQA, deepIQA, DB-CNN, BRISQUE and five FR-IQAs for third dataset

Wood species: Julbernardia pellegriniana

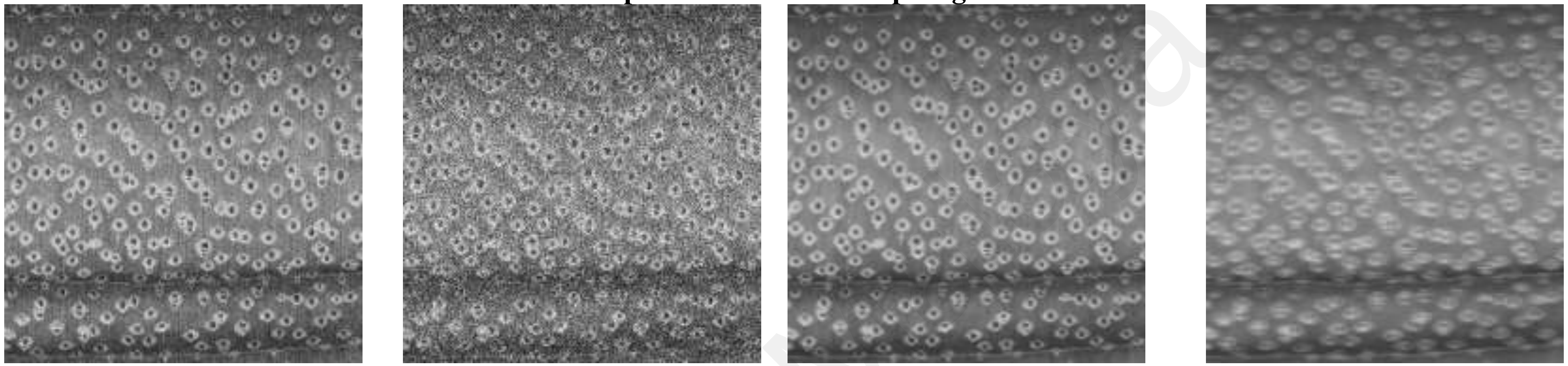

	σ_{GN} = 30		σ_{GN} = 70		σ_{MB} = 10		σ_{MB} = 16
MOS	4	MOS	1.00	MOS	4.00	MOS	1.00
GGW-IQA	3.98	GGW-IQA	1.10	GGW-IQA	3.90	GGW-IQA	1.10
MBW-IQA	4.09	MBW-IQA	1.17	MBW-IQA	3.73	MBW-IQA	1.97
BRISQUE	52.85	BRISQUE	66.74	BRISQUE	54.37	BRISQUE	57.66
deepIQA	54.91	deepIQA	70.35	deepIQA	52.23	deepIQA	64.12
DB-CNN	62.13	DB-CNN	75.13	DB-CNN	56.89	DB-CNN	54.73
MSSIM	0.87	MSSIM	0.62	MSSIM	0.94	MSSIM	0.76
SSIM	0.42	SSIM	0.13	SSIM	0.79	SSIM	0.56
FSIM	0.93	FSIM	0.79	FSIM	0.93	FSIM	0.77
IWSSIM	0.88	IWSSIM	0.66	IWSSIM	0.93	IWSSIM	0.70
GMSD	0.11	GMSD	0.22	GMSD	0.09	GMSD	0.19

Figure 6.6: Sample of wood images with MOS and quality scored from GGW-IQA, MBW-IQA, deepIQA, DB-CNN, BRISQUE and five FR-IQAs

6.5 Chapter Conclusion

In this study, a GLCM and Gabor features based No-Reference Image Quality Assessment (NR-IQA) metric, GGW-IQA was proposed to evaluate wood images prior to species classification. The GGW-IQA metric was trained using MOS and a set of GLCM and Gabor features calculated specifically for wood images. The GLCM and Gabor features were used to design GGW-IQA metric as these features are widely used for wood species recognition. The efficiency of the GGW-IQA was evaluated by comparing the correlation between MOS, GGW-IQA MBW-IQA, deepIQA, DB-CNN, BRISQUE and five FR-IQA metrics for two datasets, second dataset (reference images obtained from open database) and third dataset (reference images obtained from FRIM). The PLCC and RMSE were calculated to determine the relationship between MOS, GGW-IQA, MBW-IQA, deepIQA, DB-CNN, BRISQUE and five FR-IQAs. PLCC and RMSE values both showed that the GGW-IQA outperforms MBW-IQA, deepIQA, DB-CNN, BRISQUE and the FR-IQAs for both datasets. The results obtained shows that the GGW-IQA metric could assess the quality of wood images accurately. In addition, the GGW-IQA metric does not require a 'perfect' reference image in order to evaluate the quality of the wood images similar to the MBW-IQA. This is beneficial especially when it is impossible to obtain a perfect reference image in the dusty environment of lumber mill.

CHAPTER 7: CONCLUSION AND FUTURE WORKS

The ultimate goal of this dissertation is to design a suitable No Reference Image Quality Assessment (NR-IQA) model for wood images. To achieve this, firstly, both subjective and objective assessment of Full Reference Image Quality Assessment (FR-IQA) were performed on 190 wood images. MOS values were obtained from the subjective evaluation on the wood images. MSCN coefficients and 36 features were also calculated for the wood images.

A NR-IQA for wood images, MBW-IQA was modeled using these MOS values and 36 Generalized Gaussian Distribution (GGD) and Asymmetric Generalized Gaussian Distribution (AGGD) features to train SVR model. A well-known NR-IQA in evaluating natural images, Blind/Referenceless Image Spatial Quality Evaluator (BRISQUE) was modified to develop the MBW-IQA metric. The significant difference between the BRISQUE and the MBW-IQA metric is, BRISQUE used natural images to calculate the Mean Subtracted Contrast Normalized (MSCN) coefficients and images features; while the MBW-IQA metric used wood images for this purpose. Then, the MBW-IQA metric was compared with BRISQUE, Deep Neural Network IQA (deepIQA), Deep Bilinear Convolution Neural Network (DB-CNN) and five types of established FR-IQA metrics, i.e. Structural Similarity Index (SSIM), Multiscale SSIM (MS-SSIM), Feature Similarity (FSIM), Information Weighted SSIM (IW-SSIM) and Gradient Magnitude Similarity Deviation (GMSD).

Next, a Gray Level Co-Occurrence Matrix (GLCM) and Gabor feature-based NR-IQA, GGW-IQA metric to evaluate the quality of wood images were proposed. The GLCM and Gabor features were computed for the normalized wood images. The 44 features of GLCM and Gabor were trained together with MOS using SVR for form the

GGW-IQA metric. The GGW-IQA metric was compared with the MBW-IQA metric, BRISQUE, deepIQA, DB-CNN and five FR-IQAs and results shows that the GGW-IQA metric outperforms the MBW-IQA, BRISQUE, deepIQA, DB-CNN and FR-IQAs. The GGW-IQA metric outperforms the MBW-IQA metric as it incorporates set of widely used features for wood species recognition, namely GLCM and Gabor features. These features are widely used as it reflects the unique characteristics of wood images such as the knot and pores. Section 7.1 summarizes the main contributions of this dissertation. Section 7.2 outlines the future directions for improving this work.

7.1 Summary of Main Contributions

In this dissertation, firstly the importance of Image Quality Assessment (IQA) module in improving the rate of wood species recognition system has been studied. Results obtained from the study has shown that the wood species recognition system can be improved with IQA module where the wood image have to be evaluated first before feeding it to the recognition system. If the quality of the wood image is high, the image will be fed into the recognition system. If the quality of the wood image is low, the image will be denoised and the denoised image will be fed into the recognition system.

Next, both subjective and objective assessment of Full Reference Image Quality Assessment (FR-IQA) were performed on 190 wood images. All the wood images has their own MOS values. The study on NR-IQA model for wood images has not been done till now. Therefore, an effective and practical NR-IQA model is needed to assess the image quality produced from any new hardware or software in wood. Hence a tailored-made NR-IQA method has been proposed in this dissertation to evaluate wood images.

A NR-IQA model were proposed to evaluate wood images by modifying BRISQUE model, a renowned NR-IQA in evaluating natural images. This model is known as Modified BRISQUE Wood IQA (MBW-IQA) metric in this research. The

BRISQUE model assessed the image quality by using the locally normalized luminance coefficients. The MBW-IQA model trained a new regression model, Support Vector Machine (SVM) Regressor (SVR) using wood image features and MOS from 190 wood images. The MBW-IQA metric was compared with BRISQUE,deepIQA, DB-CNN and five types of established FR-IQA metrics, i.e. Structural Similarity Index (SSIM), Multiscale SSIM (MS-SSIM), Feature Similarity (FSIM), Information Weighted SSIM (IW-SSIM) and Gradient Magnitude Similarity Deviation (GMSD). The correlation between the MBW-IQA, BRISQUE, deepIQA, DB-CNN and FR-IQAs were computed. There was a relatively high correlation between the MBW-IQA and MOS compared to the BRISQUE and FR-IQAs.

Next, a GLCM and Gabor features-based NR-IQA were proposed and investigated. This is the proposed second NR-IQA metric in this research and it is known as GLCM and Gabor Wood IQA (GGW-IQA). In this study, 44 features of GLCM and Gabor were calculated for the normalized wood images. These features and the MOS obtained from the subjective evaluation were used to train the SVR to generate a NR-IQA metric. The efficiency of the GGW-IQA metric was compared with the MBW-IQA, BRISQUE, deepIQA, DB-CNN and five FR-IQAs. The results obtained from this study proved that the GGW-IQA outperforms the MBW-IQA, BRISQUE, deepIQA, DB-CNN and FR-IQAs. This proves that GGW-IQA metric accurately measured the image quality of wood images.

7.2 Future works

Currently, the wood images were distorted with only two types of distortions: Gaussian White Noise and Motion Blur. Hence, for the future work, more reference wood images with more distortions such as JPEG and JPEG2000 compression, JPEG blocking and interpolation could be included. Compression plays a crucial role when it involves large database. Therefore, the reliability of compression in wood images can be studies by studying the effect of compressions to the wood images. In addition, camera distortion such as JPEG blocking and interpolation will be explored and added into the wood images. Furthermore, more human subjects can be involved in order to get more MOS values. Crowdsourcing such as Amazon Mechanical Turk can be used to obtain many scores from the human subjects around the world. Thus, a larger training and testing dataset can be formed to train SVR. This process may further improve the performance of the proposed NR-IQA metric. In addition, convolution neural network technique and extreme learning machines can be incorporated with a larger training and testing dataset.

The proposed NR-IQA model can be extended to estimate noise parameters in wood images based on the calculated features. The image content measures are used to predict the noise variance in the image. The noise variance can be used to train SVR model where the features of the wood images are mapped to the noise prediction parameter. After the training phase, the automatic parameter prediction could predict the noise level in an image (Mittal et al., 2012). The noise level predicted could be used to adjust the amount of denoising strength of the filter in any filter based denoising algorithm (Martı & Manjo, 2010). The noise level estimated can be input to the filter based denosing algorithm. A higher visual quality denoised image can be produced when the noise level is predicted accurately.

List of Publications

1. Rajagopal, H., Khairuddin, A.S.M., Mokhtar, N. et al. Application of image quality assessment module to motion-blurred wood images for wood species identification system. Wood Sci Technol (2019).
2. Rajagopal, H., A.S.M., Mokhtar, N. et al. No-Reference Quality Assessment for Image-Based Assessment of Economically Important Tropical Woods. PLOS ONE (2020).
3. Rajagopal, H., Khairuddin, A.S.M., Mokhtar, N. Subjective and objective assessment on wood images. Journal of Engineering Research (Submitted on 10th January 2020)
4. Rajagopal, H., A.S.M., Mokhtar, N. et al. Gray Level Co-Occurrence Matrix (GLCM) and Gabor Features Based No-Reference Image Quality Assessment for Wood Images. (Accepted for The 2021 International Conference on Artificial Life and Robotics, 21st – 24th Jan 2021).

REFERENCES

Abang, M. Z., Ramli, M. S., & Halim, S. A. (2018). Application of blind deconvolution and Lucy-Richardson Deconvolution for image deblurring. *Journal of Fundamental and Applied Sciences*, *9*(5S), 232. https://doi.org/10.4314/jfas.v9i5s.17

Abd Latif, MH, Md. Yusof, H, Sidek, S.N, Rusli, N. (2015). Implementation of GLCM Features in Thermal Imaging Affective State Detection. In *IEEE International Symposium on Robotics and Intelligent Sensors* (Vol. 76, pp. 308–315). https://doi.org/10.1016/j.procs.2015.12.298

Angelis, G. I., Gillam, J. E., Kyme, A. Z., Fulton, R. R., & Meikle, S. R. (2018). Image-based modelling of residual blurring in motion corrected small animal PET imaging using motion dependent point spread functions. *Biomedical Physics and Engineering Express*, *4*(3). https://doi.org/10.1088/2057-1976/aab922

Aouinti, F., Nasri, M., Moussaoui, M., & Bouali, B. (2018). An improved Richardson-Lucy algorithm based on genetic approach for satellite image restoration. *International Arab Journal of Information Technology*, *15*(4), 715–720.

Aziz, F., Arof, H., Mokhtar, N., Shah, N. M., Khairuddin, A. S. M., Hanafi, E., & Talip, M. S. A. (2018). Waste level detection and HMM based collection scheduling of multiple bins. *PLoS ONE*, *13*(8), 1–14. https://doi.org/10.1371/journal.pone.0202092

Barmpoutis, P., Dimitropoulos, K., Barboutis, I., & Grammalidis, N. (2018). Wood species recognition through multidimensional texture analysis. *Computers and Electronics in Agriculture*, *144*, 241–248. https://doi.org/10.1016/j.compag.2017.12.011

Barrack, F., Scuffham, J., & McQuaid, S. (2018). Septal penetration correction in I-131 imaging following thyroid cancer treatment. *Physics in Medicine and Biology*, *63*(7). https://doi.org/10.1088/1361-6560/aab13a

Bindu, K., Ganpati, A., & Sharma, A. K. (2012). A Comparative Study of Image Compression Algorithms. *International Journal of Research in Computer Science*, *2*(5), 37–42. https://doi.org/10.7815/ijorcs.25.2012.046

Bosse, S., Maniry, D., Müller, K. R., Wiegand, T., & Samek, W. (2018). Deep Neural Networks for No-Reference and Full-Reference Image Quality Assessment. *IEEE Transactions on Image Processing*, *27*(1), 206–219. https://doi.org/10.1109/TIP.2017.2760518

Bovik,] Deepti Ghadiyaram and Alan C. (2016). Massive online crowdsourced study of subjective and objective picture quality. *IEEE Transactions on Image Processing*, *25*(1), 372–387.

Bremananth R. ; Nithya B. ; Saipriya R. (2009). Wood Species Recognition Using GLCM and Correlation. In *2009 International Conference on Advances in Recent Technologies in Communication and Computing* (Vol. 51, pp. 431–444). https://doi.org/https:/https:/10.1109/ARTCom.2009.10

Buccini, A., Donatelli, M., & Ferri, F. (2018). Weakly Constrained Lucy–Richardson with Applications to Inversion of Light Scattering Data. *Journal of Scientific Computing*, *74*(2), 786–804. https://doi.org/10.1007/s10915-017-0461-4

Chai, T., & Draxler, R. R. (2014). Root mean square error (RMSE) or mean absolute error (MAE)? -Arguments against avoiding RMSE in the literature. *Geoscientific Model Development*, *7*(3), 1247–1250. https://doi.org/10.5194/gmd-7-1247-2014

Chandler, D. M. (2013). Seven Challenges in Image Quality Assessment: Past, Present, and Future Research. *ISRN Signal Processing*, *2013*, 1–53. https://doi.org/10.1155/2013/905685

Chandler, D. M., & Hemami, S. S. (2007). VSNR : A Visual Signal-to-Noise Ratio for Natural Images. *IEEE Transactions on Image Processing*, *16*(9), 2284–2298.

Chang, Chih-Chung and Lin, C.-J. (2011). LIBSVM: A library for support vector machines. *ACM Transactions on Intelligent Systems and Technology*, *2*(3), 27:1--27:27.

Chih-Wei Hsu, Chih-Chung Chang, and C.-J. L. (2016). *A Practical Guide to Support Vector Classication*. *Department of Computer Science National Taiwan University, Taipei 106, Taiwan*. https://doi.org/10.1162/089976600300015565

Chow, L.S., Rajagopal, H., & Paramesran, R. (2016). Correlation between subjective and objective assessment of magnetic resonance (MR) images. *Magnetic Resonance Imaging*, *34*(6), 820–831. https://doi.org/10.1016/j.mri.2016.03.006

Chow, Li Sze, Rajagopal, H., & Paramesran, R. (2016). Correlation between subjective and objective assessment of magnetic resonance (MR) images. *Magnetic Resonance Imaging*, *34*(6), 820–831. https://doi.org/10.1016/j.mri.2016.03.006

Daassi-Gnaba, H., Oussar, Y., Merlan, M., Ditchi, T., Géron, E., & Holé, S. (2018). Moisture content recognition for wood chips in pile using supervised classification. *Wood Science and Technology*, *52*(5), 1195–1211. https://doi.org/10.1007/s00226-018-1023-0

Defoirdt, N., Sen, A., Dhaene, J., De Mil, T., Pereira, H., Van Acker, J., & Van den

Bulcke, J. (2017). A generic platform for hyperspectral mapping of wood. *Wood Science and Technology*, *51*(4), 887–907. https://doi.org/10.1007/s00226-017-0903-z

Engelke, U., Kusuma, M., Zepernick, H. J., & Caldera, M. (2009). Reduced-reference metric design for objective perceptual quality assessment in wireless imaging. *Signal Processing: Image Communication*, *24*(7), 525–547. https://doi.org/10.1016/j.image.2009.06.005

Esteban, L. G., de Palacios, P., Conde, M., Fernández, F. G., García-Iruela, A., & González-Alonso, M. (2017). Application of artificial neural networks as a predictive method to differentiate the wood of Pinus sylvestris L. and Pinus nigra Arn subsp. salzmannii (Dunal) Franco. *Wood Science and Technology*, *51*(5), 1249–1258. https://doi.org/10.1007/s00226-017-0932-7

Funck, J. W., Zhong, Y., Butler, D. A., Brunner, C. C., & Forrer, J. B. (2003). Image segmentation algorithms applied to wood defect detection. *Computers and Electronics in Agriculture*, *41*(1–3), 157–179. https://doi.org/10.1016/S0168-1699(03)00049-8

Gazo, R., Wells, L., Krs, V., & Benes, B. (2018). Validation of automated hardwood lumber grading system. *Computers and Electronics in Agriculture*, (June), 0–1. https://doi.org/10.1016/j.compag.2018.06.041

Gu, I. Y. H., Andersson, H., & Vicen, R. (2010). Wood defect classification based on image analysis and support vector machines. *Wood Science and Technology*, *44*(4), 693–704. https://doi.org/10.1007/s00226-009-0287-9

Guang-sheng, C., & Peng, Z. (2012). Sensors and Actuators A : Physical Dynamic wood slice recognition using image blur information. *Sensors & Actuators: A. Physical*, *176*, 27–33. https://doi.org/10.1016/j.sna.2011.12.056

Gulame, M., Joshi, K. R., & Kamthe, R. S. (2013). A Full Reference Based Objective Image Quality Assessment. *International Journal of Advanced Electrical and Electronics Engineering (IJAEEE)*, *2*(6), 13–18.

Gupta, P., Moorthy, A. K., Soundararajan, R., & Bovik, A. C. (2018). Generalized Gaussian Scale Mixtures : A Model for Wavelet Coefficients of Natural Images. *Signal Processing: Image Communication*, *66*, 87–94. https://doi.org/10.1016/j.image.2018.05.009

Hou, G., Zhao, X., Pan, Z., Yang, H., Tan, L., & Li, J. (2020). Benchmarking Underwater Image Enhancement and Restoration, and beyond. *IEEE Access*, *8*, 122078–122091. https://doi.org/10.1109/ACCESS.2020.3006359

Ibrahim, I., Khairuddin, A. S. M., Abu Talip, M. S., Arof, H., & Yusof, R. (2017). Tree species recognition system based on macroscopic image analysis. *Wood Science and Technology*, *51*(2), 431–444. https://doi.org/10.1007/s00226-016-0859-4

Iglesias, C., Anjos, O., Martínez, J., Pereira, H., & Taboada, J. (2015). Prediction of tension properties of cork from its physical properties using neural networks. *European Journal of Wood and Wood Products*, *73*(3), 347–356. https://doi.org/10.1007/s00107-015-0885-1

Jain, Anil K., and F. F. (1991). Unsupervised Texture Segmentation Using Gabor Filters. *Pattern Recognition*, *24*(12), 1167–1186.

Khalid, M., Lee, E. L. Y., Yusof, R., & Nadaraj, M. (2008). Design of an intelligent wood species recognition system. *International Journal of Simulation System, Science and Technology*, *9*(3), 9–19.

Konda Naganathan, G., Cluff, K., Samal, A., Calkins, C. R., Jones, D. D., Meyer, G. E., & Subbiah, J. (2016). Three dimensional chemometric analyses of hyperspectral images for beef tenderness forecasting. *Journal of Food Engineering*, *169*, 309–320. https://doi.org/10.1016/j.jfoodeng.2015.09.001

Kurimo, E., Lepistö, L., Nikkanen, J., Grén, J., Kunttu, I., & Laaksonen, J. (2009). The Effect of Motion Blur and Signal Noise on Image Quality in Low Light Imaging. In *Scandinavian Conference on Image Analysis* (pp. 81–90). Berlin, Heidelberg: Springer. https://doi.org/https://doi.org/10.1007/978-3-642-02230-2_9

Larson, E. C., & Chandler, D. M. (2010). Most apparent distortion: full-reference image quality assessment and the role of strategy. *Journal of Electronic Imaging*, *19*(1), 011006-011006–011021. https://doi.org/10.1117/12.810071

Lasmar, N. E., Stitou, Y., & Berthoumieu, Y. (2009). Multiscale skewed heavy tailed model for texture analysis. In *Image Processing (ICIP), 2009 16th IEEE International Conference on* (pp. 2281–2284). https://doi.org/10.1109/ICIP.2009.5414404

Li, C., Guan, T., Zheng, Y., Zhong, X., Wu, X., & Bovik, A. (2021). Blind image quality assessment in the contourlet domain. *Signal Processing: Image Communication*, *91*, 116064. https://doi.org/10.1016/j.image.2020.116064

Li, R., Buongiorno, J., Turner, J. A., Zhu, S., & Prestemon, J. (2008). Long-term effects of eliminating illegal logging on the world forest industries, trade, and inventory. *Forest Policy and Economics*, *10*(7–8), 480–490.

https://doi.org/10.1016/j.forpol.2008.04.003

Longuetaud, F., Mothe, F., Kerautret, B., Krähenbühl, A., Hory, L., Leban, J. M., & Debled-Rennesson, I. (2012). Automatic knot detection and measurements from X-ray CT images of wood: A review and validation of an improved algorithm on softwood samples. *Computers and Electronics in Agriculture*, *85*, 77–89. https://doi.org/10.1016/j.compag.2012.03.013

Martı, L., & Manjo, V. (2010). Adaptive Non-Local Means Denoising of MR Images With Spatially Varying Noise Levels. *Journal OF Magnetic Resonance Imaging*, *31*(1), 192–203. https://doi.org/10.1002/jmri.22003

Meier, E. (2007). The Wood Database. Retrieved August 16, 2018, from https://www.wood-database.com/

MICT Image Quality Evaluation Database. (n.d.).

Mittal, A., Moorthy, A. K., & Bovik, A. C. (2012, December). No-Reference Image Quality Assessment in the Spatial Domain. https://doi.org/10.1109/TIP.2012.2214050

Moorthy, A. K., & Bovik, A. C. (2011). Blind Image Quality Assessment: From Natural Scene Statistics to Perceptual Quality. *IEEE Transactions on Image Processing*, *20*(12), 3350–3364. https://doi.org/10.1109/TIP.2011.2147325

Noor, M. N. H. M., Kadir, R., & Muhamad, S. (2020). Illegal Logging and Forest Offences in Peninsular Malaysia: Perceived Opportunity Factors. *Journal of Nusantara Studies (JONUS)*, *5*(2), 86–102. https://doi.org/10.24200/jonus.vol5iss2pp86-102

Pan, S., & Kudo, M. (2011). Segmentation of pores in wood microscopic images based on mathematical morphology with a variable structuring element. *Computers and Electronics in Agriculture*, *75*(2), 250–260. https://doi.org/10.1016/j.compag.2010.11.010

Patrick Le Callet, F. A. (2005). Subjective quality assessment IRCCyN/IVC database. Retrieved from http://www.irccyn.ec-nantes.fr/ivcdb/

Ponomarenko, N, Lukin, V., Egiazarian, K., Astola, J., Carli, M., & Battisti, F. (2008). Color image database for evaluation of image quality metrics. In *Multimedia Signal Processing, 2008 IEEE 10th Workshop on* (pp. 403–408). IEEE.

Ponomarenko, Nikolay, Jin, L., Ieremeiev, O., Lukin, V., Egiazarian, K., Astola, J., … Jay Kuo, C.-C. (2015). Image database TID2013: Peculiarities, results and perspectives. *Signal Processing: Image Communication*, *30*, 57–77. https://doi.org/10.1016/j.image.2014.10.009

Qin, R., Qiu, Q., Lam, J. H. M., Tang, A. M. C., Leung, M. W. K., & Lau, D. (2018). Health assessment of tree trunk by using acoustic-laser technique and sonic tomography. *Wood Science and Technology*, *52*(4), 1113–1132. https://doi.org/10.1007/s00226-018-1016-z

Rahman, T., Haque, M. R., Rozario, L. J., & Uddin, M. S. (2014). Gaussian Noise Reduction in Digital Images Using a Modified Fuzzy Filter. In *International Conference on Computer and Information Technology (ICCIT)* (pp. 217–222).

Rajagopal, H., Khairuddin, A.S.M., Mokhtar, N. et al. (2019). Application of image quality assessment module to motion-blurred wood images for wood species identification system. *Wood Science and Technology*, 1–15.

Ratnasinga, J., Ioras, F., Swan, T. T., Yoon, C. Y., & Thanasegar, G. (2011). Determinants of Occupational Accidents in the Woodworking Sector: The Case of the Malayasian Wooden Furniture Industry. *Journal of Applied Sciences*, *11*(3), 561–566. https://doi.org/10.3923/jas.2011.561.566

Recommendation, I. T. U. R. B. T. (2002). 500-11. (2000). *Methodology for the Subjective Assessment of the Quality of Television Pictures*. *Recommendation ITU-R BT. 500-11. ITU Telecom. Standardization Sector of ITU.*

Rohaly, A. M., Corriveau, P. J., Libert, J. M., Webster, A. A., Baroncini, V., Beerends, J., ... & Winkler, S. (2000). Video quality experts group: Current results and future directions. In *SPIEVisual Communication and Image Processing* (pp. 742–753).

Rubiyah Yusof, Nenny Ruthfalydia Rosli, M. K. (2010). Using Gabor Filters as Image Multiplier for Tropical Wood Species Recognition System. In *International Conference on, Computer Modeling and Simulation, International Conference* (pp. 289–294). https://doi.org/10.1109/UKSIM.2010.61

Saad, M. A., Bovik, A. C., & Charrier, C. (2012). Blind Image Quality Assessment: A Natural Scene Statistics Approach in the DCT Domain. *IEEE Transactions on Image Processing*, *21*(8), 3339–3352. https://doi.org/10.1109/TIP.2012.2191563

Sharifi, K., & Leon-Garcia, A. (1995). Estimation of shape parameter for generalized Gaussian distributions in subband decompositions of video. *IEEE Transactions on Circuits and Systems for Video Technology*, *5*(1), 52–56. https://doi.org/10.1109/76.350779

Sheikh, H.R., Sabir, M. F., & Bovik, A. C. (2006). A Statistical Evaluation of Recent Full Reference Image Quality Assessment Algorithms. *IEEE Transactions on Image*

Processing, *15*(11), 3440–3451. https://doi.org/10.1109/TIP.2006.881959

Sheikh, Hamid Rahim, & Bovik, A. C. (2006). Image information and visual quality. *IEEE Transactions on Image Processing : A Publication of the IEEE Signal Processing Society*, *15*(2), 430–444. https://doi.org/10.1109/tip.2005.859378

Shivashankar, S. (2018). Automatic Wood Classification using a Novel Color Texture Features. *International Journal of Computer Applications*, *180*(27), 34–38.

Song, X.-K. (2007). *Correlated data analysis: modeling, analytics, and applications*. Springer Science & Business Media.

Taylor, R. (1990). Interpretation of the Correlation Coefficient: A Basic Review. *Journal of Diagnostic Medical Sonography*, *6*(1), 35–39. https://doi.org/10.1177/875647939000600106

Tou, J. Y., Tay, Y. H., & Lau, P. Y. (2009). A Comparative Study for Texture Classification Techniques on Wood Species Recognition Problem. In *2009 Fifth International Conference on Natural Computation* (pp. 8–12). IEEE. https://doi.org/10.1109/ICNC.2009.594

Venkatachalapathy, K., & Sudhakar, P. (2014). An Intelligent Recognition System for Identification of Wood Species. *Journal of Computer Science*, *10*(7), 1231–1237. https://doi.org/10.3844/jcssp.2014.1231.1237

Wang, J., & Wang, Z. (2014). Perceptual Quality of Asymmetrically Distorted Stereoscopic Images : The Role of Image Distortion Types. In *International Workshop on Video Processing and Quality Metrics for Consumer Electronics (VPQM)*.

Wang, Z.; (2011). Applications of objective image quality assessment methods. *Signal Processing Magazine, IEEE*, *28*(6), 137–142. https://doi.org/10.1109/MSP.2011.942295

Wang, Zhou, Bovik, A. C., Sheikh, H. R., & Simoncelli, E. P. (2004). Image quality assessment: From error visibility to structural similarity. *Image Processing, IEEE Transactions On*, *13*(4), 600–612. https://doi.org/10.1109/TIP.2003.819861

Wang, Zhou, & Li, Q. (2011). Information content weighting for perceptual image quality assessment. *IEEE Transactions on Image Processing*, *20*(5), 1185–1198. https://doi.org/10.1109/TIP.2010.2092435

Wang, Zhou, Simoncelli, E. P., & Bovik, A. C. (2003). Multi-Scale Structural Similarity for Image Quality Assessment. In *Asilomar Conference on Signals, Systems and Computers* (Vol. 2, pp. 1398–1402). IEEE.

Wilson, M. D. (2008). Support Vector Machines. In *Encyclopedia of Ecology* (Vol. 16, pp. 3431–3437). Elsevier. https://doi.org/10.1016/B978-008045405-4.00168-3

Wu, J., Zeng, J., Dong, W., Shi, G., & Lin, W. (2019). Blind image quality assessment with hierarchy: Degradation from local structure to deep semantics. *Journal of Visual Communication and Image Representation*, *58*, 353–362. https://doi.org/10.1016/j.jvcir.2018.12.005

Xiao, B., Tang, H., Jiang, Y., Li, W., & Wang, G. (2018). Brightness and contrast controllable image enhancement based on histogram specification. *Neurocomputing*, *275*, 2798–2809. https://doi.org/10.1016/j.neucom.2017.11.057

Xue, W., Zhang, L., Mou, X., & Bovik, A. C. (2014). Gradient magnitude similarity deviation: A highly efficient perceptual image quality index. *Image Processing, IEEE Transactions On*, *23*(2), 684–695.

Yusof, R., Khalid, M., & Anis, A. S. (2013). Application of kernel-genetic algorithm as nonlinear feature selection in tropical wood species recognition system. *Computers and Electronics in Agriculture*, *93*, 68–77. https://doi.org/10.1016/j.compag.2013.01.007

Zamri, M. I. P., Cordova, F., Khairuddin, A. S. M., Mokhtar, N., & Yusof, R. (2018). Tree species classification based on image analysis using Improved-Basic Gray Level Aura Matrix. *Computers and Electronics in Agriculture*, (124), 227–233. https://doi.org/https://doi.org/10.1016/j.compag.2016.04.004

Zhang, L., Zhang, D., & Mou, X. (2011). FSIM: a feature similarity index for image quality assessment. *Image Processing, IEEE Transactions On*, *20*(8), 2378–2386.

Zhang, W., Ma, K., Yan, J., Deng, D., & Wang, Z. (2018). Blind Image Quality Assessment Using A Deep Bilinear Convolutional Neural Network. *IEEE Transactions on Circuits and Systems for Video Technology*, *PP*(c), 1. https://doi.org/10.1109/TCSVT.2018.2886771

Zhang, Y., Moorthy, A. K., Chandler, D. M., & Bovik, A. C. (2014). Signal Processing : Image Communication C-DIIVINE : No-reference image quality assessment based on local magnitude and phase statistics of natural scenes. *Signal Processing : Image Communication*, 1–23. https://doi.org/10.1016/j.image.2014.05.004